THE CYANIDE CATALYZED DIMERIZATION OF

2,3 NAPHTHALENEDICARBOXALDEHYDE;

A UNIQUE OXIDATIVE CONDENSATION PRODUCT AND DERIVATIVES

By

Colin McGill

RECOMMENDED:

Tom Allen

Brian Radley

Thomas K. Green

Advisory Committee Chair

Tom Allen

Department Chair

APPROVED:

Dean, College of Natural Science and Mathematics

Susan M. Kennicks

Dean of the Graduate School

April 12, 2005

Date

THE CYANIDE CATALYZED DIMERIZATION OF 2,3 NAPHTHALENEDICARBOXALDEHYDE; A UNIQUE OXIDATIVE CONDENSATION PRODUCT AND DERIVATIVES

A

THESIS

Presented to the Faculty

of the University of Alaska Fairbanks

in Partial Fulfillment of the Requirements

for the Degree of

MASTER OF SCIENCE

By

Colin McGill, B.S.

Fairbanks, Alaska

May 2005

ABSTRACT

2,3 Naphthalenedicarboxaldehyde (NDA), in the presence of cyanide, is commonly used for the derivitization of amino acids and peptides to fluorescent 2-substituted 1-cyanobenzo[f]isoindoles, providing high sensitivity in capillary electrophoresis (CE) and high performance liquid chromatography (HPLC) separations. CE studies of the neurotransmitters glutamate and aspartate have shown the formation of a number of competitive side products. Although mentioned in the literature, these side products have not been characterized. The product, 15-hydroxybenzo[g]benzo [6,7]isochromeno[4,3-c]isochromen-7(15H)-one (**2**), is reported here, as a dimerization of NDA in the presence of cyanide and atmospheric oxygen. The structure is confirmed by IR, LRFAB-MS, IRMS, and NMR spectra. Possible mechanisms for the formation of **2**, its air oxidation, and an alternative benzoin condensation product are discussed.

15-hydroxybenzo[g]benzo [6,7]isochromeno[4,3-c]isochromen-7(15H)-one (**2**) is easily converted to full acetals via reflux in an alcohol solvent in the presence of an acid catalyst. Oxidation by NaOCl (aq) yields 3-(3-chloro-1,4-dioxo-3,4-dihydro-1H-benzo[g]isochromen-3-yl)-2-napthaldahyde (**4**) by capturing hypochlorite at the position α the enolate. Oxidation by pyridinium chlorochromate (PCC) yields naptho[2,3-c]furan-1,3-dione (**5**) by multiple oxidations and the formation of the anhydride.

TABLE OF CONTENTS

LIST OF FIGURES

LIST OF TABLES

ACKNOWLEDGEMENTS

I would like to thank my committee. Without the regular contribution of their ideas, perspectives and guidance I would have constantly struggled to stay oriented. Each of them contributed in their own way, and did so constantly throughout the duration of my research. Dr. Brian Rasley provided an analytical perspective to problem solving, regularly identifying variables in synthesis I had overlooked. Dr. Thomas Clausen contributed greatly to constructing plausible mechanisms and particularly difficult structure determinations. His patience and helpfulness at all times were second to none. Dr. Thomas Green's constant input of ideas kept the project moving. His enthusiasm for the research was infectious, and his expertise, irreplaceable.

Sheila Chapin was helpful (ok, life saving) more times than I can count. Emily Reiter lent regular moral support and perspective, especially throughout the writing and revisions. And Kristian Swearingen deserves mention for not only sharing work space for the last three years, but contributing his ideas and time to the early stages of this project before diverging in his own research.

Finally, my wife, Crystal, has been supportive and inspirational from the day we met. She constantly amazes me, and I honestly cannot imagine doing this without her.

1.0. Introduction

2,3 naphthalenedicarboxaldehyde (NDA) **1** in the presence of cyanide was first introduced as a reagent for the fluorescent detection of amino acids and peptides by Carlson et al. in 1986.[1,2] The reagent has been shown to react rapidly with amino groups to form stable, highly fluorescent 2-substituted 1-cyanobenzo[f]isoindoles, as shown below. Since that time, NDA has become a widely used analytical reagent for amino acid analysis by HPLC[3] and capillary electrophoresis (CE).[4]

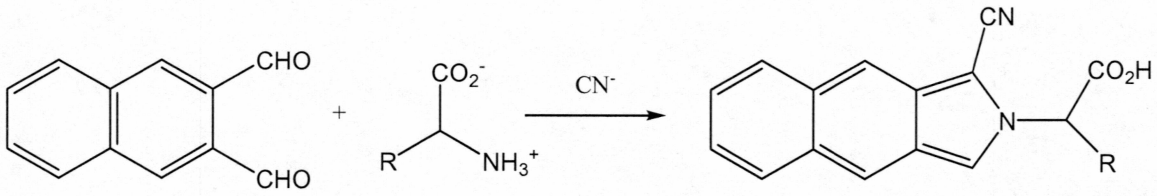

NDA amino isoindole

As initially reported, sodium cyanide is added to a methanolic solution of NDA, immediately followed by an aqueous solution of amino acid.[1] The formation of a pale yellow solution after the cyanide but prior to the amino acid was reported, but no characterization of possible side products was made. Prior experience in the capillary electrophoresis coupled to laser induced fluorescent detection (CE-LIFD) study of the amino acid glutamate has consistently shown the online formation of numerous NDA derivative side products which obscure the electropherograms over a broad region. Identification and characterization of an NDA condensation product is thus described along with associated chemical derivatives and competitive reactions.

We report here the structure of the product, 15-hydroxybenzo[g]benzo [6,7]isochromeno[4,3-c]isochromen-7(15H)-one (**2**), that forms when NDA is reacted

with cyanide and atmospheric oxygen, in the absence of an amino acid, as shown in Figure 1. The product is isolated within 10 minutes reaction time at room temperature as a yellow crystalline solid. It is conveniently reacted to full acetals, **3a** and **3b**, in alcohol and HCl catalyst. Attempted oxidation of the hydroxyl functionality by NaOCl yields a unique ring open product, **4**, via halogenation through the enolate intermediate. Oxidation by PCC yields the anhydide derivative of NDA, **5**.

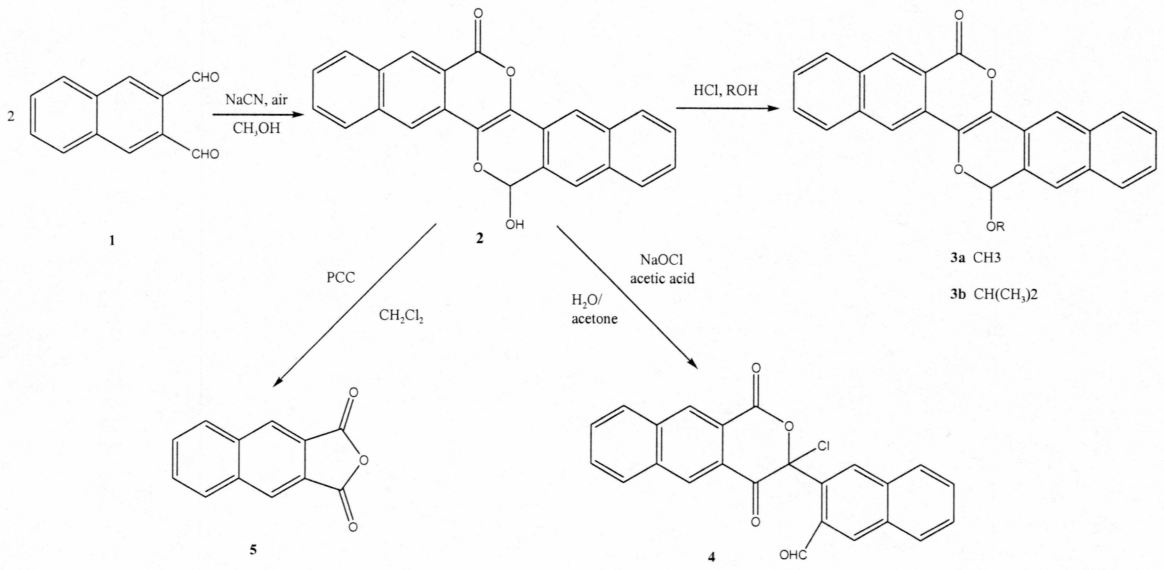

Figure 1: Summary of Synthetic Routes. Condensation of NDA to **2**, the formation of acetals **3a** and **3b,** the reaction to **4** via capturing of an open ring intermediate by chlorination, and the formation of the anhydride derivative, **5**.

The following sections will provide proof of structure for products **2**, **3a** and **3b**, **4**, and **5**. Possible mechanisms for the formation of **2**, **4**, and **5** are also discussed.

2.0. Results and Discussion

2.1. Identification of 15-hydroxybenzo[g]benzo [6,7]isochromeno[4,3-c]isochromen-7(15H)-one

The molecular weight (366.1 g/mol) indicates that the product is a dimer of NDA. The reagents used are not commonly associated with the modification of aromatic rings; therefore, the napthalene rings are likely intact. A strong IR absorption at 3439.5 cm^{-1} and MS fragmentation patterns both indicate the presence of a hydroxyl functionality, and LRFAB-MS shows a single exchange in a lithium enriched 3-NBA matrix, indicating a single, readily exchangable proton. ^{1}H NMR indicates 14 hydrogens, and analysis of ^{13}C NMR spectra show 11 quaternary and 13 C-H carbons, primarily in the aromatic region. Resonances at 160.1 ppm and 93.1 ppm indicate the presence of an ester and a hemiacetal. Congruence between NMR and IRMS demonstrate the molecular formula to be $C_{24}H_{14}O_4$. Of the 18 degrees of unsaturation, 14 are accounted for in the NDA components.

The structure, 15-hydroxybenzo[g]benzo [6,7]isochromeno[4,3-c]isochromen-7(15H)-one (**2**), is proposed on the above chemical evidence and the determination of a plausible mechanism for its formation. The structure of **2** is confirmed by its IR spectrum, mass spectrum, elemental analysis, and NMR spectra including ^{1}H, ^{13}C, gCOSY, gHSQC, and gHMBC spectra. Assignments of all ^{1}H resonances and all but two ^{13}C resonances are made. These are shown pictorally in the NMR discussion of **2** and tabularly in Appendix A.

2.1.1. Discussion of Infrared Spectrum (IR) Results

The IR (KBr) spectrum (Figure 2) shows absorbances at 3439, 1715, 1624, 1280, and 1155 cm^{-1}. The very broad absorption at 3439 cm^{-1} is characteristic of a hydroxyl functionality and accounts for the hemiacetal. The strong absorptions at 1715, 1280, and 1155 cm^{-1} can be attributed to the ester functionality due to its adjacency to conjugation.[7] The overlapping absorption centered at 1624 cm^{-1} are typical of naphthalene hydrogens at both α and β positions.[8]

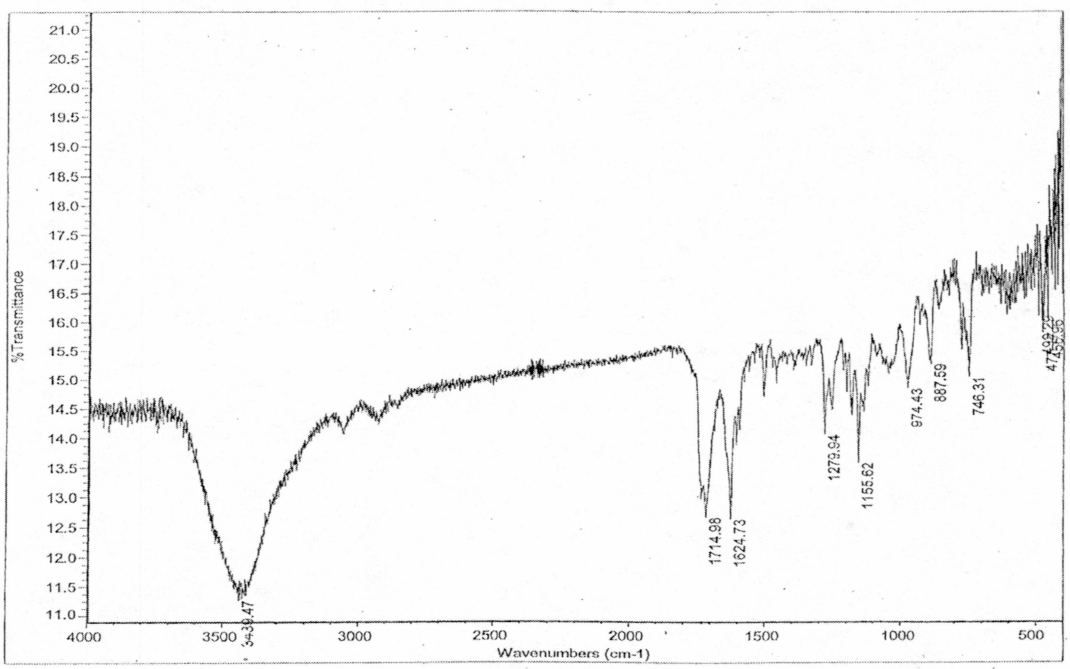

Figure 2: The Infrared Spectrum (KBr) of 2. Note the broad abrorbance at 3439 cm^{-1} (hydroxyl), strong absorbances at 1715, 1280, and 1155 cm^{-1} (ester), and 1624 (naphthyl).

2.1.2. Discussion of Low Resolution Fast Atom Bombardment Mass Spectroscopy (LRFAB-MS) Spectra

Low Resolution Fast Atom Bombardment Mass Spectroscopy (LRFAB-MS) of **2** was performed in desorption matrixes of 3-nitrobenzyl alcohol (3-NBA) and 3-NBA enriched with lithium (3-NBA/Li), as shown in Figures 3 and 4. When run with 3-NBA, a peak was measured at 349.1 m/z and 366.1 m/z. Adjacent, smaller peaks were determined at 348.1 m/z and 367.1 m/z. The 3-NBA control showed no interfering peaks near 360 m/z. When run with 3-NBA/Li, all previous peaks were still present, and a new peak at 373.1 m/z appeared, indicating the 366.1 m/z parent molecular ion had picked up a lithium ion. A less intense peak at 372 m/z indicates ^{6}Li adducting to the analyte.

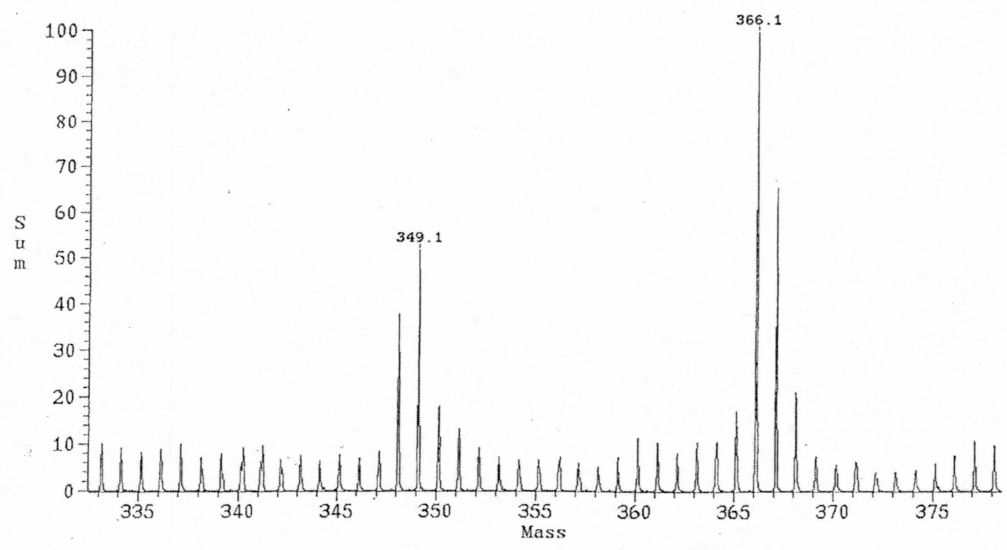

Figure 3: The LRFAB-MS Spectra in a 3-NBA Matrix. The parent molecular ion [M^{+}] is determined at 366.1 m/z with [$M+H^{+}$] at 367.1 m/z. Fragments at 349.1 m/z and 348.1 m/z are determined to be [$M-OH^{+}$] and [$M-H_2O^{+}$], respectively.

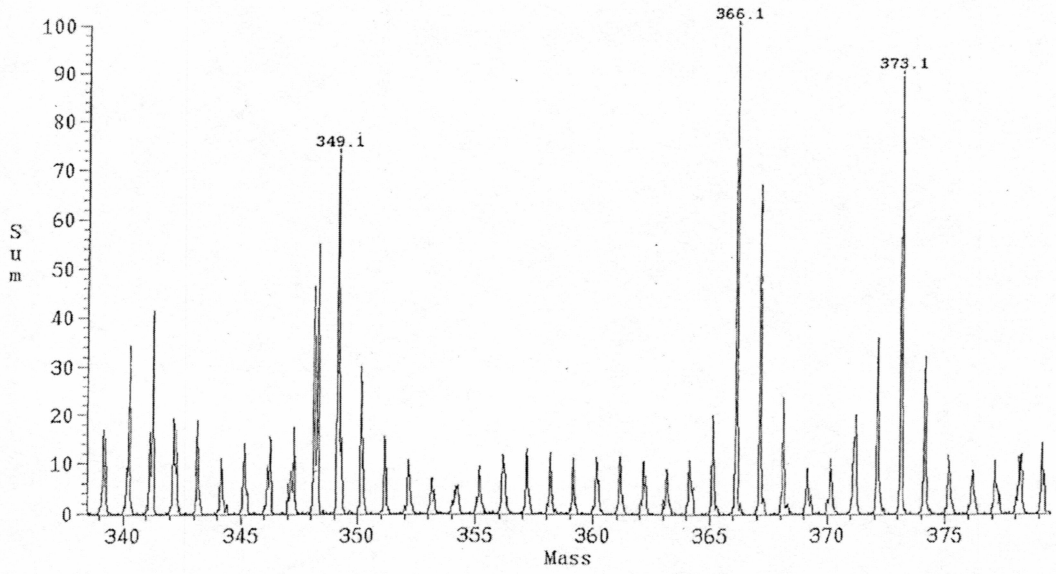

Figure 4: The LRFAB-MS Spectra of 2 in a 3-NBA/Li Matrix. The new peak at 373.1 m/z correspondsto a $[M+Li]^+$ ion. The peak at 372.1 m/z shows ^6Li adducting to the parent molecular ion.

The lack of a shift in the 349.1 m/z peak indicates that it is not the molecular ion, and is most likely the fragmentation product $[M\text{-}OH^+]$. Similarly, the peak of 348.1 m/z is due to an $[M\text{-}H_2O]^+$ fragment. The peak at 366.1 is the parent ion, **2**, and the abnormal isotopic distribution of the parent compound is due to the presence of the protonated cation form $[M+H]^+$ at 367.1[9]. The complex $[M+Li^+]$ forms in the 3-NBA/Li matrix and is shown in peak at 373.1 m/z. The presence of a single lithium atom indicates that **2** has a single, readily exchangable proton. The peak at 372.1 m/z shows the adducting of the ^6Li (natural isotopic abundance of 7.59 %) to the parent molecular ion.

2.1.3. Discussion of Isotope Ratio Mass Spectrometry (IRMS)

Elemental analysis using isotope ratio mass spectrometry (IRMS) was performed in triplicate for percent N and C, and for percent H and O (Table 1). The presence of nonstoichiometric levels of nitrogen indicated the presence of NaCN in the sample which had not been completely removed in the aqueous washes. The presence of the contaminant NaCN was also suggested by the sum of C, N, O, and H being slightly less than 100%, due to the Na present.

Table 1: The IRMS Elemental Analysis for 2. N, C, H, and O are shown. A comparison is made for the adjustment of mean values based on the presence of residual NaCN in the test samples.

Sample #	Sample mass (mg)	Conc. N %	Conc. C %	Conc. H %	Conc. O %
1	0.295 (N, C) 0.198 (H, O)	0.23	77.73	3.89	16.58
2	0.288 (N, C) 0.228 (H, O)	0.22	77.68	3.96	17.55
3	0.294 (N, C) 0.214 (H, O)	0.23	77.99	3.90	16.40
Mean +/- 95% int.	NA	0.23 +/- 0.01	77.80 +/- 0.413	3.92 +/- 0.09	16.84 +/- 1.55
Correction for NaCN	NA	0.00	78.86 +/- 0.405	3.98 +/- 0.11	17.12 +/- 1.56
Theoretical	NA	0.0	78.7	3.85	17.50

The IRMS results were adjusted to account for the presence of NaCN contamination. The average concentration N due to NaCN in the sample was 0.227 %. Correcting for molecular mass differences, the concentrations of C and Na due to NaCN contamination were 0.194 % and 0.372 % respectively. The contaminating C was removed from the total concentration of C, and the values for C, H, and O percent were totaled to 98.366 %. The final values for C, H, and O percent were adjusted for the reduced total mass in the system.

The corrected IRMS results for C, H, and O percent are 78.9 %, 3.98 %, and 17.12 %, respectively. With the molecular weight of 366.1 g/mol demonstrated by LRFAB-MS, the prediction of molecular formula is 24.05 C, 14.57 H, and 3.92 O. The ^{1}H and ^{13}C NMR confirms this prediction, with 24 C and 14 H in the spectra. Degree of unsaturation for the product is 18. This high degree of unsaturation is concurrent with the condensation of NDA, and given the dynamics of the reaction, it is unlikely that the naphthalene functionalities would be modified.

2.1.4. Discussion of Nuclear Magnetic Resonance (NMR) Spectra

Assignments of ^{1}H and ^{13}C NMR resonances are shown in Figure 5. All ^{1}H NMR, and all but two ^{13}C NMR resonances are unambiguous. Points of entry for the analysis were the carbonyl at position 7, the single sp^2 hybridized carbon at position 15, and the hydroxyl functionality. A point by point rationale of all assignments is available in Table A.2 of Appendix A.

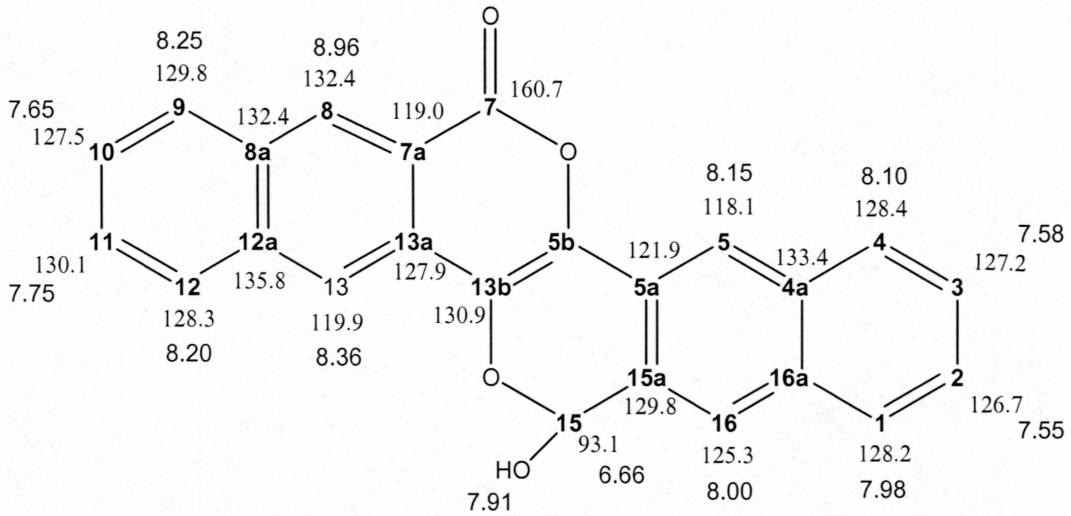

Figure 5: Assignments of ^{1}H and ^{13}C NMR spectra for 2.

The singlet ^{1}H NMR resonance at 8.96 ppm shows the only gHMBC ($^{3}J_{CH}$) coupling to the carbonyl ester, and therefore must be assigned to position H-8. Irradiation of H-8 shows positive NOE correlation to the hydrogen at 8.25 ppm, which is assigned to position H-9. H-10, H-11, and H-12 are all assigned by gCOSY connectivities. Irradiation of the singlet hydrogen at 8.36 ppm shows positive NOE correlation to position H-12, and is assigned to H-13. Carbon assignments to all

identified positions are determined by gHSQC. All relevant gCOSY and NOESY correlations are illustrated in Figure 6.

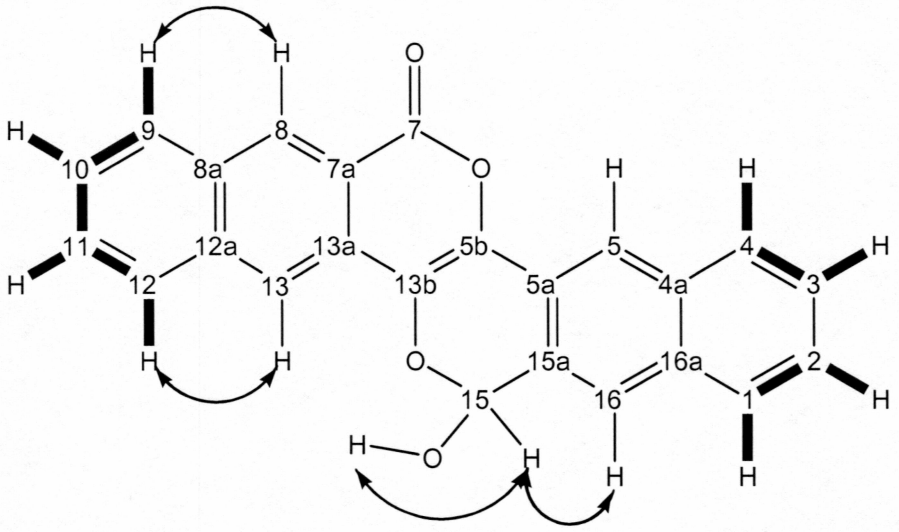

Figure 6: gCOSY and NOE Difference Correlations. The important gCOSY (solid bars) and NOE difference (arrows) correlations obseved for product **2**.

Irradiation of the anomeric hydrogen at position H-15 demonstrates positive NOE correlation to both the hydroxyl hydrogen (H-OH) and the singlet hydrogen at 8.00 ppm, which must be H-16. The final singlet hydrogen (8.15 ppm) is assigned to position H-5. Assignment of H-1 and H-4 are made via gHSQC to adjacent carbons and gHMBC correlations to H-16 and H-5, respectively. Pertinent gHMBC correlations are shown in Figure 7.

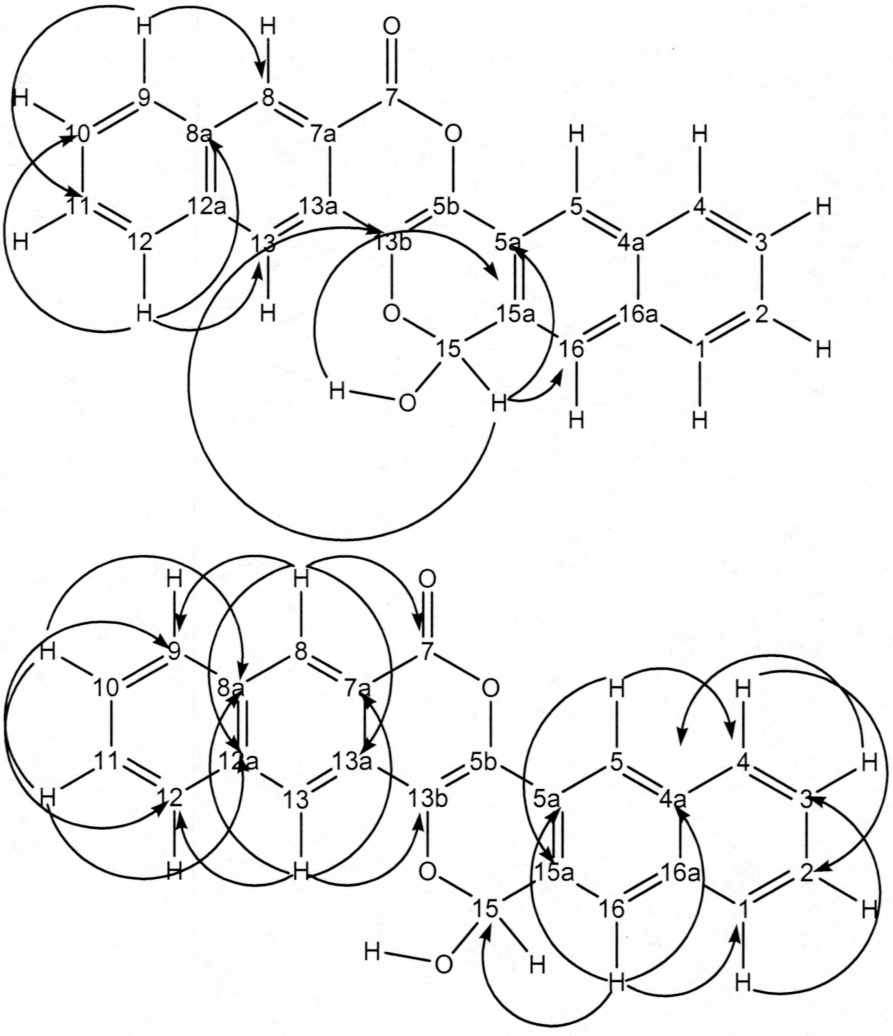

Figure 7: The gHMBC Proof of Structure for Product 2.

Assignments made previously via gCOSY, NOESY, and gHSQC are in agreement with gHMBC observations. Quaternary carbons are easily assigned via multiple gHMBC correlations and descrimination between quaternary and nonquaternary carbons in the ^{13}C NMR spectra. Only C-5b and C-16a are unassigned. Both are seen only by H-5 in the gHMBC spectra, and the chemical shifts are too similar to assign by using model compounds.

2.1.5. Discussion of Possible Mechanisms

The structure of the product demands that an oxidation of NDA takes place. The reaction conducted with the exclusion of air failed to yield **2**, although a slower-forming, competetive condensation was apparently unaffected. Thus, we can propose a viable reaction pathway, shown in Figure 8, which involves (1) cyanide catalyzed air oxidation of NDA to the methyl ester **1a**, (2) cyanide catalyzed benzoin condensation to **1b**, (3) cyclization to a lactone **1c**, (4) enolization to **1d**, and finally formation of the hemiacetal in product **2**. All steps following the oxidation are reversible.

It is important to note that although the cyanide catalyzed oxidation of NDA to the methyl ester **1a** has been shown to be a viable intermediate to the formation of **2**, it is also possible that the benzoin condensation to **1b** proceed via an acyl cyanide intermediate, prior to the formation of the methyl ester. The acyl cyanide, discussed later and illustrated in Scheme 3, would provide a superior leaving group; however, no spectroscopic evidence for the formation of the acyl cyanide has been obtained. It is also possible that an equilibria exists between the acyl cyanide, **1a**, and **2**. The acyl cyanide could form both **1a** and **2**. The **1a** produced would also lead to the formation of **2**, as described.

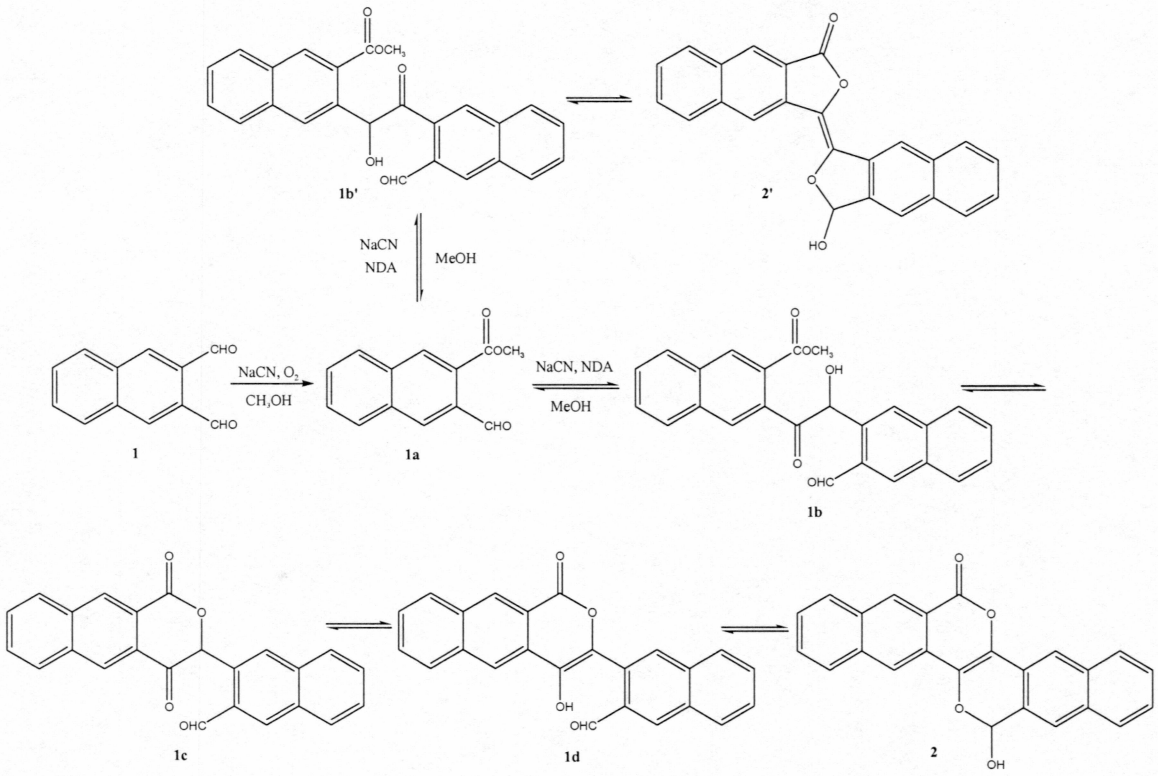

Figure 8: A Proposed Reaction Mechanism for the Formation of 2.

2.1.6. Model Compound Oxidations

No direct spectroscopic evidence for intermediate **1a** has been obtained; however, it has been reported that aromatic aldehydes oxidize to form methyl esters in methanol in the presence of manganese dioxide and cyanide[5]. This oxidation was shown to proceed via oxidation of a cyanohydrin to an acyl cyanide, followed by methyl ester formation. One can envision a similar reaction here, only with atmospheric oxygen as the oxidizing agent, as shown in Figure 9. It is surprising that the oxidation takes place so readily under the mild conditions.

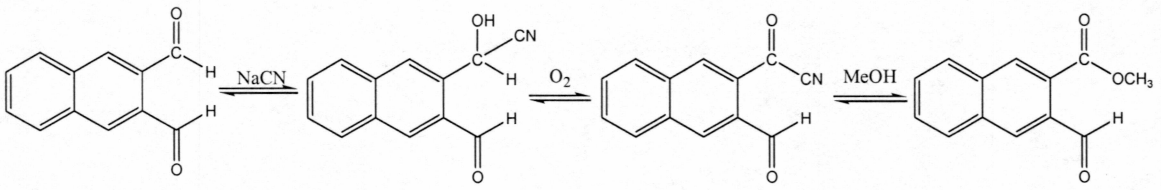

Figure 9: A Possible Mechanism for the Reaction of the Aldehyde to the Methyl Ester. The reaction may proceed from the aldehyde to methyl ester via cyanohydrin and acyl cyanide intermediates. Both the acyl cyanide and the methyl ester could function as leaving groups in a benzoin condensation.

The acyl cyanide would also provide an excellent leaving group for a benzoin condensation; however, no evidence for this hypothesis was obtained. The proposed mechanism for the formation of **2** would be valid via either intermediate, and may proceed through a combination of both.

Under identical reaction conditions to the synthesis of **2**, we found that the model compound, 2-napthaldahyde, yields less than 10% methyl ester formation (by NMR integration) in 1 hour. Notably, most of the conversion to the methyl ester occurred in the solvent removal phase of the synthesis due to the heating of the solution. Color in the reaction mixture appears indicative of product formation. The initial reporting of derivitization of amino groups via NDA reported the formation of a pale yellow color in the solution prior to the addition of the amino acid[1]. The addition of cyanide to the methanolic solution of NDA results in the immediate development of a yellow color prior to the precipitation of **2** from methanol. Prior to heating, no change in the reaction mixture's color was observed; however, immediately upon increasing the temperature a

yellow color developed. The true yield is likely much lower than the value calculated following solvent removal. The low degree of oxidation in the model compound suggests that only aldehydes activated by electron donating groups and conjugation, such as NDA, are efficiently air oxidized to methyl esters in the abbreviated time frame of this reaction.

In support of this hypothesis, we found that both acetylbenzaldehyde and terepthaldehyde were converted to methyl 4- acetyl benzoate and dimethyl terepthalate, respectively, in less than 20 minutes at room temperature in a methanolic solution of NaCN and atmospheric O_2. A summary of the model compounds' methyl ester formation is shown in Figure 10. Both reactions demonstrated immediate change in color upon the addition of the cyanide catalyst at room temperature. The low yield for the formation of dimethyl terepthalate is due to multiple benzoine condensations between terepthaldehyde molecules, resulting in aqueous soluble side products. No evidence of terepthaldehyde was present in the side product's NMR. The ^1H NMR of both $CDCl_3$ soluble products clearly show the presence of the methyl ester and very low (less than 5%) levels of aldehyde. The reaction of the activated aldehyde to methyl ester via air oxidation of a cyanohydrin is clearly a plausible mechanism.

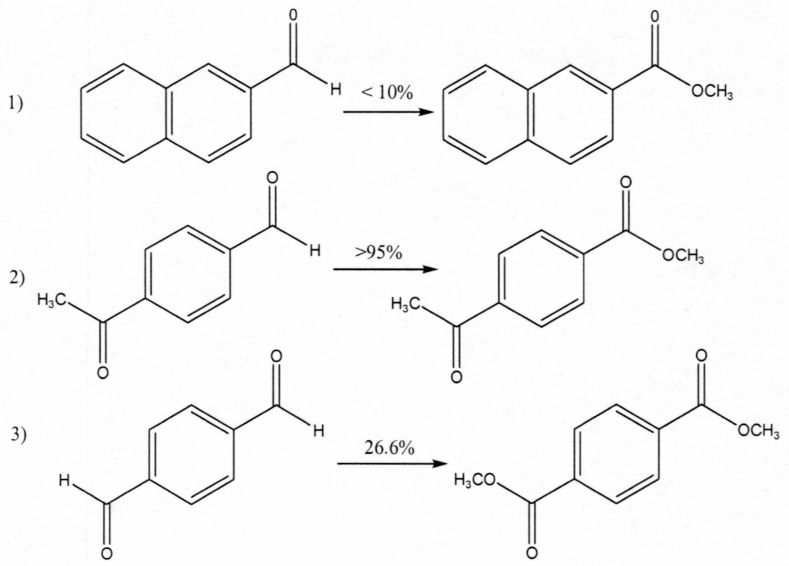

Figure 10: Yields of Conversion of Model Compounds to Methyl Esters. Model compounds 1) 2-napthaldehyde, 2) acetylbenzaldehyde, 3) terepthaldehyde, and corresponding yields of methyl ester derivatives.

2.1.7. Discussion of Alternative Benzoin Condensation Products

All of the steps in the proposed mechanism for the formation of **2** are reversible except the oxidation and subsequent methyl ester formation. Thus **2'** (Figure 8**)** could hypothetically form due the alternative benzoin intermediate **1b'**, with a similar reaction pathway as proposed for **2**. Products **2** and **2'** would be difficult to distinguish by ^{13}C and ^{1}H spectra alone, according to ACD NMR predictive software[11]. However, the gHMBC spectrum of the isolated product reveals a three bond coupling ($^{3}J_{CH}$) between C-13b (131.5 ppm) and both H-13 (8.36 ppm) and H-15 (6.66 ppm), shown in Figure 11.

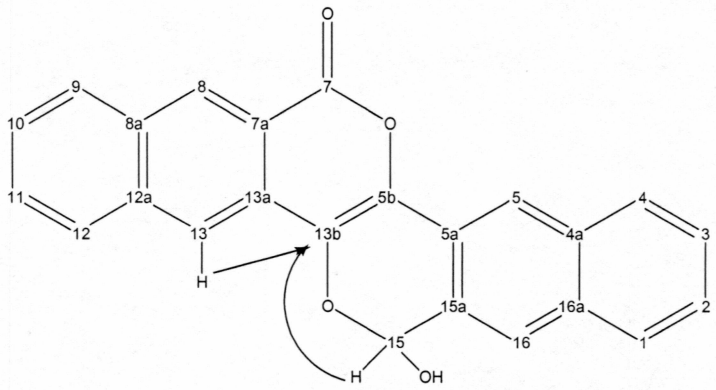

Figure 11: gHMBC Correlation Proving the Structure of 2. The illustrated correlations refute the alternative benzoin product **2'**.

There is no carbon in **2'** that would show a $^{3}J_{CH}$ gHMBC correlation with both of the hydrogen atoms. Additionally, AM1 calculations yield a heat of formation of -46.3 kcal/mol for **2** and – 30.9 kcal/mol (trans) and -26.8 kcal/mol (cis) for **2'**. Due to the reversibility of the benzoin mechanism, **2** is highly favored under equilibrating conditions.

2.2. Identification of Acetal Derivatives

Product **2** is quantitatively converted to acetals **3a** and **3b** via reflux in R-OH with an acid catalyst. Both products are isolated in high yield by cooling, centrifugation, and multiple washes with cold water. The NMR analyses of **3a** and **3b** are straight forward and can be accomplished without the use of ^{13}C or 2-D NMR techniques. Comparison of **3a** to **2** shows the lack of a hydroxyl H at 6.90, and H-15 shifts from 6.66 to 6.54. The methoxy ester shows a clear singlet at 3.64 which integrates for three hydrogens. **3b** also shows a lack of a hydroxyl hydrogen at 6.90, and H-15 shifts from 6.66 to 6.41. The

isopropyl acetal shows a septet centered at 4.5 which integrates for one hydrogen and two doublets (1.2 and 1.4 ppm) which integrate for three hydrogen each. Difference in the chemical shift in the aromatic region are small and, in the case of **3b,** partially due to the use of d-chloroform versus DMSO-d_6.

The formation of the acetal dramatically reduces solubility in DMSO and increases solubility in chloroform. The advantages in working microscale are clear: the formation of the acetal only nominally decreases the overall yield while allowing for NMR in a recoverable solvent. Further advantages include superior separation of ^{1}H NMR resonances in the aromatic region. Removal of the hydroxyl hydrogen at 6.90 also deconvolutes the aromatic region of the ^{1}H NMR.

2.3. Attempted Oxidation of the Hemiacetal

The hemiacetal functionality on **2** should be easily oxidized to a carboxylic ester, producing a symmetric isocoumarin with extended conjugation, as shown in Figure 12. NMR spectra of the resulting product would be significantly less complicated than **2**, due to the symmetry, and provide an excellent proof of structure of **2**. All carbons would posses sp^2 hybridization, and potentially demonstrate strong fluorescent properties.

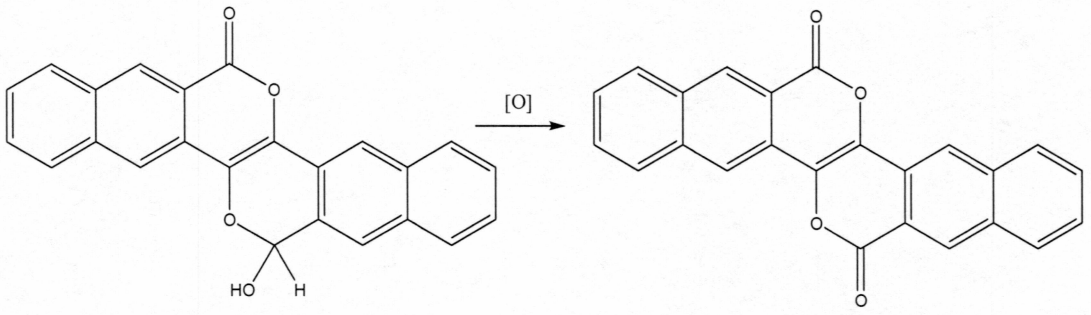

Figure 12: The Attempted Oxidation of 2 at the Hemiacetal. The symmetric isocoumarin should be formed by the selective oxidation of the hemiacetal to the carboxylic ester.

Two oxidative methods were applied: oxidation via NaOCl (aq) and oxidation by pyridinium chlorochromate (PCC) in dichloromethane. Neither method produced the isocoumarin, but both yielded unexpected products which demonstrated the reversibility in the mechanism of **2** and the reactivity of the activated π bond located between positions 13b and 5b.

2.3.1. Product of Sodium Hypochlorite Oxidation: 3-(3-chloro-1,4-dioxo-3,4-dihydro-1H-benzo[g]isochromen-3-yl)-2-napthaldahyde

The attempted sodium hypochlorite oxidation of **2**, yielded a unique white crystalline product which we have identified as 3-(3-chloro-1,4-dioxo-3,4-dihydro-1H-benzo[g]isochromen-3-yl)-2-napthaldahyde (**4**). The product separates within 5 minutes from the 50% aqueous acetone solvent in high yield. Essentially, **4** is the reversible, lactone intermediate **1c**, capturing a hypochlorite cation at the 3 position of the isochromenyl group. The structure of **4** is confirmed by IR spectrum, mass spectrum, elemental analysis, and NMR spectra including ^{1}H, ^{13}C, gCOSY, gHSQC, gHMBC, and NOESY spectra. All assignments but two ^{13}C resonances have been made.

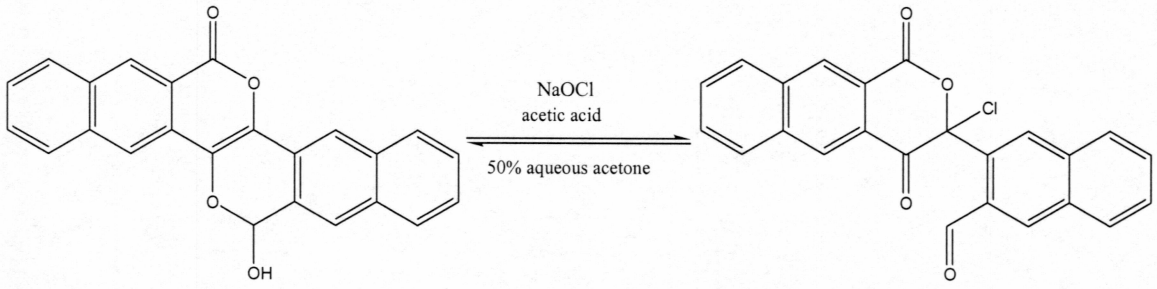

Figure 13: The Reaction of Product 2 to Product 4. Product **2** is converted to **4** in a ring opening recation with NaOCl (aq) and acetic acid catalyst inn a 50% aqueous acetone solution.

2.3.2. Discussion of Infrared Spectrum (IR) Results

IR (KBr) spectral analysis of **4** shows a few notable differences from the IR of **2**. Absorbencies at 1751, 1716, 1684 cm^{-1} (Figure 14) , are likely representative of the carboxylic ester, ketone and aromatic aldehyde functionalities, respectively[7,8]. The medium absorbancies at 2750 cm^{-1} and 1410 cm^{-1}, not present in IR of **2**, are also characteristic of aromatic aldehydes. The broad absorbance at 3450 cm^{-1} indicates either the presence of an alcohol, due to minor contamination of the sample, or the presence of water. Comparison of the IR spectra to that of **2** shows a substantial reduction in relative intensities between the alcohol and carboxylic ester absorptions.

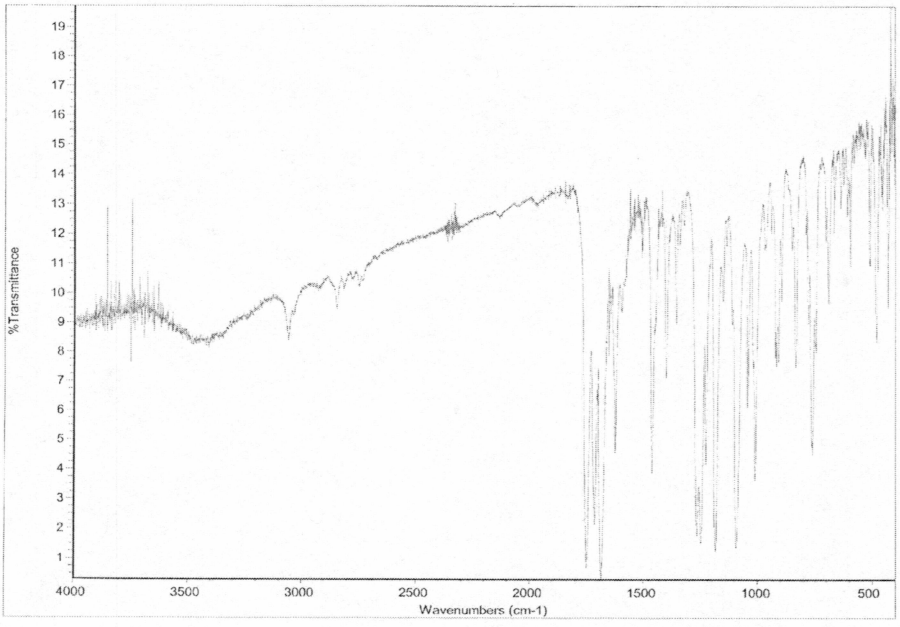

Figure 14: The IR (KBr) Spectrum of Product 4. The spectrum indicates small levels of either starting material or water, evident by the weak, broad absorption at 3450 cm^{-1}.

2.3.3. Discussion of Electrospray Ionization Mass Spectrometry (ESI-MS) Spectra

The LRFAB-MS of **4** was of low quality, so electrospray ionization mass spectrometry (ESI-MS) of **4** was performed by spraying the sample in $CHCl_3$/MeOH at a concentration of approximately 100μM. Results are shown in Figure 15. No absorption was verified at the expected $[M+H]^+$ ion m/z of 401.5. However, an intense absorption occurred at m/z of 365.08, which represents the loss of HCl from the protonated molecular ion. A smaller absorption can also be seen at 366.08, which simply represents the loss of Cl from the protonated parent molecule. These findings confirm the presence of chlorine in **4**, and suggests a molecular weight of 400.58, a clear agreement with the theoretical molecular weight.

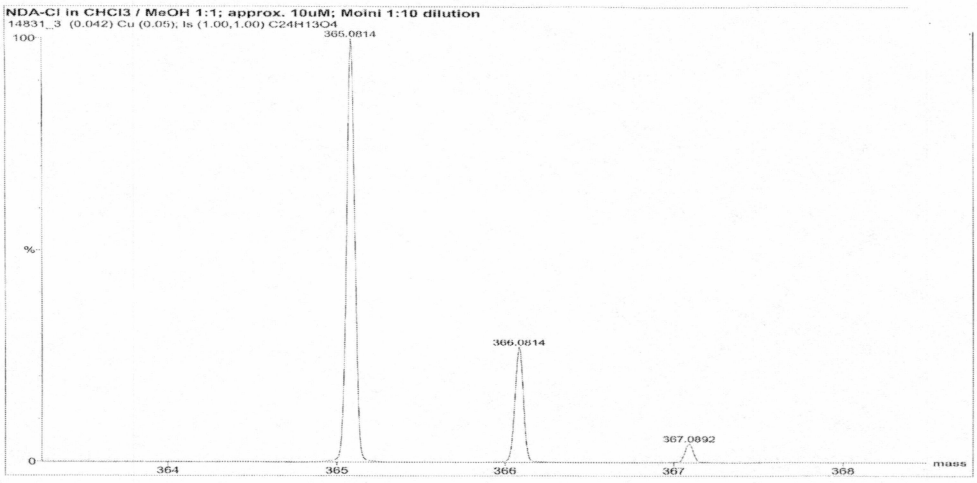

Figure 15: ESI-MS Analysis of Product 2. The parent molecular ion was not present, but $[M-HCl]^+$ is present as m/z of 366.08, predicting a mass of 400.58 for the parent molecule.

2.3.4. Discussion of Isotope Ratio Mass Spectrometry (IRMS)

Elemental analyses in the form of IRMS were performed in triplicate for percent N and C, and for percent H and O (Table 2). No N was detected. The mean total percent accounted for by C, H, and O was 70.7 %, 3.6 %, and 17.2 %, respectively. The unaccounted 8.5 % is due to the presence of the Cl atom, as shown by the ESI-MS analysis. The slight discrepancies between calculated and theoretical percent mass is likely due to the capture of the solvent, water, in the crystalline product. The presence of water in the crystal lattice would result in the decrease in concentration of C and Cl and the increase in concentration of H and O, relative to the theoretical values.

Table 2: The IRMS Elemental Analysis of 4. Measured mean percent concentration of C, H, and O, and implied mean percent concentration Cl are showm. Comparison of theoretical values to measured values are made.

Sample #	Sample mass (mg)	Conc. N %	Conc. C %	Conc. H %	Conc. O %	Conc. Cl % by Δ
1	0.146 (N,C) 0.166 (H,O)	0.0	71.2	3.59	16.83	8.38
2	0.163 (N,C) 0.125 (H,O)	0.0	70.9	3.61	17.49	8.0
3	0.122 (N,C) 0.124 (H,O)	0.0	70.1	3.6	17.33	8.97
Mean +/- 95%	N/A	0.0	70.7 +/- 1.4	3.60 +/- 0.03	17.22 +/- 0.70	8.45 +/- 1.21
theoretical	N/A	0.0	71.9	3.20	16.00	8.90

2.3.5. Discussion of Nuclear Magnetic Resonance (NMR) Spectra

Assignments for H and C resonances of **4** are shown in Figure 16. All ^{1}H NMR, and all but two ^{13}C NMR resonances are unambiguously assigned. Points of entry for the analysis were the carbonyl ester on position 1', the ketone on position 4', and the aldehyde on position 2. The carbon assignments for positions 7' and 8' are ambiguous. The overlap in both ^{1}H and ^{13}C spectra, and the lack of good gCOSY in the region, made definitive assignment impossible.

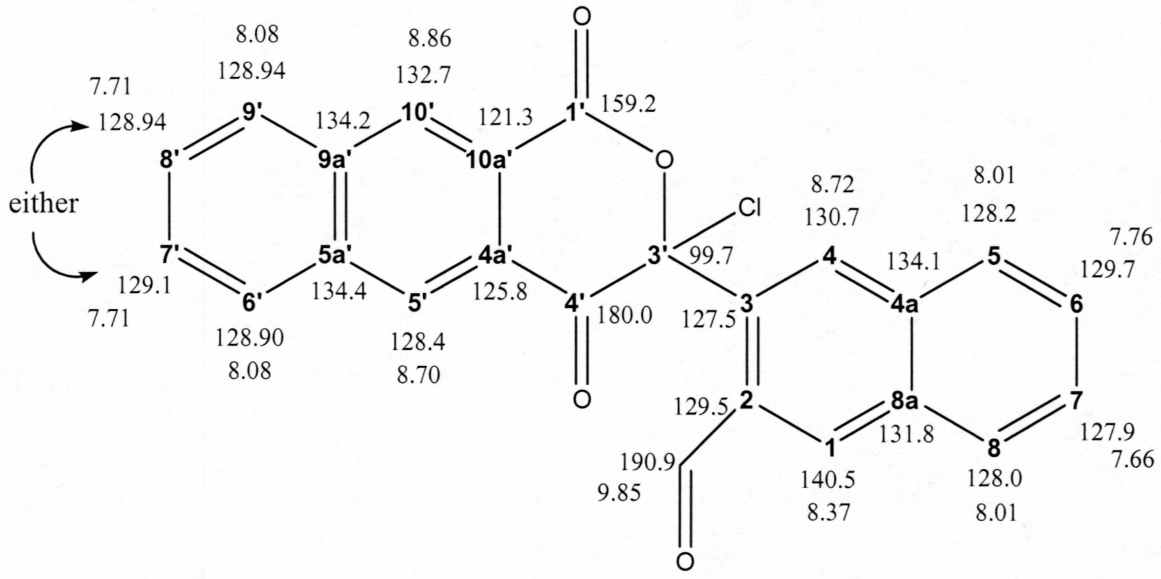

Figure 16: The Assignments for H and C NMR Spectra for Product 4.

The gCOSY spectra provided little usable data for the proof of structure. The low intensity of the correlations in the naphthyl rings were difficult to discern from noise and long-range effects. The chemical assignments for **4** were made predominantly with the

use of gHMBC and gHSQC spectra. Quaternary carbons were determined by ^{13}C, and two correlations in the NOE difference spectra contributed to the solution.

Irradiation of H-1 (s, 8.37 ppm) showed positive NOE correlations to the aldehydic hydrogen (H-A) and H-8 (8.01 ppm). The NOESY and gHMBC connectivities are illustrated in Figure 17. All assigments on the naphthaldehyde group were made based on redundant gHMBC couplings, gHSQC, and process of elimination, recognizing quaternary versus nonquaternary carbons. H-A show a $^{2}J_{CH}$ coupling to C-2 via the gHMBC. The unusually short coupling appears as a doublet in the 2-D spectrum. The effect is unobscured by interfering resonances and cannot be confused for multiple correlations. H-4 shows the only coupling to the chlorinated carbon, C-3', evident by its unique chemical shift. It is important to recognize the presence of two hydrogens at 8.01 ppm, located at H-5 and H-8. The assignment of H-6 was made by gHMBC couplings to C-4a and C-8.

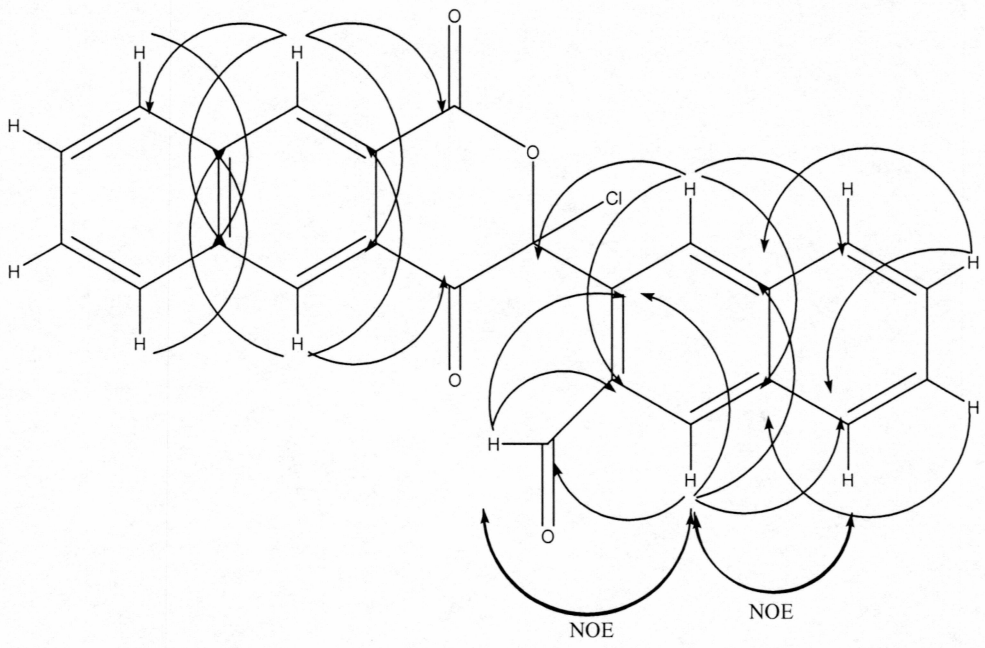

Figure 17: The gHMBC and NOE Proof of Structure for Product 4. The relevant gHMBC (one sided arrows)and NOE difference (two sided arrows) correlations used in the proof of structure for product **4** are shown. The gHSQC correlations are implicit in all observed C-H bonds.

H-5' was identified by its gHMBC correlation to the ketone, and H-10' by its correlation to the ester. H-6' and H-9' both have chemical shifts of 8.08 ppm. The assignment of H-9' was made by by gHSQC to C-9'. H-9' and H-10' share a common $^{3}J_{CH}$ coupling to the quaternary carbon, C-5a', and H-10' also shows a coupling to C-9', as shown in Figure 14. Assignment of H-6' is analogous, but the assignment of C-6' is made by default in the gHSQC spectra, due to the lack of a coupling from H-5'.

Positions H-7' and H-8' both exhibit chemical shifts of 7.71 ppm. Both C-8' and C-9' have chemical shifts of 128.937 ppm. The degree of overlap in the NMR spectra

makes the assignment of positions 7' and 8' ambiguous. The lack of assignment does not affect the determination of structure for product **4**.

2.3.6. Discussion of Possible Mechanisms

The mechanism for the formation of **4** can be viewed from two perspectives: 1) as the donation of **2**'s activated π bond electrons to a hypochlorite cation, resulting in ring opening and the formation of an aldehyde, or 2) product **2** is solvent-driven to its enolate form which is captured by hypochlorous acid. Both scenarios are illustrated in Figures 18 and 19.

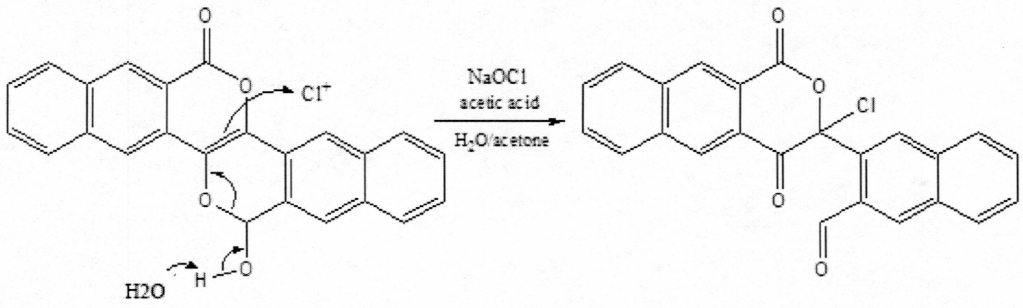

Figure 18: An Elementary Mechanism for the Reaction of Product 2 to Product 4. The π bond is activated by dual adjacent electron donating groups and conjugation. The strong electrophile, hypochlorite (essentially chlorine cation), attacks the π system, causing subsequent ring opening and the formation of the aldehyde in product **4**. The reaction is acid catalyzed.

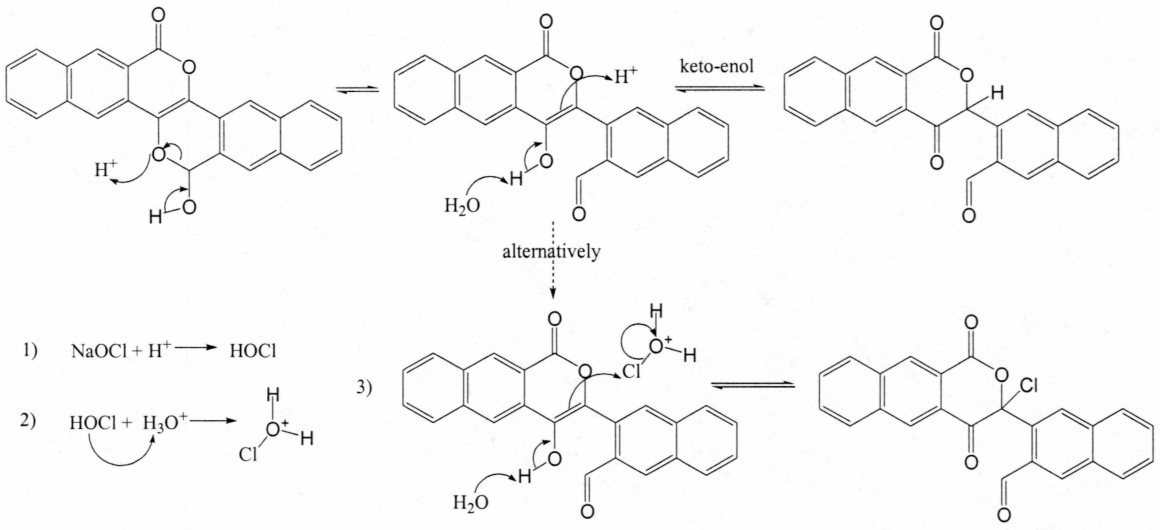

Figure 19: The Halogenation of 2 at the α Position via an Enolate Intermediated. It is important to note that NaOCl reacts with the acetic acid catalyst, forming hypoclorous acid, HOCl. HOCl provides the source of chlorine cation which out competes protons for the α position of the enolate.

The formation of **4**, opposed to the isocoumarin, is a surprising result which can be attributed primarily to two factors. **2** did not demonstrate good solubility in the solvent system. The enol form of **2** exhibits solubility in polar solvents superior to that of **2**. This is demonstrated during the synthesis of **2**, because the enol form remains soluble in methanol, while **2** precipitates rapidly. The aqueous/acetone mixture would favor the enol form due to solvent polarity, eliminating the secondary alcohol (position 15) as a target for oxidation. Secondly, the π electrons located between position 13b and 5b are high activated by adjacent electron donating groups and extended conjugation. This position is therefore extremely reactive to strong electrophiles such as hypochlorite, and may present a target more desirable than the secondary alcohol.

2.3.7. Product of Pyridinium Chlorochromate Oxidation: naptho[2,3-c]furan-1,3-dione

2 was treated with 2 equivalents PCC in dichloromethane under mild conditions for 96 hours. PCC is commonly used as an oxidant of primary alcohols which selectively reacts them to aldehyde form without the formation of the carboxylic acid. The combination of a favorable solvent, a targeted oxidant, and a product exhibiting extended conjugation to drive the reaction seemed a probable formula for the synthesis of the isocoumarin. No evidence for any production of the isocoumarin was obtained following analysis of the column fractions. The primary products were unreacted **2** and what appears to be naptho[2,3-c]furan-1,3-dione (**5**), the anhydride of 2,3-naphthalenedicarboxilic acid, shown as the product in Figure 20.

Due to the small scale, no ^{13}C or 2-D NMR is available; however, numerous points indicate the proposed structure. The H-NMR is highly symmetric, with a singlet and two multiplets in the aromatic region. The reagents used would leave the naphthalene rings intact, which would immediately account for the observed peaks. Formation of the diacid would provide the symmetry in the aromatic region but would also show the carboxylic hydrogen. The only probable functionalities at the 2 and 3 positions which would not add resonances to the spectrum would be the anhydride. H-NMR spectra of **5** also shows excellent agreement with ACD modeling predictions for chemical shift and coupling constants in the multiplets.

2.3.8. Discussion of Possible Mechanism

The formation of **5** is also supported by a realistic mechanism involving multiple oxidations by PCC in the presence of water, as shown in Figure 20. The combination of the stated obsevations shows naptho[2,3-c]furan-1,3-dione (**5**) to be the clear product.

The expected isocoumarin was probably not obtained due to the water contamination. PCC is commonly used to selectively oxidize secondary alcohols to ketones and primary alcohols to aldehydes without the formation of carboxylic acids. This specialization is a function of the solvent system, usually dichloromethane. The hydrate functionality is the source of the second oxygen in the carboxylic acid, and although PCC is a very strong oxidizing agent, the exclusion of water prevents hydrate formation. In the synthesis of **5,** the solvent was not dried appropriately, and contained enough water to make the formation of hydrates viable.

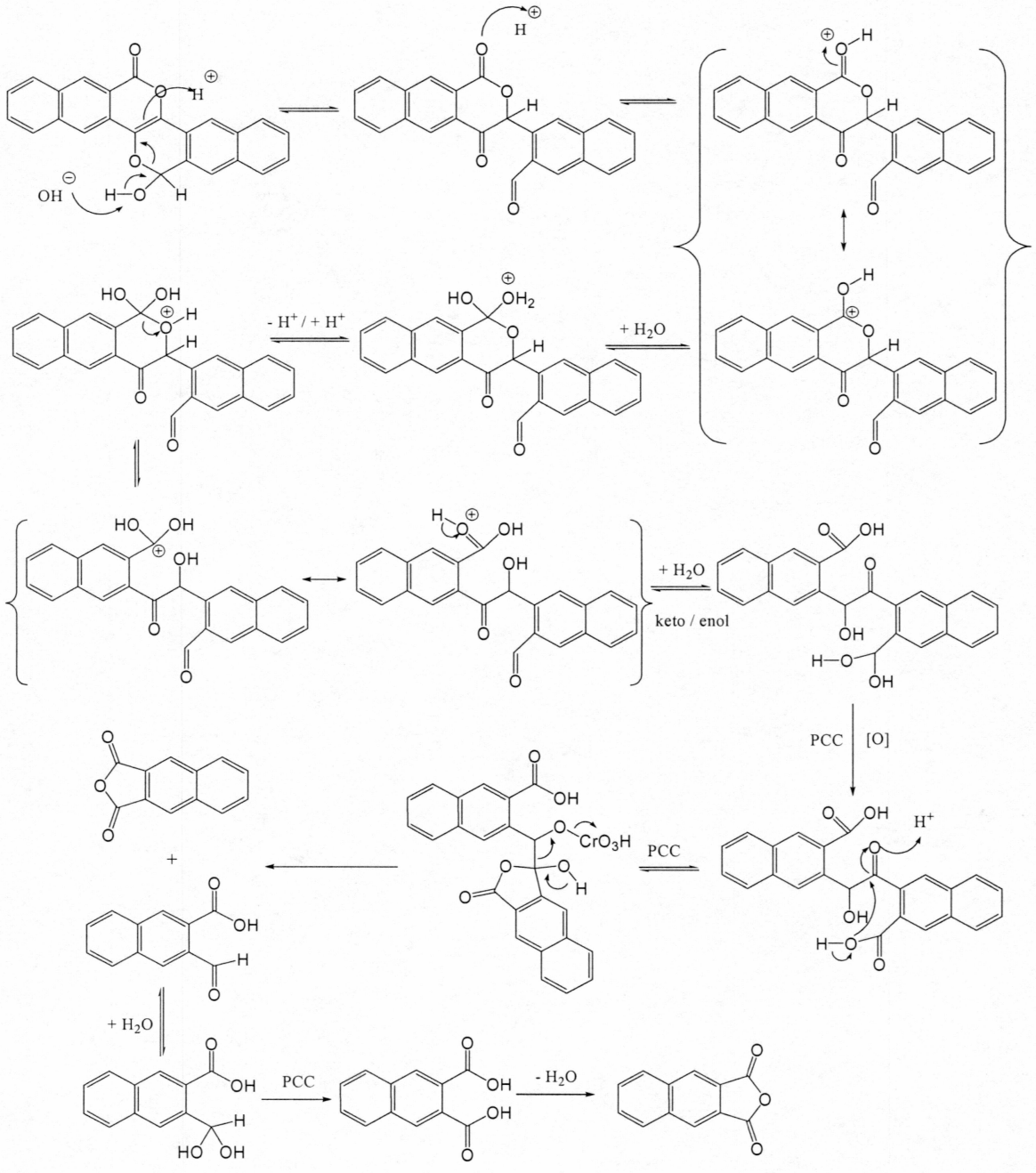

Figure 20: The Proposed Mechanism for the Formation of Product 5. Two units of **5** are formed a reverse Fischer esterification of **2**, PCC oxidation of the hydrate, cleavage via a PCC leaving group, further oxidation, and anhydride formation.

Two equivalents of PCC were used in the reaction, based on the single alcohol functionality present in **2**. Despite the extended reaction time (4 days), significant amounts of **2** were unreacted. This was a result of the multiple PCC oxidations in the formation of **5**. What was thought to be two equivalents was more likely half an equivalent, based on the mechanism proposed in Figure 20. Following the biphase separation, only low levels of side products were evident in H NMR of the unseparated product.

2.4. Competitive Non-Oxidized Condensation of NDA

The synthesis of **2** is complicated by a slower-forming, competitive condensation reaction of NDA which occurs without an oxidation step. If the reaction is allowed to proceed beyond 10 minutes, significant contamination occurs due to the precipitation of the slower forming product. This contaminant can be easily isolated by column chromatography, as described in the Experimental section. Due to the small scale, only ^{1}H-NMR was obtained, and is shown in the Supplementary section.

The non-oxidized condensation product can also be directly synthesized by attempting the synthesis of **2** in the absence of O_2 (g). The contaminant obtained by direct synthesis is structurally different than the contaminant isolated chromatographically. Upon addition to chloroform, the product isomerizes completely to its recognizable form within 30 minutes. This structural isomer is identical to the product recovered by column chromatography. Minor spectroscopic differences occur between the two due to the different solvents. The column product, analyzed in DMSO-d_6, separation of H singlets at 7.42 and 7.62 ppm. The same H in $CDCl_3$ overlap at 7.58 ppm. Although there are small differences in shift, the splitting patterns for the multiplets and the relative orientation identify a common product.

Due to the small quantities obtained, no positive identification has been made for the contaminant. There are likely several more unresolved condensations of NDA which take place online, competing with amino groups during derivitization.

3.0. Experimental Section

3.1. Synthesis of 15-hydroxybenzo[g]benzo [6,7]isochromeno[4,3-c]isochromen-7(15H)-one (**2**)

NDA (35 mg, 0.22mmol) was dissolved in 3.8 mL dry methanol. NaCN (12.3 mg, 0.25 mmol) was added and the solution was sonicated or stirred to vortex for 10 minutes in an open reaction vessel. A yellow precipitate began to crystallize within 5 minutes. The solution was cooled for 10 minutes in an ice bath, centrifuged, and supernatant decanted. The precipitate was washed twice with cold water to remove excess sodium cyanide. The product was dried under vacuum and identified as 6-hydroxybenzo[g]benzo-[5,6]indeno[1,2-c]isochromen-14(6H)-one **(2)**. 29.5%, mp 287-289, IR (KBr): 3439 (OH), 1725 (doublet, O-C=O), 1624, 1279, 1155. ^{1}H NMR (300 MHz, DMSO-d_6): δ (ppm) 8.96 (s, 1H, H-8), 8.36 (s, 1H, H-13), 8.25 (d, 1H, 8.3 Hz, H-9), 8.20 (d, 1H, 8.3 Hz, H-12), 8.15 (s, 1H, H-5), 8.10 (dd, 1H, 8.3 Hz, 1.3 Hz, H-4), 8.00 (s, 1H, H-16), 7.98 (dd, 1H, 8.3 Hz, 1.3 Hz, H-1), 7.91 (d, 1H, 6.9 Hz, OH), 7.75 (ddt, 1H, 8.3 Hz, 7.0 Hz, 1.3 Hz, H-11), 7.65 (ddt, 1H, 8.3 Hz, 7.0 Hz, 1.3 Hz, H-10), 7.58 (ddt, 1H, 8.3 Hz, 7.0 Hz, 1.3 Hz, H-3), 7.55 (ddt, 1H, 8.3 Hz, 7.0 Hz, 1.3 Hz, H-2), 6.66d, 1H, 6.9 Hz, H-15); ^{13}C NMR (75 MHz, DMSO-d_6): δ (ppm) 160.7 (C-7), 135.8 (C-12a), 133.8, 132.7 (C-5b, C-16a), 133.4 (C-4a), 133.1 (C-8), 132.4 (C-8a), 130.9 (C-13b), 130.1 (c-11), 129.8 (C-9), 129.83 (C-15a), 128.5 (C-13a), 128.4 (C-4), 128.3 (C-12), 128.2 (C-1), 127.5 (C-10), 127.2 (C-3), 126.7 (C-2), 125.3 (C-16), 121.9 (C-5a), 119.9 (C-13), 119.0 (C-7a), 118.1 (C-5), 93.1 (C-15). gCOSY, gHMBC, gHSQC, and NOESY spectra are available

in the Supporting Information. Mass Spectrometry; LRFAB (3-NBA) m/z 349.1 (M^+-OH), 366.1 (M^+) (3-NBA-Li) 373.1 (M^++Li) Anal. Calcd for $C_{24}H_{14}O_4$: C, 78.7; H, 3.85; O, 17.5. Found C, 77.8; H, 3.92; O, 16.8.

3.2. Methyl Ester Synthesis **(3a)**

2 (8.0mg, 0.022mmol) was dissolved in 3mL methanol and 40 μL HCl was added. The reaction was refluxed for 1 hour and cooled to 0^0 C. The precipitate was centrifuged , washed with cold water, dried and analyzed without further purification. 90% mp 220-222 ^{1}H NMR (DMSO-d_6): δ (ppm) 9.02 (s, 1H, H-8), 8.52 (s, 1H, H-13), 8.29 (d, 1H, H-9), 8.26 (d, 1H, H-12), 8.23 (s, 1H, H-5), 8.16 (d, 1H, H-4), 8.11 (s, 1H, H-16), 8.03 (d, 1H, H-1), 7.78 (dt, 1H, H-11), 7.70 (dt, 1H, H-10), 7.63 (dt, 1H, H-3), 7.59 (dt, 1H, H-2), 6.54 (s, 1H, H-15), 3.64 (s, 3H, OCH_3).

3.3. Isopropyl Ester Synthesis (**3b)**

2 (5 mg, 0.014 mmol) was dissolved in 1 mL isopropanol and 3 drops of 6N HCl was added. The reaction was refluxed for 10 minutes and cooled to 0^0 C. The precipitate was centrifuged, washed with cold water, dried and analyzed without further purification. 85%, mp 208-210, ^{1}H NMR ($CDCl_3$): δ (ppm) 8.93 (s,1H, H-8), 8.25 (s, 1H, H-13 or H-5), 8.23 (s, 1H, H-13 or H-5), 8.00 (d, 1H, H-9), 7.97 (d, 1H, H-12), 7.88 (d, 1H, H-4), 7.81 (d, 1H, H-1), 7.74 (s, 1H), 7.63 (dt, 1H, H-11), 7.53 (dt, 1H, H-10), 7.48 (dt, 1H, H-3), 7.44 (dt, 1H, H-2), 6.41 (s, 1H, H-15), 4.48 (sept, 1H, isopropyl H), 1.39 (d, 3H, isopropyl methyl), 1.21 (d, 3H, isopropyl methyl).

3.4. Conversion of 2-napthaldehyde to methyl 2-napthoate

2-napthaldehyde (35.5 mg, 0.2275 mmol) was added to 4.55 mL dry methanol. NaCN (11.2 mg, 0.2275 mmol) was added and the solution was sonicated or stirred to vortex at room temperature for 1 hour 15 minutes. No visible change in reaction composition occurred. Methanol was removed by rotovaporization. The heating and concentration of the reagents initiated formation of the product, indicated by the darkening of the solution and color change. A biphase separation was performed in equal parts methylene chloride and water. The organic phase was treated with anhydrous Na_2SO_4 (s), separated via centrifugation and the solvent removed by rotovaporization. Percent yield was only 6.7 % by NMR integration. Analytical resonances ^{1}H NMR ($CDCl_3$): δ (ppm) 10.068 (s, 2-naphthaldehyde aldehydic H), 3.895 (s, methyl 2-napthoate methoxy H)

3.5. Conversion of acetylbenzaldehyde to methyl 4-acetylbenzoate

Acetylbenzaldehyde (49.2 mg, 0.3324 mmol) was added to 6.65 mL dry methanol. NaCN (16.3 mg, 0.3324 mmol) was added and the solution reacted by sonication or stirring to vortex at room temperature for 15 minutes. Upon addition of NaCN, the reaction mixture immediately turned a dark yellow. In the absence of mixing, a brown color forms which reverts to yellow when mixing is recommenced. Methanol was removed by rotovaporization, and a biphasic separation was performed in equal parts methylene chloride and water. The organic phase was treated with anhydrous Na_2SO_4 (s), separated via centrifugation and the solvent removed by rotovaporization. ^{1}H-NMR was performed in $CDCl_3$. Yield 4-acetyl benzoate is 86.7 %. The reaction to methyl

ester appears quantitative by NMR. ^{1}H NMR ($CDCl_3$): δ (ppm) 8.04 (d, 2H, benzo-ester side), 7.95 (d, 2H, benzo-acyl side), 3.878 (s, 3H, methyl ester), 2.572 (s, 3H, acyl methyl)

3.6. Conversion of terepthaldehyde to dimethyl terepthalate

Terepthaldehyde (248.7 mg, 1.85 mmol) was added to 37.1 mL dry methanol. NaCN (90.65 mg) was added and the solution reacted by sonication or stirring to vortex at room temperature for 15 minutes. Upon addition of NaCN, the reaction mixture developed a dark red color, which proved temperature dependent. The product remained highly soluble in methanol. Methanol was removed by rotovaporization, and a biphasic separation was performed with equal parts methylene chloride and water. The organic phase was treated with anhydrous Na_2SO_4 (s), separated via centrifugation and the solvent removed by rotovaporization. Significant side reactions between aldehydes produced water soluble contaminants. Only 66.1 mg (26.6%) material was retained in the organic phase. ^{1}H NMR ($CDCl_3$): δ (ppm) 8.031 (s, 4H, benzo), 3.878 (s, 6H, methoxy ester)

3.7. Synthesis of 3-(3-chloro-1,4dioxo-3,4-dihydro-1H-benzo[g] isochromen-3-yl)-2-napthaldahyde **(4)**

15 mL (50/50) acetone and water solution was prepared. 100 μL glacial acetic acid catalyst was added followed by 1.00 mL 5.25% NaOCl (aq). **2** (15.0 mg) was added with moderate stirring for 10 minutes. The reaction proceeds visibly in the first few minutes;

the reduction in conjugation causes the color to change from yellow to white. The mixture is cooled on ice for 15 minutes, centrifuged and separated, and washed twice with cold water. Yield is 88.0 %. IR (KBr): 1751, 1716, 1684, 1267, 1250, 1185, 1095. ^{1}H NMR (300 MHz, $CDCl_3$): δ (ppm) 9.85 (s, 1H, H-CHO), 8.86 (s, 1H, H-10'), 8.71 (s, 1H, H-4), 8.69 (s, 1H, H-5'), 8.37 (s, 1H, H-1), 8.08 (dd, 1H, H-6'), 8.08 (dd, 1H, H-9'), 8.01 (d, 1H, 8.8 Hz, H-5), 8.01 (d, 1H, 8.8 Hz, H-8), 7.76 (ddt, 1H, C-6), 7.71 (ddt, 1H, H-7'), 7.71 (ddt, 1H, H-8'), 7.66 (ddt, 1H, H-7); ^{13}C NMR (75 MHz, CD_2Cl_2): δ (ppm) 190.917 (C-CHO), 180.012 (C-4'), 159.189 (C-1'), 140.495 (C-1), 134.435 (C-5a'), 134.234 (C-9a'), 134.071 (C-4a), 132.671 (C-10'), 131.825 (C-8a), 130.725 (C-4), 129.670 (C-6), 129.453 (C-2), 129.104 (C-7'), 128.937 (C-8' or 9'), 128.937 (C-8' or 9'), 128.900 (C-6'), 128.421 (C-5'), 128.152 (C-5), 128.027 (C-8), 127.932 (C-7), 127.465 (C-3), 128.849 (C-4a'), 121.269 (C-10a'), 99.665 (C-3'). gCOSY, gHMBC, gHSQC, and NOESY spectra are available in the Supporting Information. Mass Spectrometry; HRESI ($CHCl_3$/MeOH 1:1) m/z 365.08 (M^+-Cl) 366.08 (protonated M^+-Cl) Anal. Calcd for $C_{24}H_{13}O_4Cl$: C, 70.7, H, 3.60, O, 17.22, Cl, 8.45.

3.8. Synthesis of naphtho[2,3-c]furan-1,3-dione (**5**)

2 (7.6 mg, 0.211 mmol) was added to 2.00 mL methylene chloride. 9.0 mg (2 molar equivalents) PCC was added and the solution was stirred constantly in a sealed system for 4 days. The reaction mixture forms an opaque brown color within the first few minutes of PCC addition, which clears to a transparent blue within 8 hours. A biphasic separation in dichloromethane and water isolates the organic products. The organic phase is dried

by anhydrous Na_2SO_4 (s), isolate by centrifugation, and evaporated to an appropriate loading volume and separated via silica column chromatography coupled to UV florescence, providing adequate fraction resolution. A 100% methylene chloride mobile phase elutes two florescent fractions: one violet and one yellow. The fraction which fluoresced yellow in UV is **2**. The fraction which fluoresces violet is PCC oxidized to either the di-acid or anhydride form. ^{1}H NMR (300 MHz, $CDCl_3$): δ (ppm) 8.493 (s, 2H), 8.087 (dd, 2H), 7.755 (dt, 2H)

3.9. Synthesis and Isolation of the Competetive Condensation Product

N_2 (g) is bubbled through 1.00 mL methanolic solution containing NDA (11.5 mg) for 15 minutes. 0.25 ml methanolic solution containing NaCN (4.1 mg) is injected via syringe. The solution is sonicated, continuing N (g) perfusion. A dark precipitate forms within 12 minutes. The mixture is cooled on ice for 10 minutes, centrifuged and washed with cold water. Alternatively, the non-oxidized condensate can be isolated as a contaminant in the synthesis of **2**. If the reaction time is extended to 15-20 minutes, significant contamination of **2** occurs due to competitive condensation reactions of NDA. Isolation of both products can be achieved via flash column chromatography. **2** is visible in the column (yellow) and is easily separated in 100% methylene chloride mobile phase. Following the complete collection of **2**, the non-oxidized product (orange) can be isolated rapidly with a 5% methanol modified methylene chloride mobile phase. It is important to note that the product is synthesized in a conformation other than the stable isomer measured in chloroform. The isomerization is completed within 30 minutes of addition

to CH_2Cl_2 or $CHCl_3$. ^1H NMR (300 MHz, $CDCl_3$): δ (ppm) 8.925 (s, 1H), 8.814 (s, 1H), 8.073 (m, 2H), 8.028 (s, 1H), 7.929 (s, 1H), 7.842 (m, 2H), 7.676 (m, 2H), 7.576 (s, 1H), 7.576 (s, 1H), 7.496 (m, 2H)

4.0 References

1. Carlson, R.G.; Srinivasachar, K.; Givens, R.S.; Matuszewski, B.K. "New Derivitizing Agents for Amino Acids and Peptides. 1 Facile Synthesis of N-Substituted 1-Cyanobenz[f]isoindoles and their Spectroscopic Properties." *J. Org. Chem.* **1986**, 51, 3978-3983.

2. De Montigny, P.; Stobaugh, J.F.; Givens, R.S.; Carlson, R.G.; Srinivasachar, K.;Sternson, L.A.; Higuchi, T. "Napthalene-2,3-Dicarboxaldehyde/Cyanide Ion: A Rationally Designed Fluorogenic Reagent for Primary Amines." *Anal. Chem.* **1987**, 59, 1096-101.

3. De Antonis, K.M.; Brown, P.R. "Analysis of Derivatized Peptides Using High Performance Liquid Chromatography and Capillary Electrophoresis." *Advances in Chromatography* (New York) **1997**, 37, 425-452.

4. Waterval, J.C.M.; Lingeman, H.; Bult, A.; Underberg, W.J.M. "DerivitizationTrends in Capillary Electrophoresis." *Electrophoresis* **2000**, 21, 4029-4045.

5. Corey, E.J.; Gilman, N.W.; Ganem, B.E. "New Methods for the Oxidation of Aldehydes to Carboxylic Acids and Esters." *J.A.C.S.* **1968**, 9, 5616-5617.

6. Lai, G.; Anderson, W.K. "A Simplified Procedure for the Efficient Conversion of Aromatic Aldehydes into Esters." *Synth. Commun.* **1997**, 27, 1281-1283.

7. Wade, L.G. *Organic Chemistry, Fourth Edition*, Prentice Hall, Inc.: New Jersey, **1999**, p.1207-1211.

8. Breitmaier, E. *Structural Elucidation by NMR in Organic Chemistry*, John Wiley and Sons: Chichester, **1999**.

9. Skoog, D.; Holler, F.; Newman, T. *Principles of Instrumental Analysis, Fifth Edition,* Harcourt Brace College Publishing: Philadelphia, **1998**, p. 498-534.

10. Silverstein, R.M.; Bassler, G.C.; Morrill, T.C. *Spectrometric Identification of Organic Compounds, Fifth Edition,* John Wiley and Sons: Chichester, **1991**, p. 91-164.

11. ACD/HNMR Predictor v. 4.56, Advanced Chemistry Development, Ontario, Canada

APPENDIX A

Supplementary Spectra for Product **2**

Table A.1. A Summary of NMR Correlations for Product **2**.

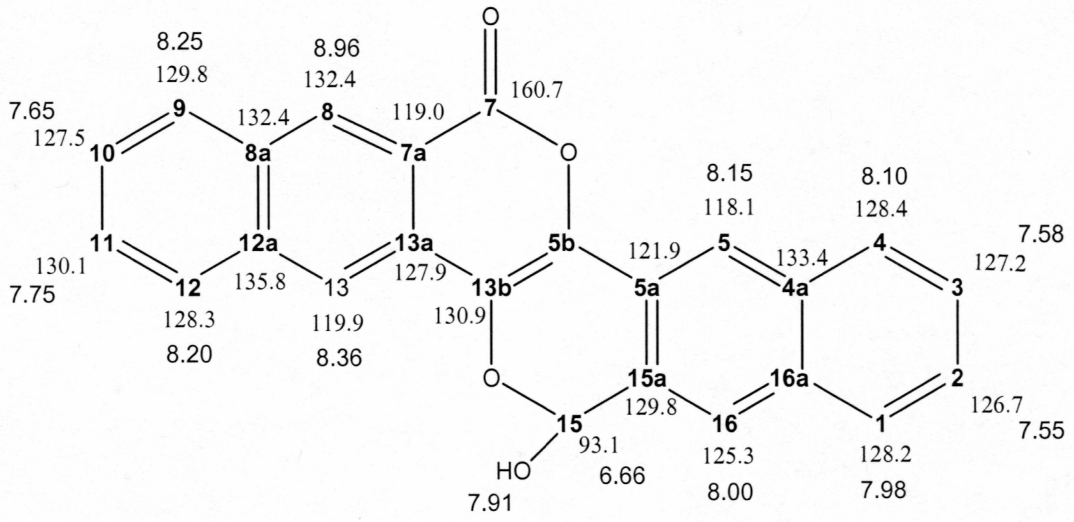

δ_H, ppm	H-#	J_{HH}	gCOSY	One bond δ_c	Three Bonds δ_c[1]
8.96 (s)	H-8	--	--	132.4	127.9, 129.8, 135.8, 160.1
8.36 (s)	H-13	--	--	119.9	119.0, 128.3, 130.9, 132.0
8.25 (d)	H-9	8.3, 1.3	7.65	129.8	130.1, 132.4
8.20 (d)	H-12	8.3, 1.3	7.75	128.3	119.9, 127.5, 132.0
8.15 (s)	H-5	--	--	118.1	128.4, 129.8 (3 Hz)
8.10 (dd)	H-4	8.3, 1.3	7.58	128.4	126.7
8.00 (s)	H-16	--	--	125.3	93.1, 121.9, 128.2, 133.1
7.98 (dd)	H-1	8.3, 1.3	7.55	128.2	127.3
7.91 (d)	H-OH	6.9	6.66	--	129.8
7.75 (ddt)	H-11	1.3, 7.0, 8.3	7.65, 8.20	130.1	135.8, 129.8
7.65 (dt)	H-10	1.3, 7.0, 8.3	7.75, 8.25	127.5	128.3, 132.0
7.58 (dt)	H-3	1.3, 7.0, 8.3	7.55, 8.10	127.2	133.4 (3 Hz)
7.55 (dt)	H-2	1.3, 7.0, 8.3	7.58, 7.98	126.7	--
6.66 (d)	H-15	6.9	7.91	93.1	121.9, 125.2, 130.9

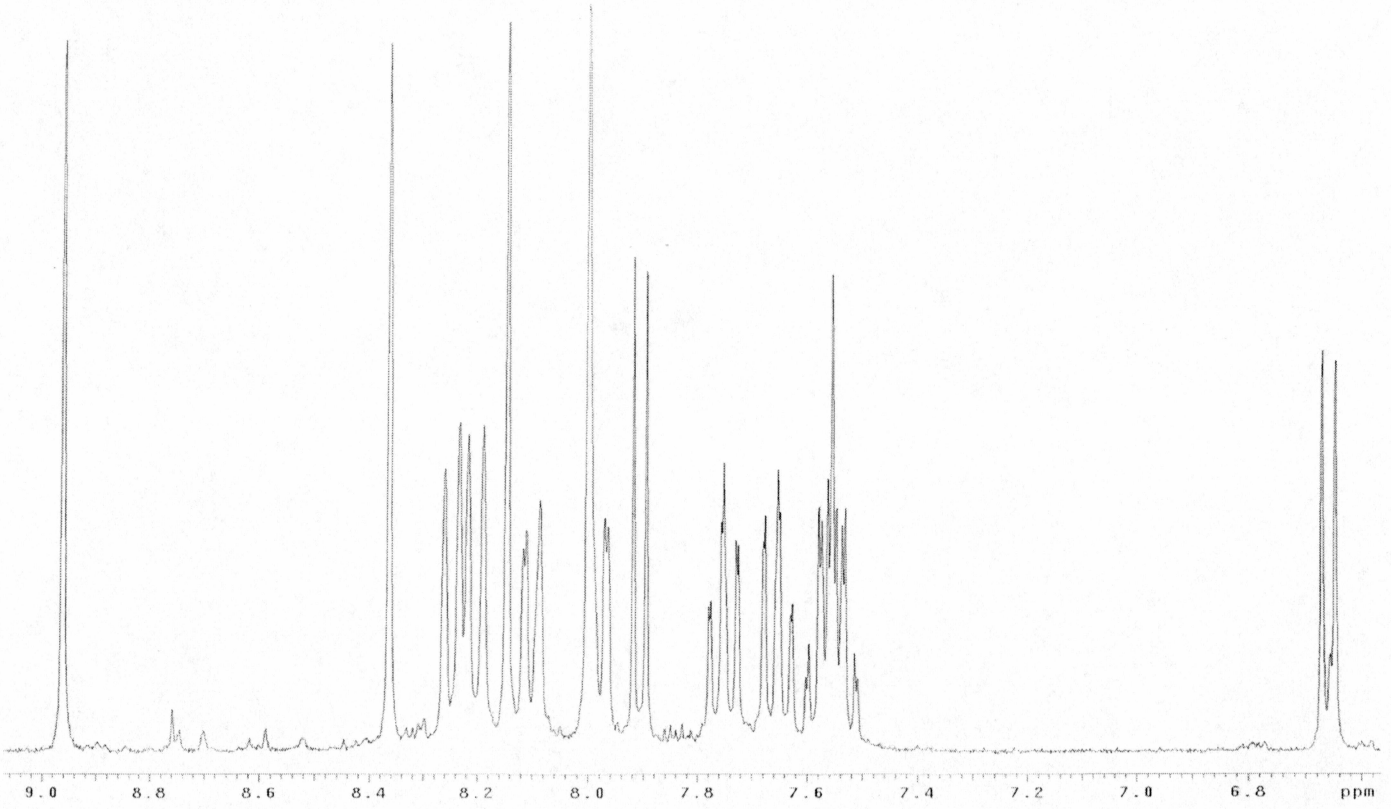

Figure A.2. H NMR of **2** in DMSO-d_6

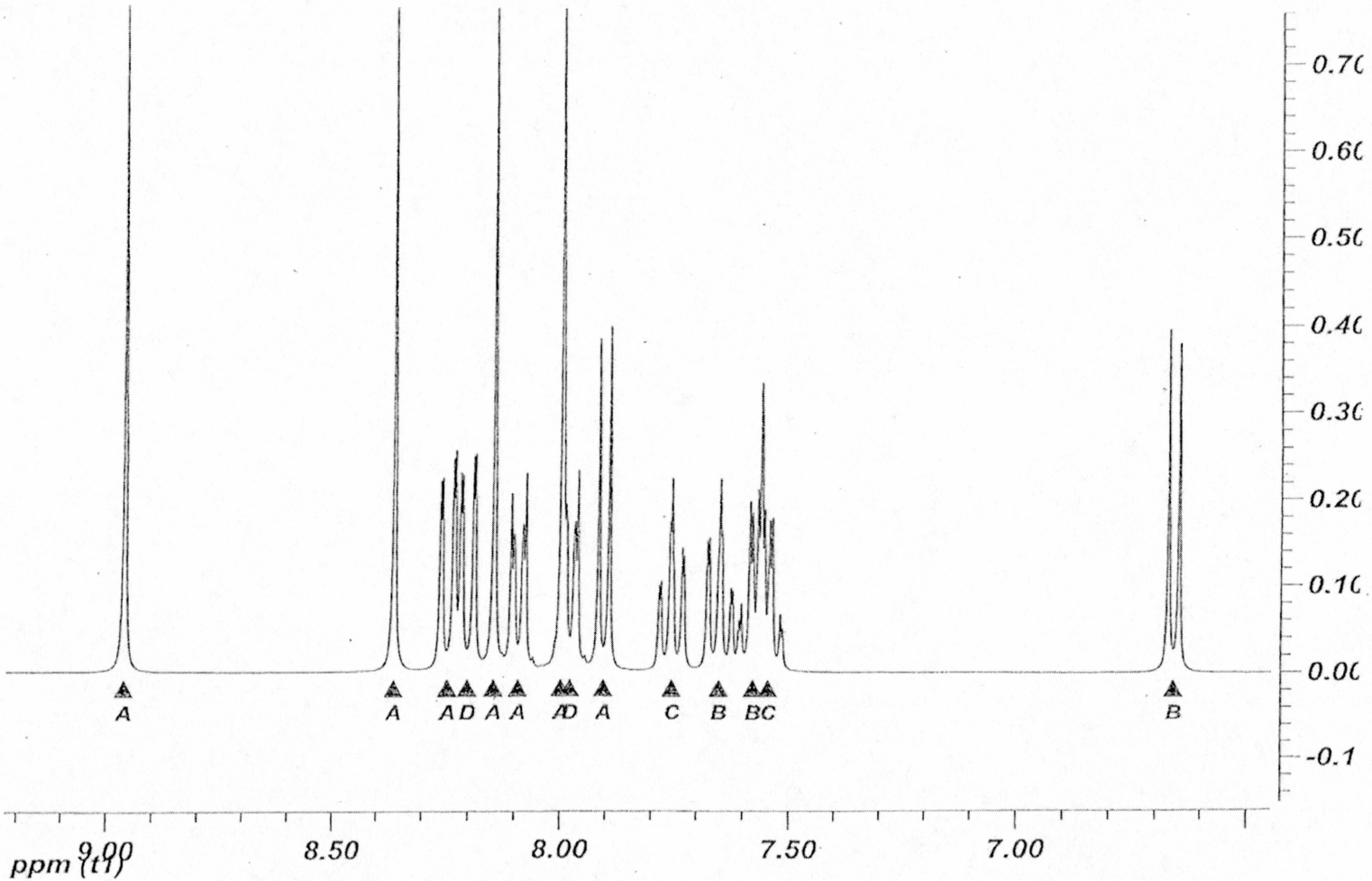

Figure A.3. The Simulated H-NMR Spectrum for Product **2**. Coupling constants were taken form A.1.1. Note the excellent agreement between predicted and observed specra.

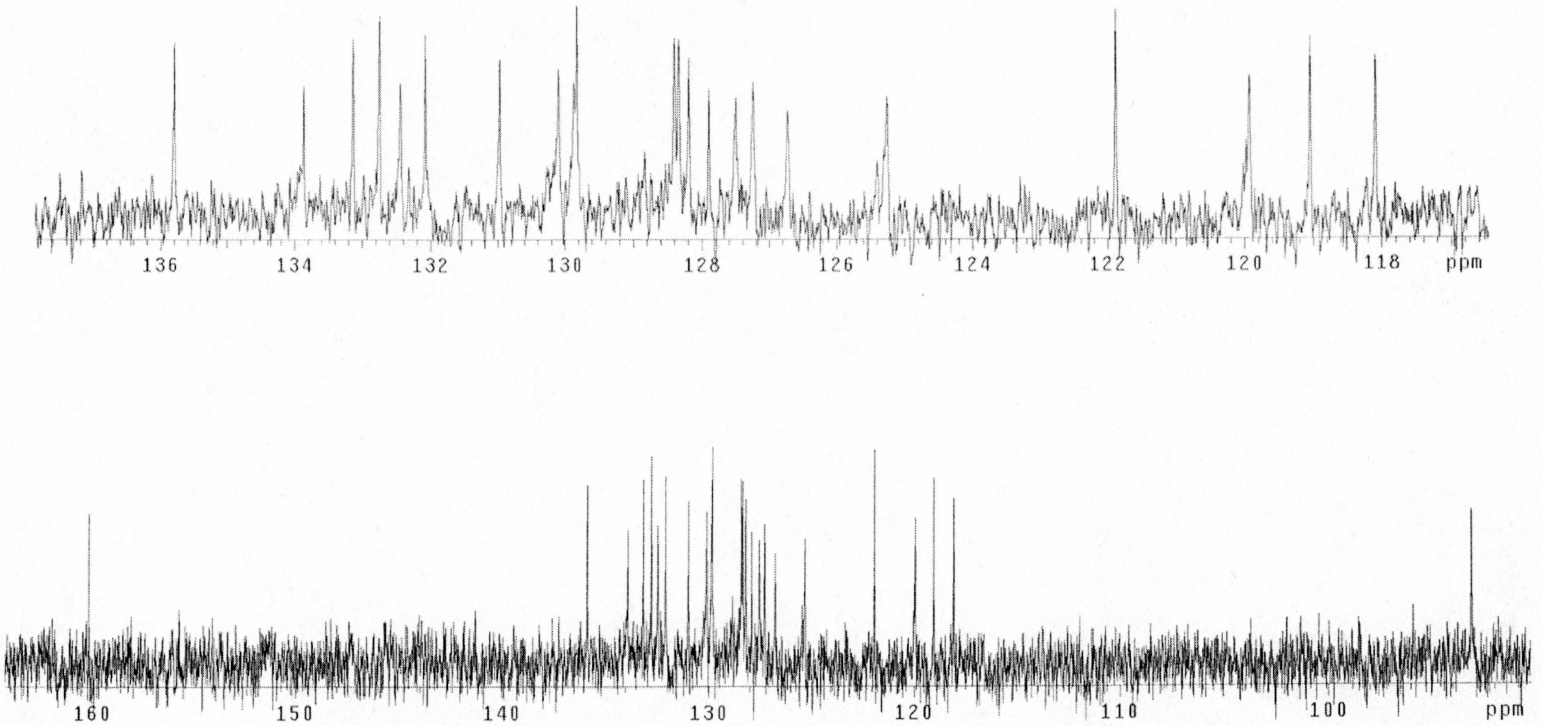

Figure A.4. ^{13}C NMR of **2** in DMSO-d_6

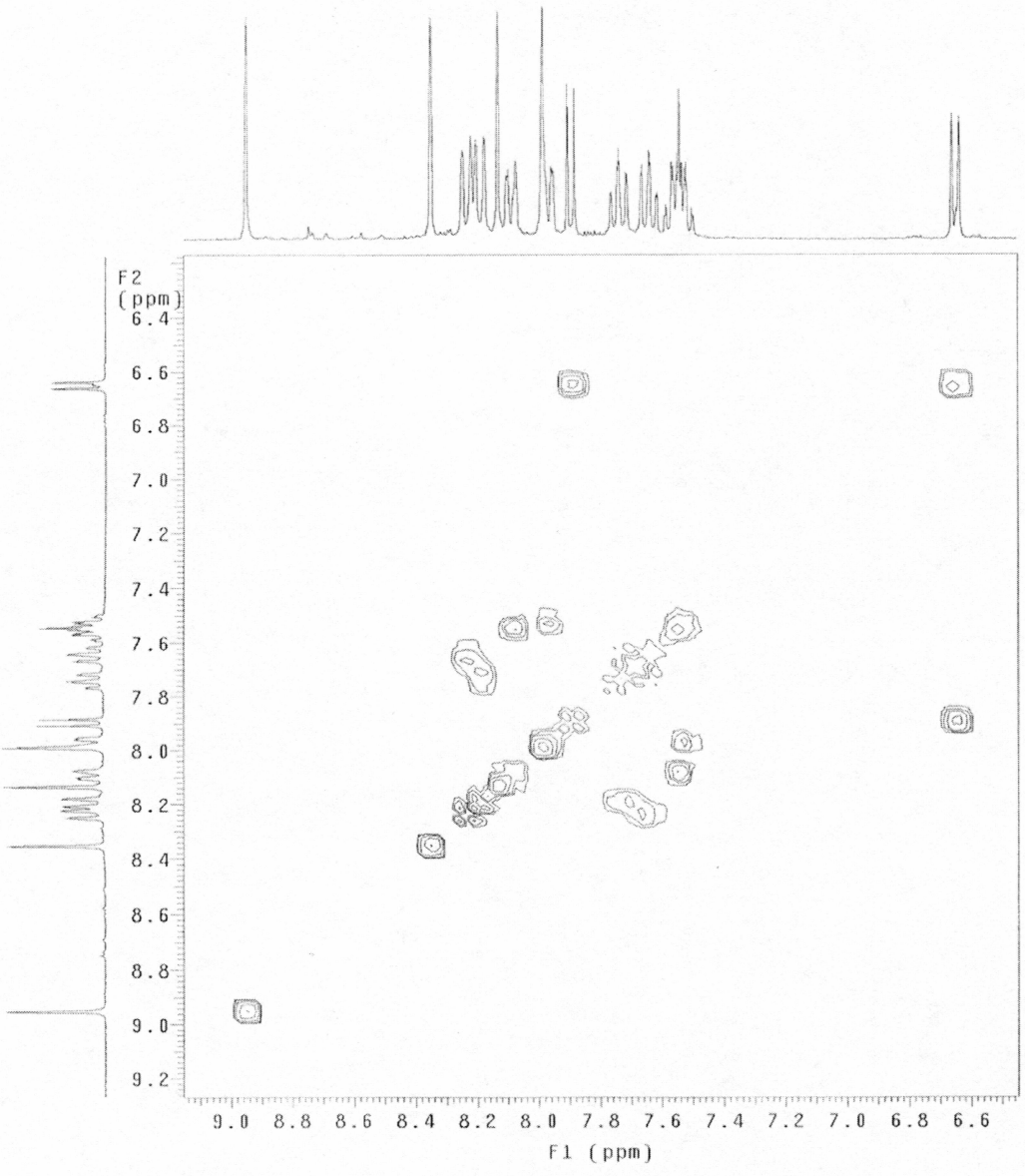

Figure A.5. gCOSY of **2** in DMSO-d_6

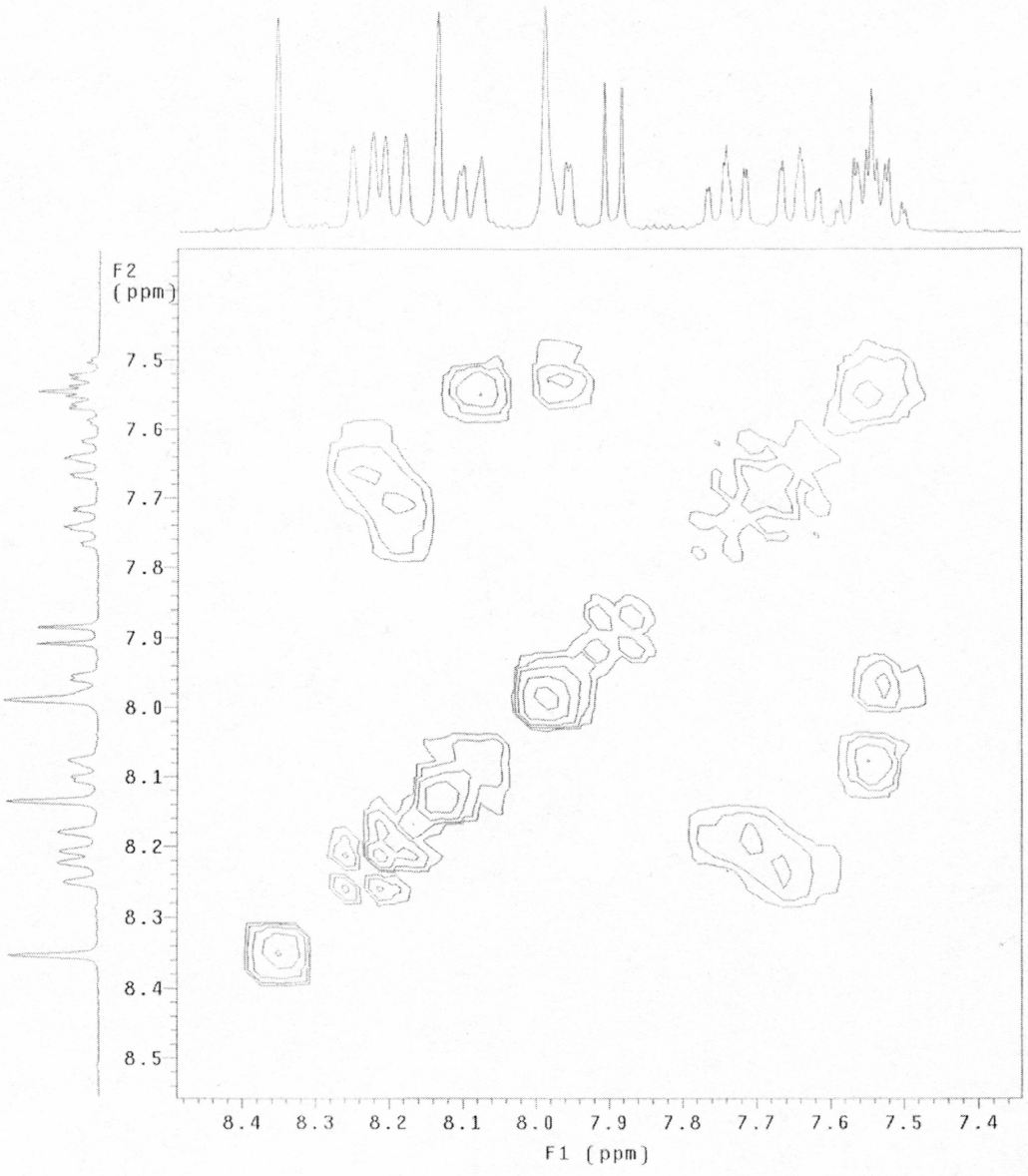

Figure A.6. Expanded gCOSY of **2** in DMSO-d_6

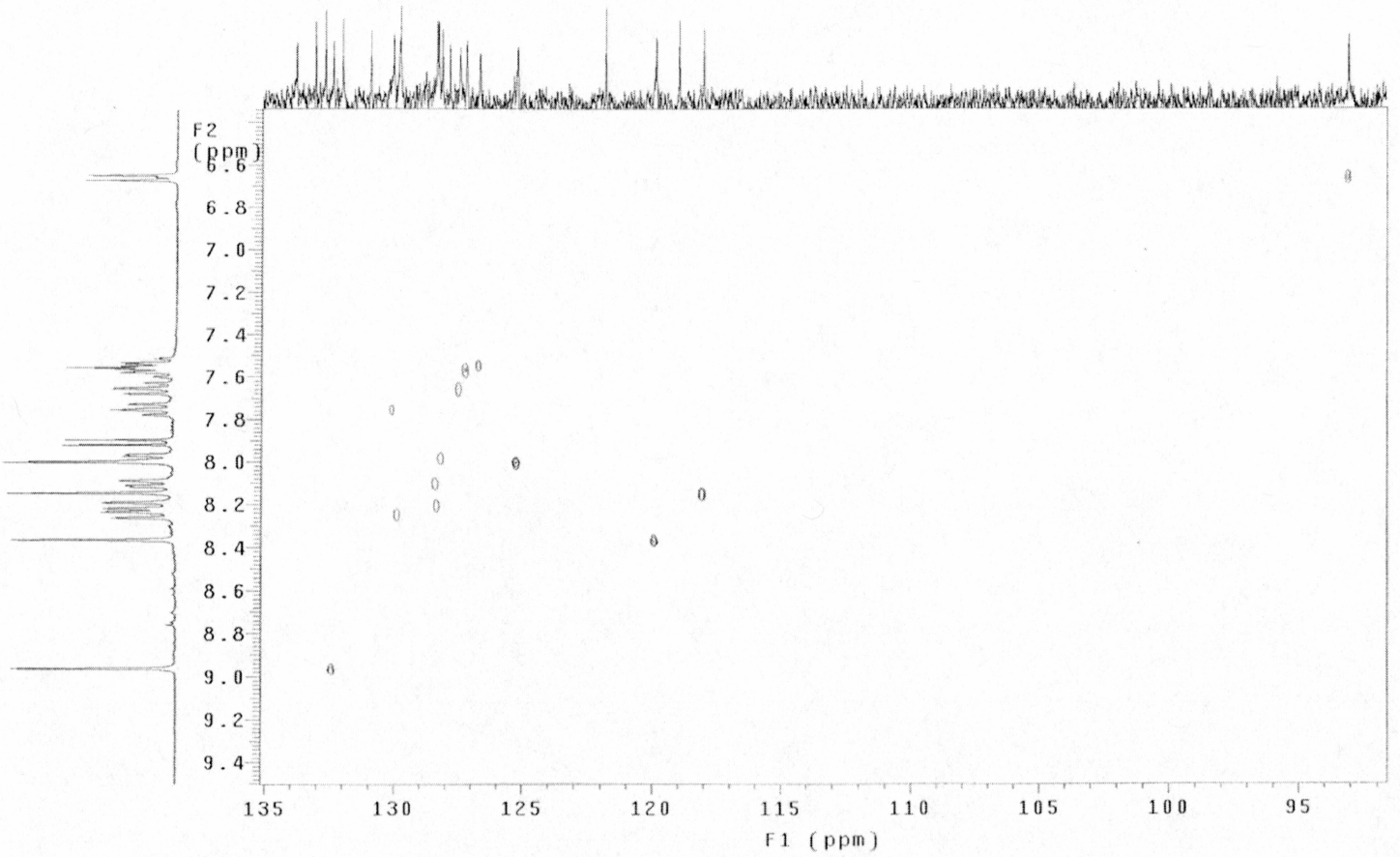

Figure A.7. Full gHSQC of **2** in DMSO-d_6

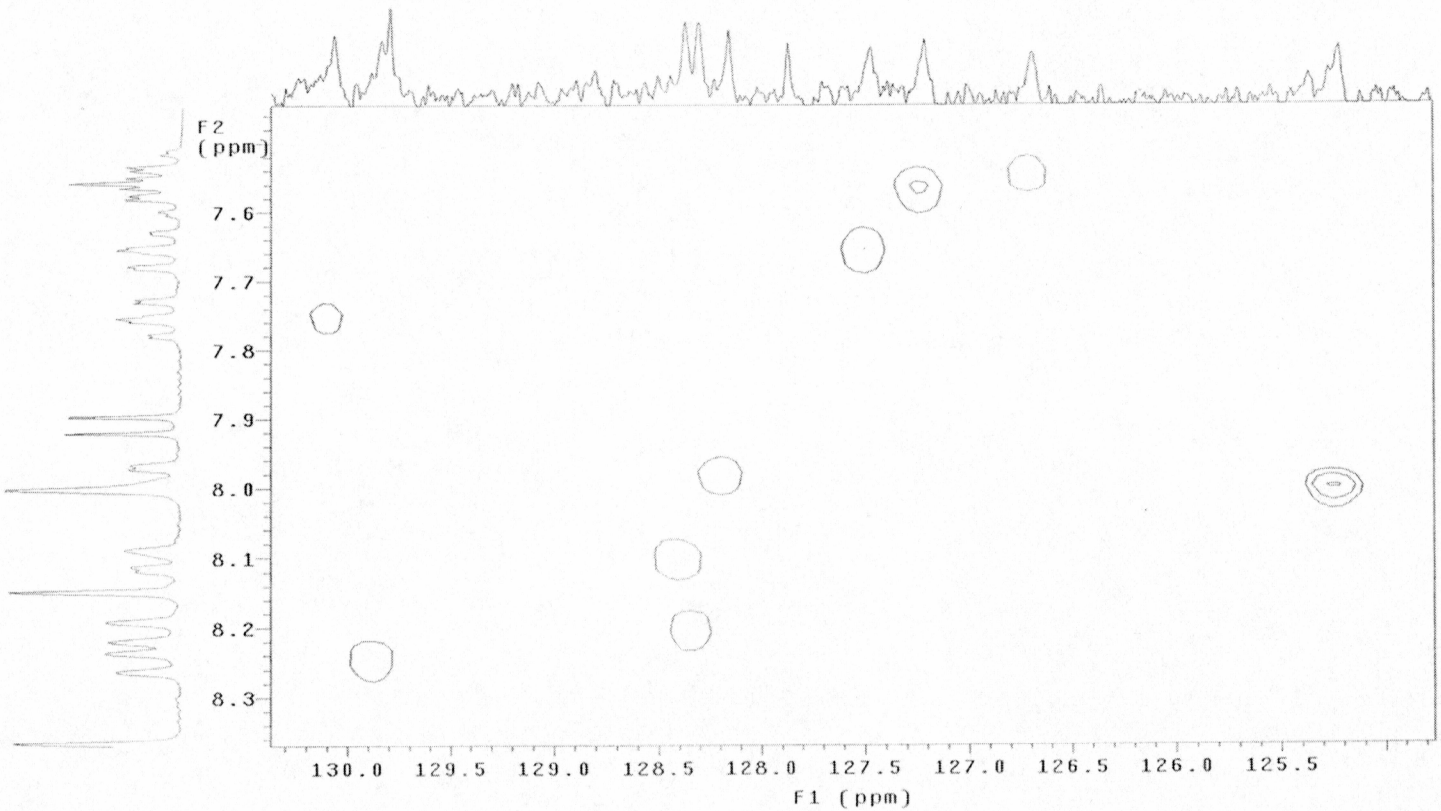

Figure A.8. Expanded gHMBC of **2** in DMSO-d_6

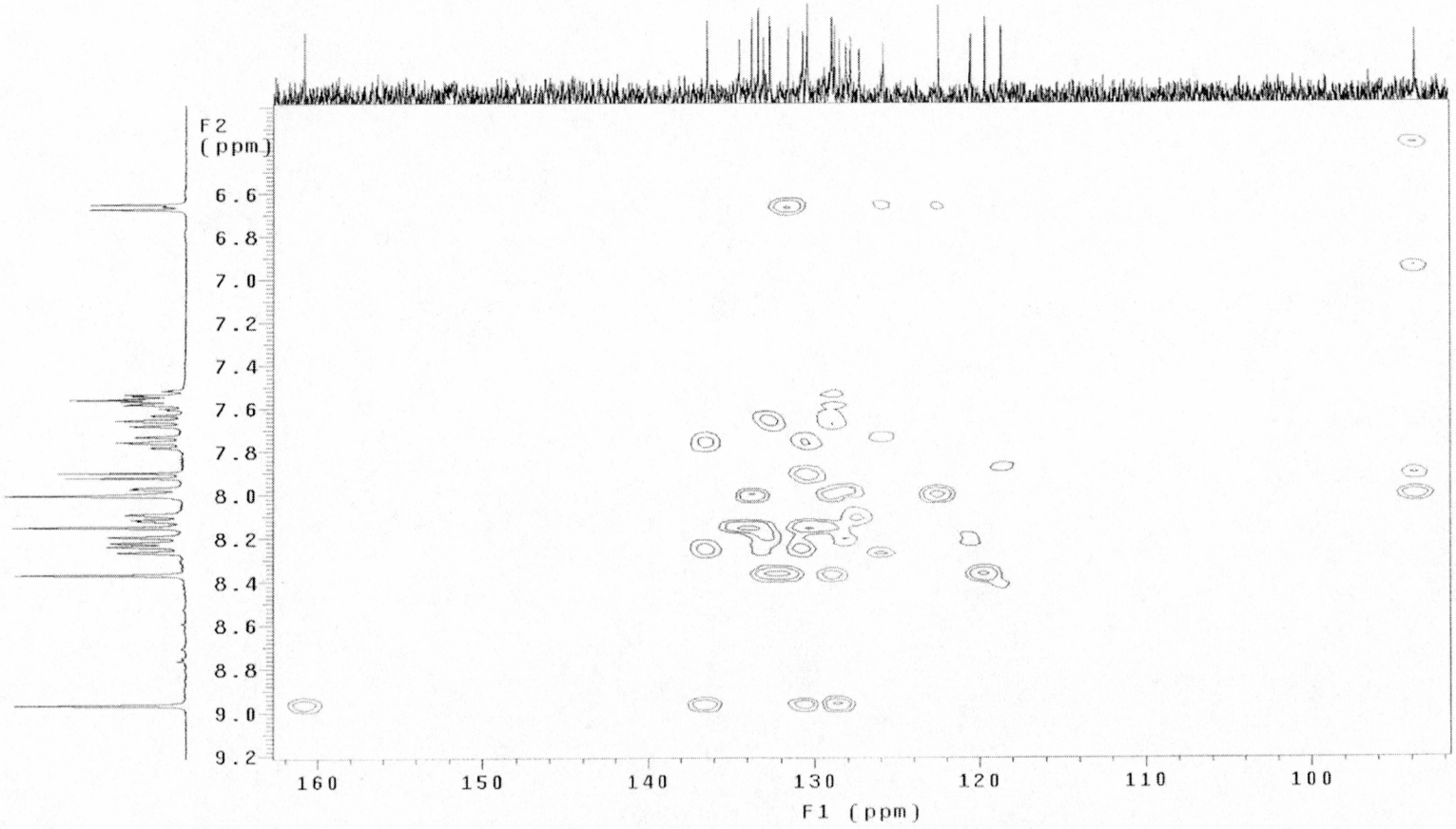

Figure A.9. Full gHMBC of **2** in DMSO-d_6 using a mixing time corresponding to 8 hz coupling

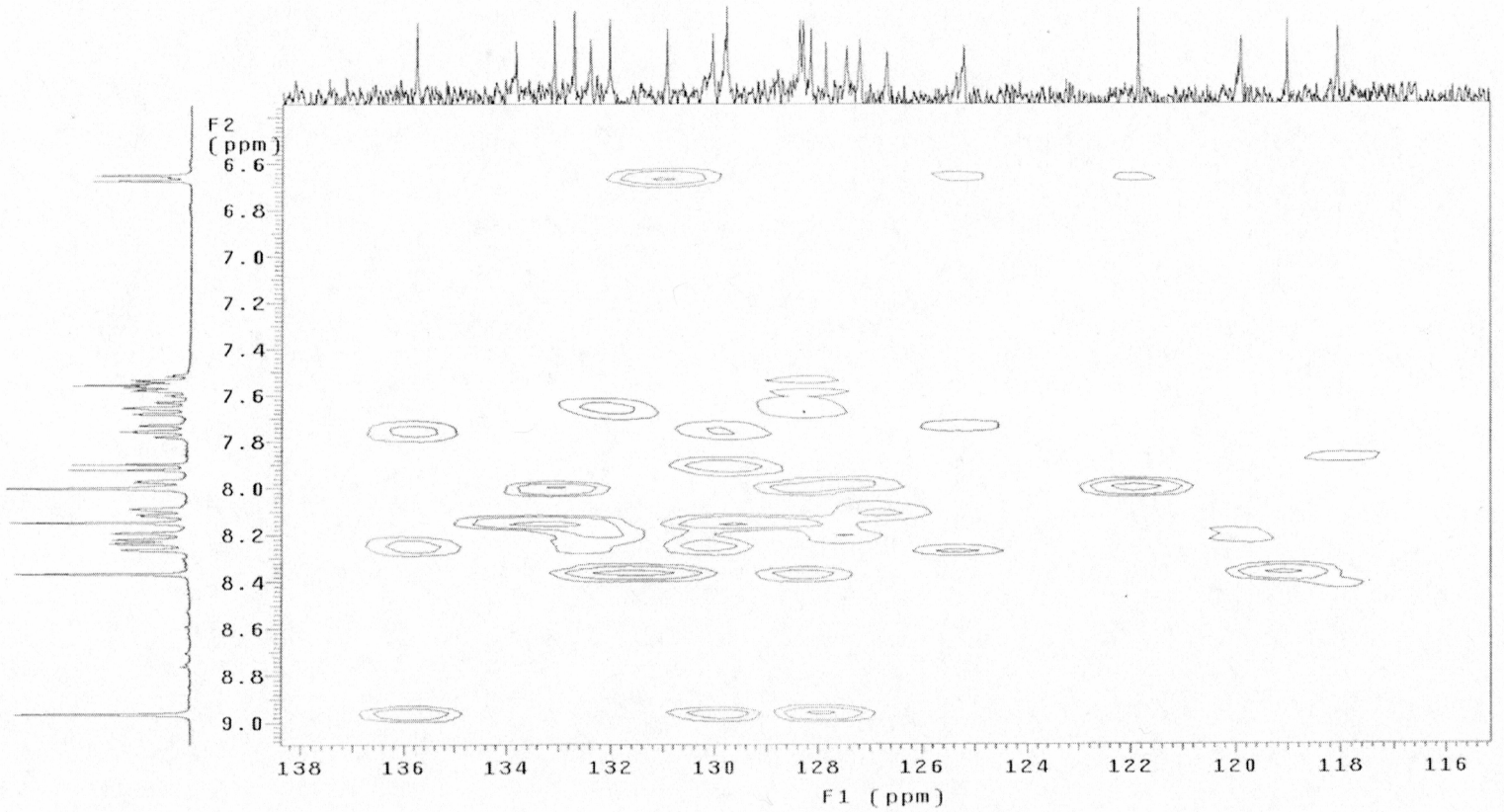

Figure A.10. Expanded gHMBC of **2** in DMSO-d_6 using a mixing time corresponding to 8 hz coupling

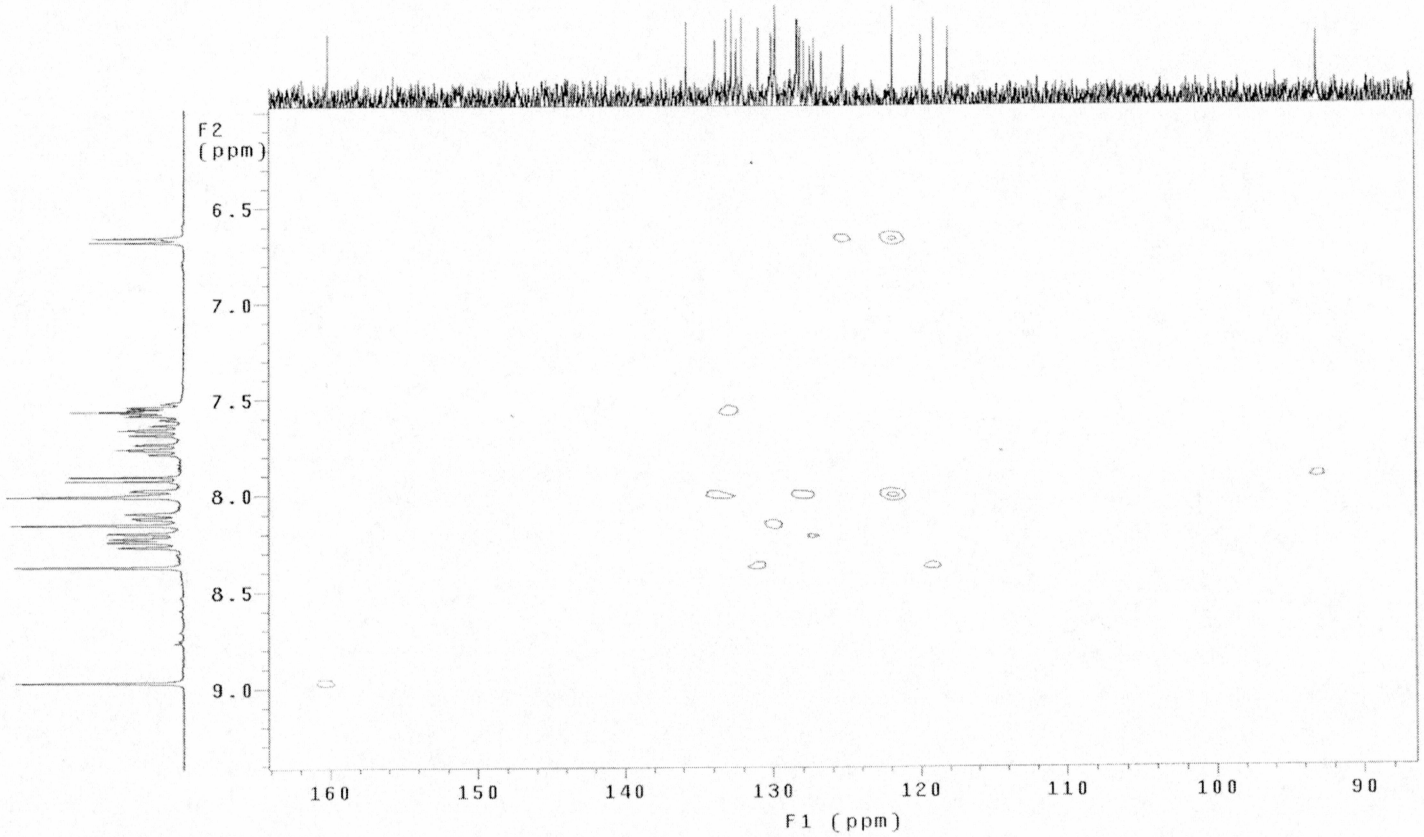

Figure A.11. Full gHMBC of **2** in DMSO-d_6 using a mixing time corresponding to 3 hz coupling

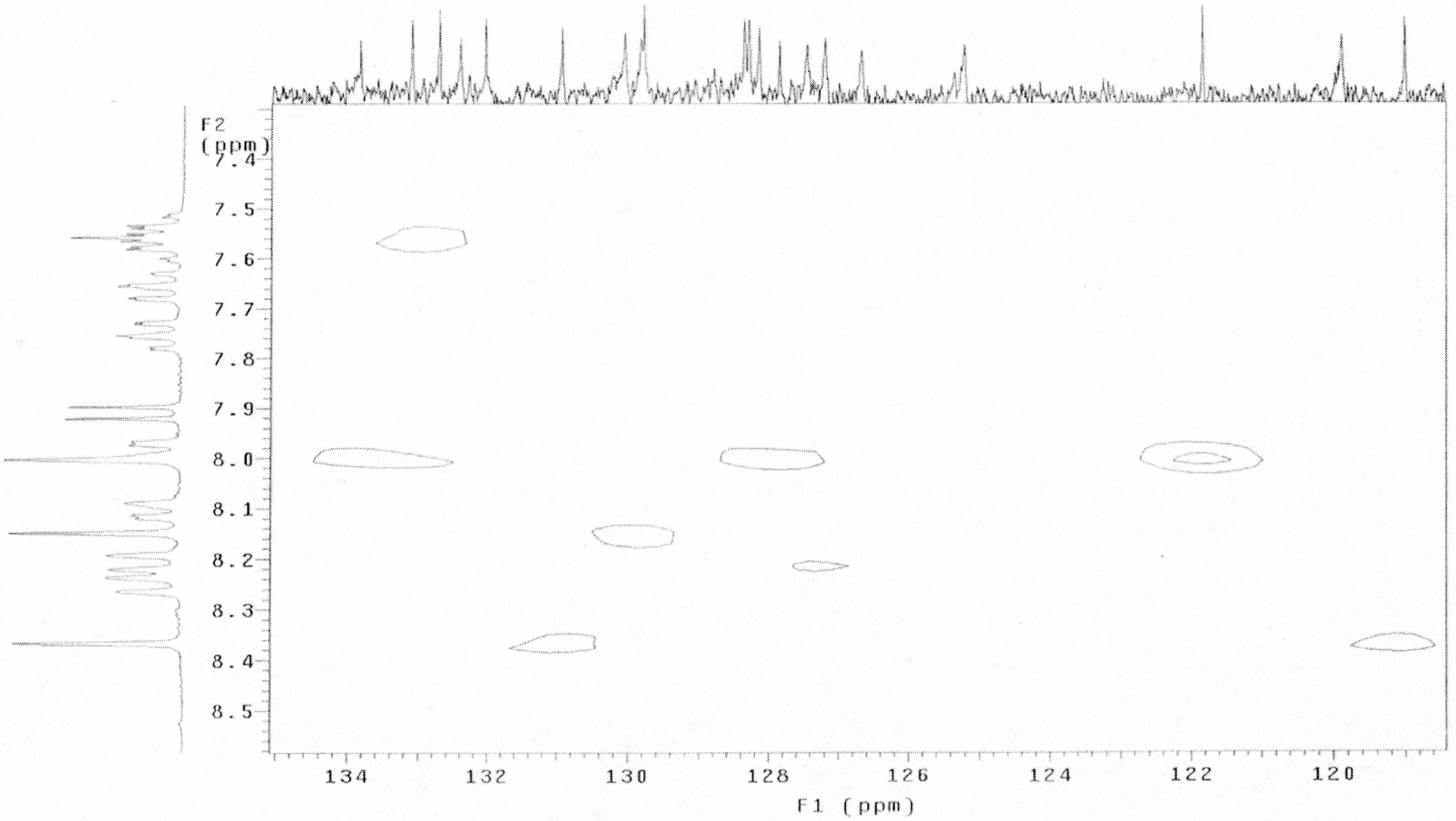

Figure A.12. Expanded gHMBC of **2** in DMSO-d_6 using a mixing time corresponding to 3 hz coupling

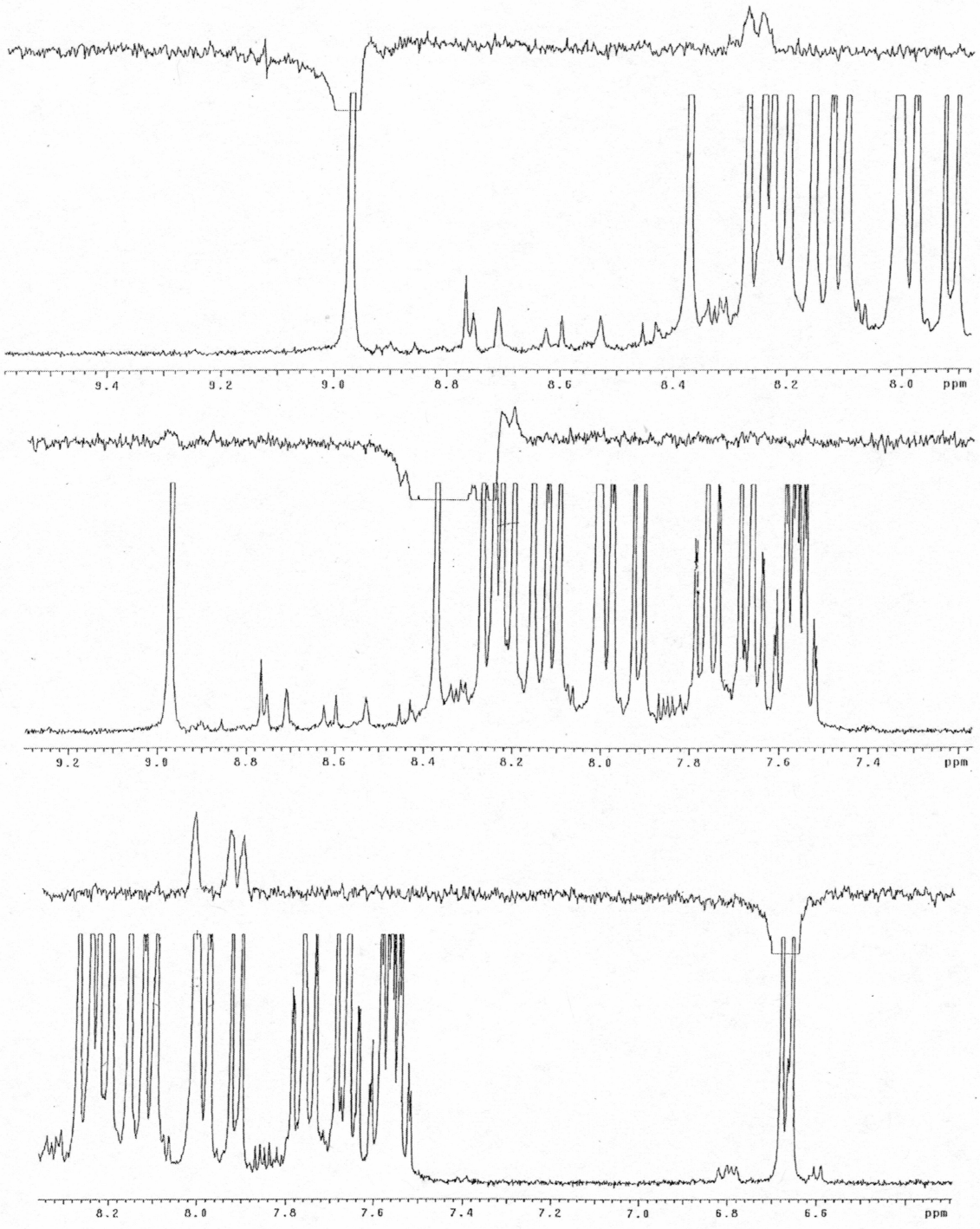

Figure A.13. NOESY 1D of **2** in DMSO-d_6 with irradiation at (from top to bottom) 8.97, 8.37, and 6.67 ppm

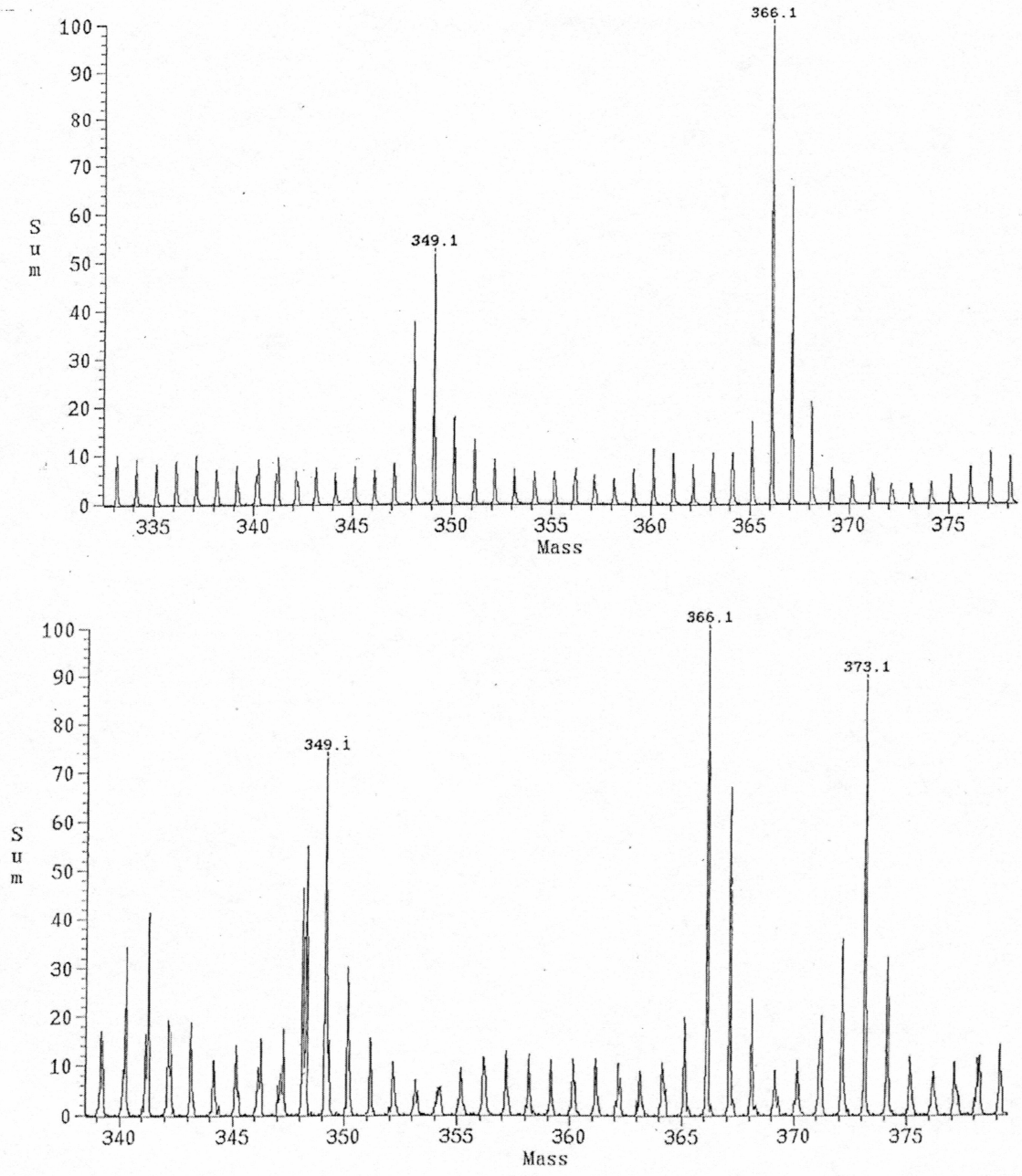

Figure A.14. LRFAB-MS of **2** in 3-NBA (top) and 3-NBA/Li (bottom)

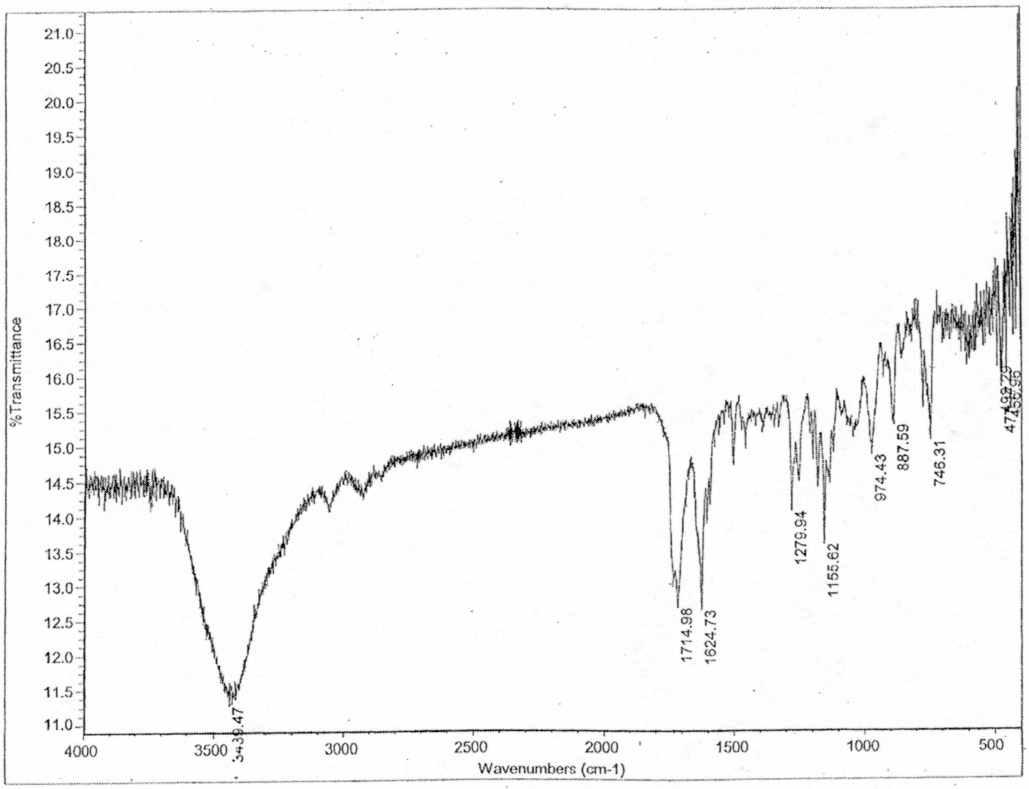

Figure A.15. IR (KBr) of Product **2**

APPENDIX B

Supplementary Spectra for the Model Compounds

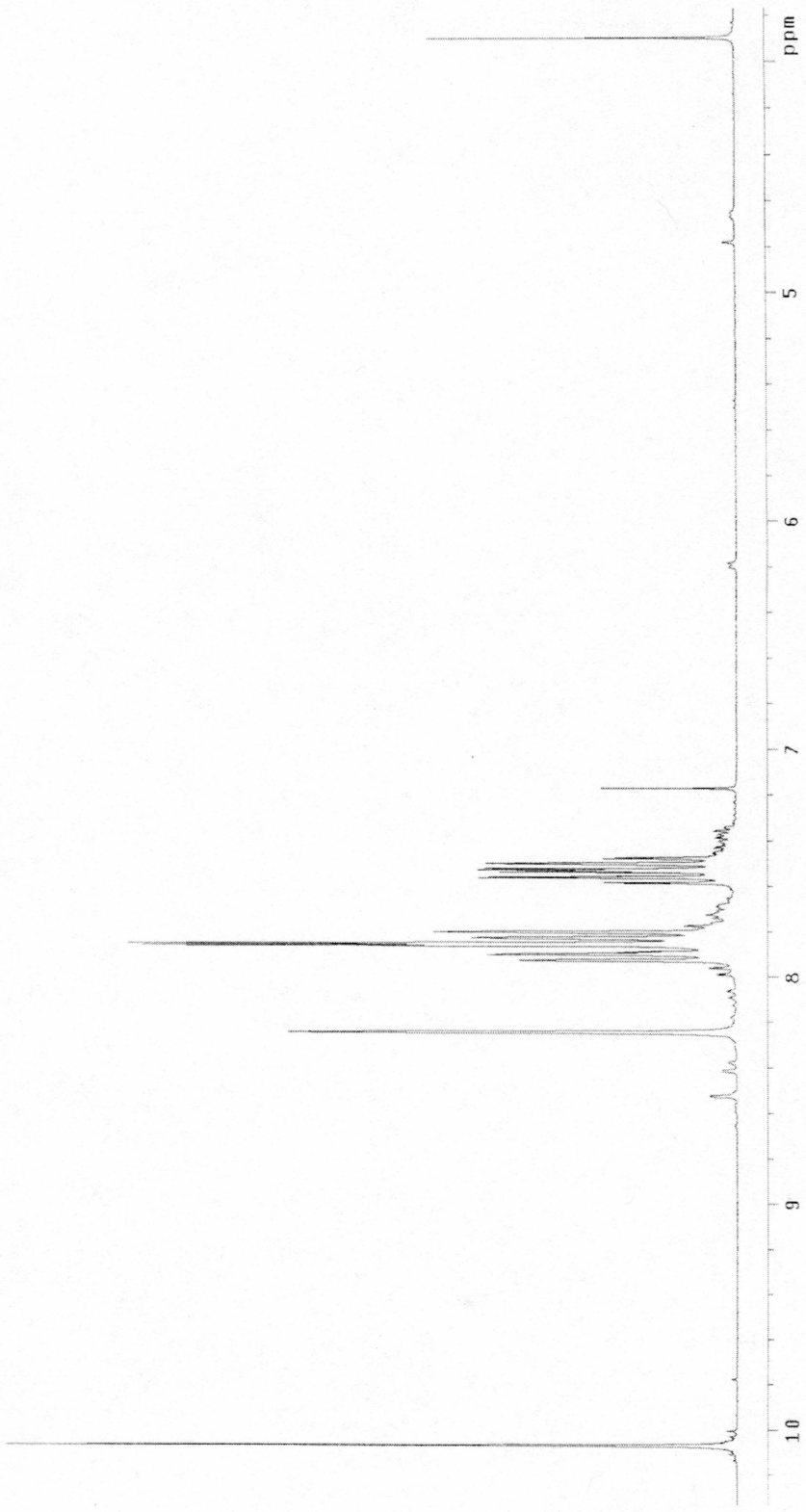

Figure B.1. ^{1}H NMR of 2-napthaldehyde in $CDCl_3$ with 10% methyl 2-napthoate derivative

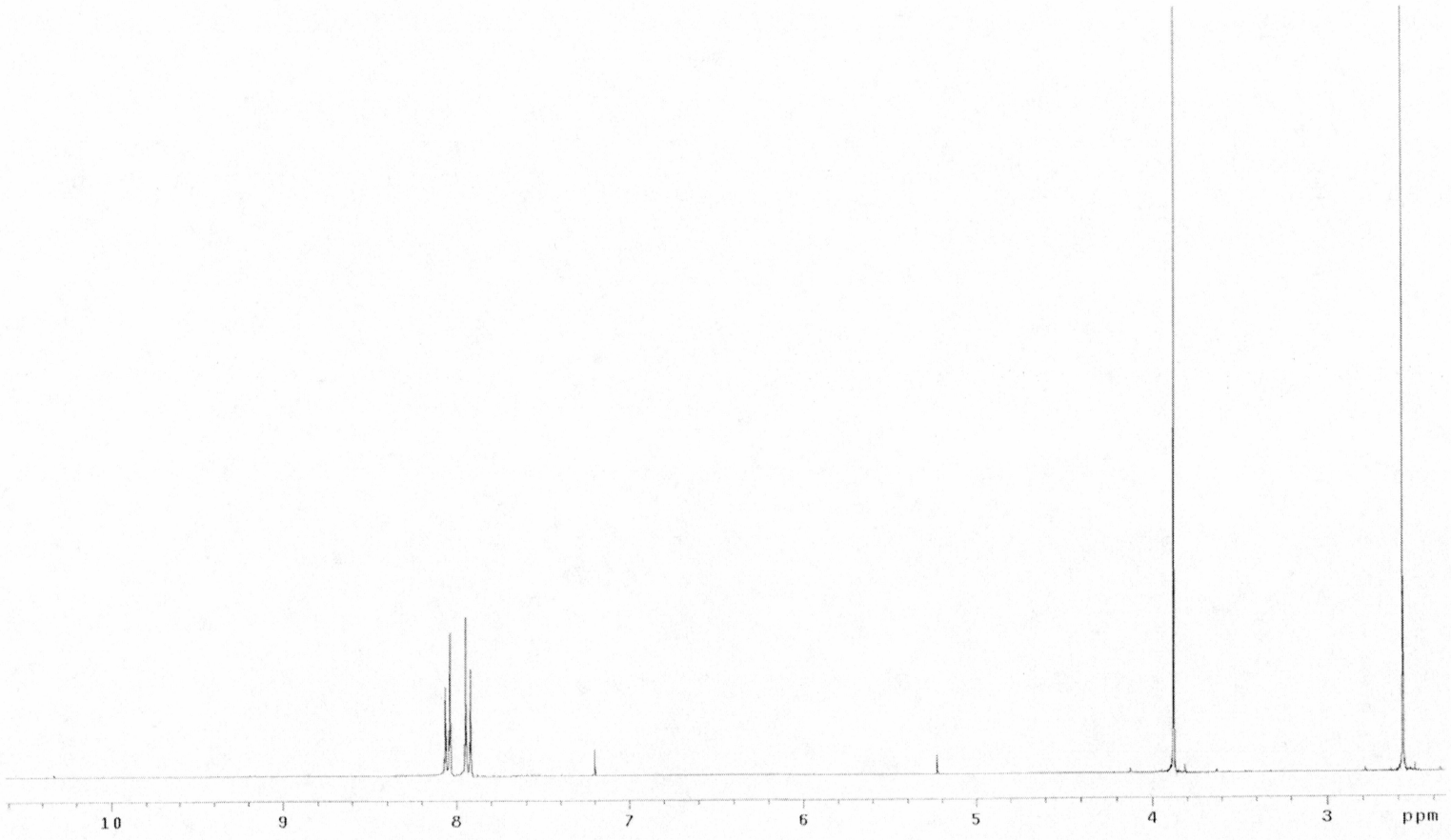

Figure B.2. ^{1}H NMR of methyl 4-acetylbenzoate in $CDCl_3$

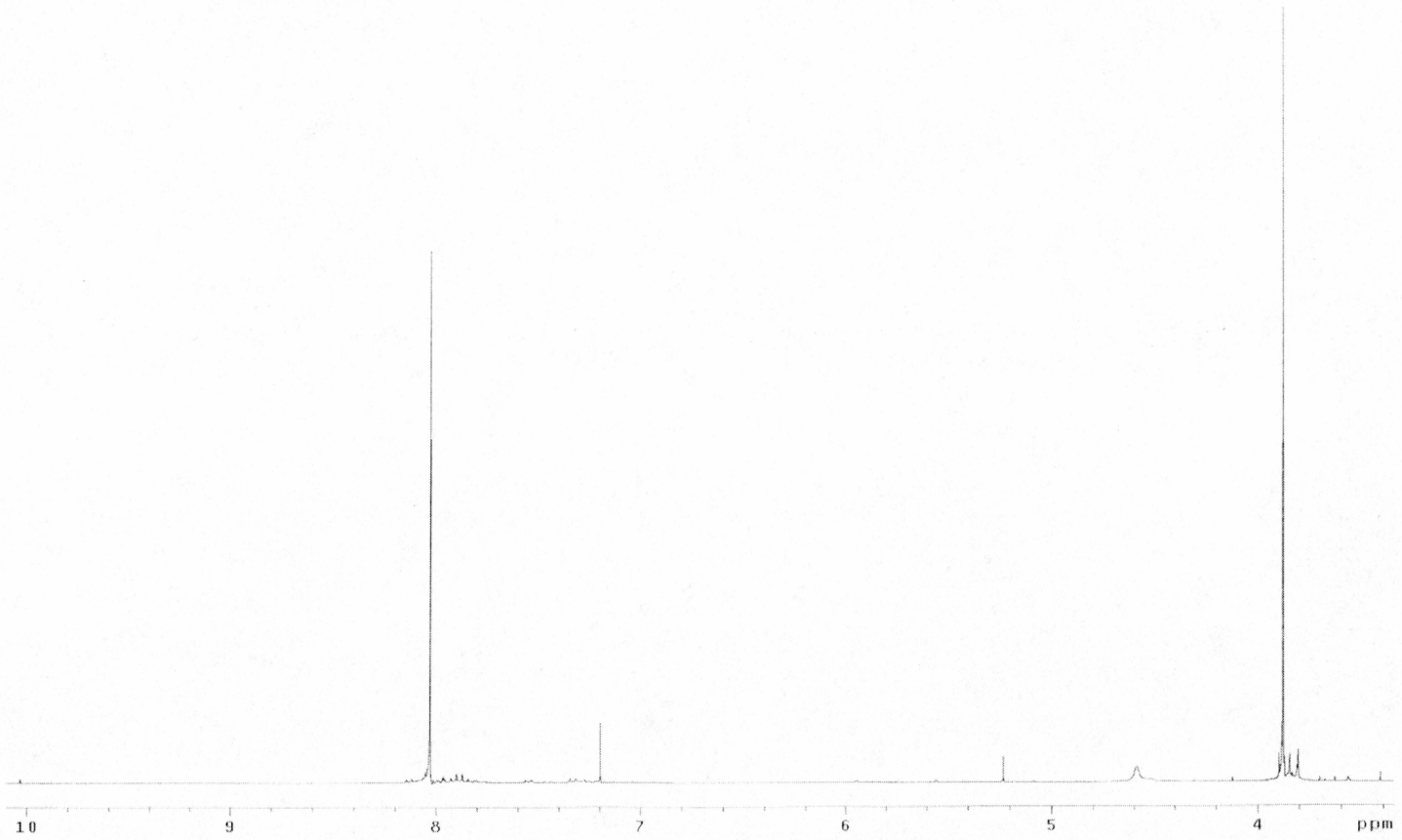

Figure B.3. ^{1}H NMR of dimethyl terepthalate in $CDCl_3$

APPENDIX C

Supplementary Spectra for the Acetal Derivatives

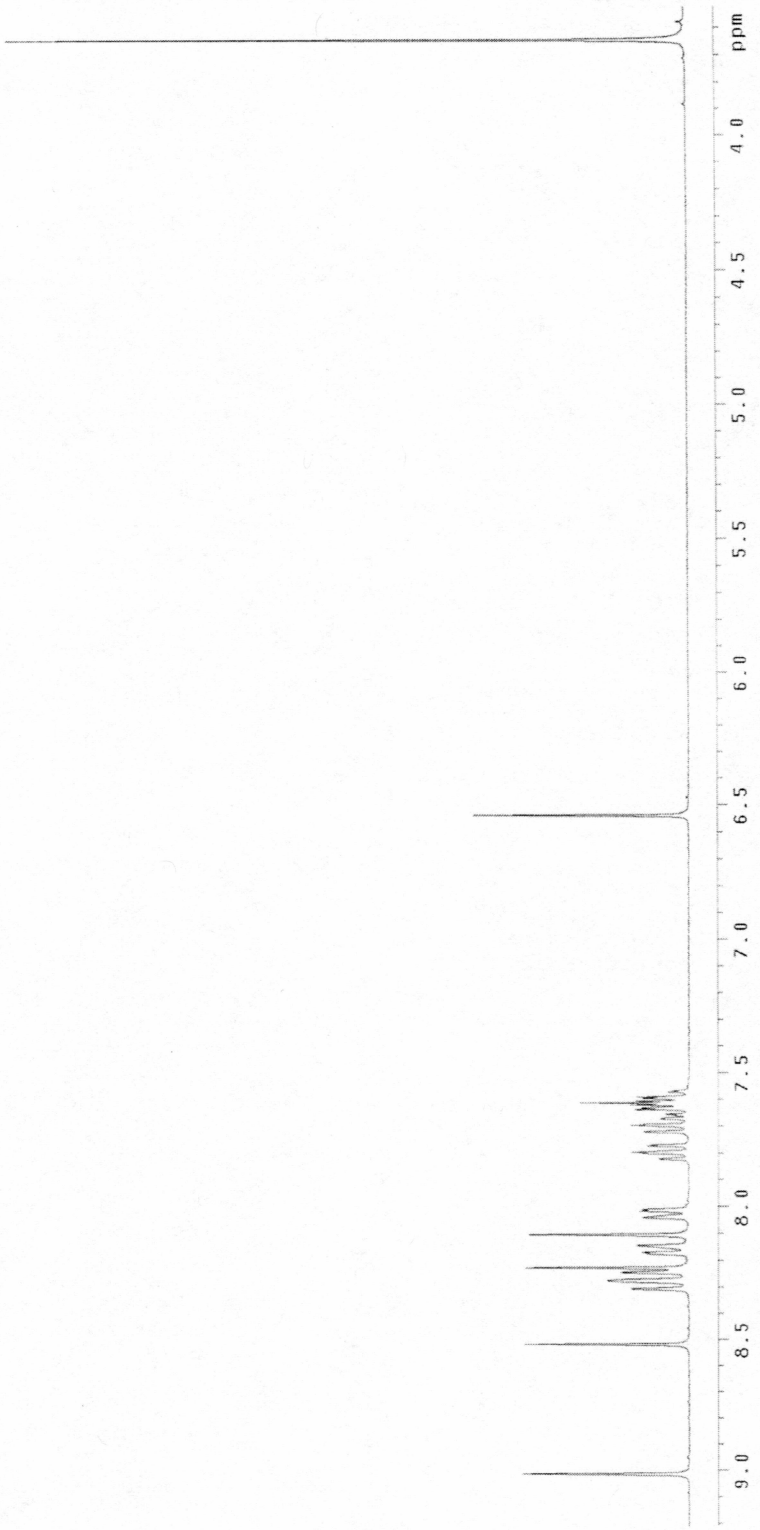

Figure C.1. ^{1}H NMR of the methyl ester derivative of **2** in DMSO-d_6

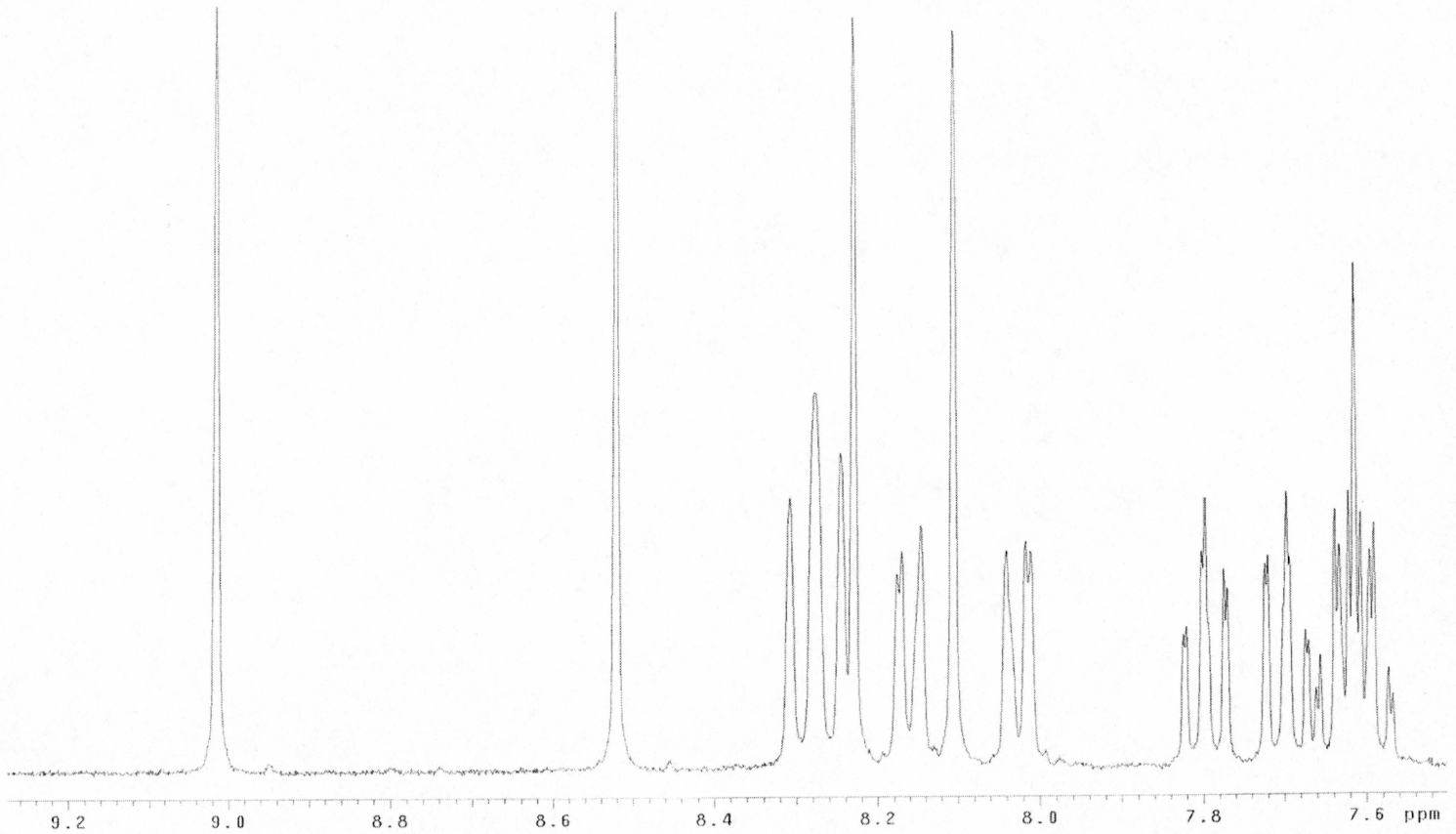

Figure C.2. Expanded ^{1}H NMR of the methyl ester derivative of **2** in DMSO-d_6, showing superior resolution in the couplings of the aromatic hydrogens

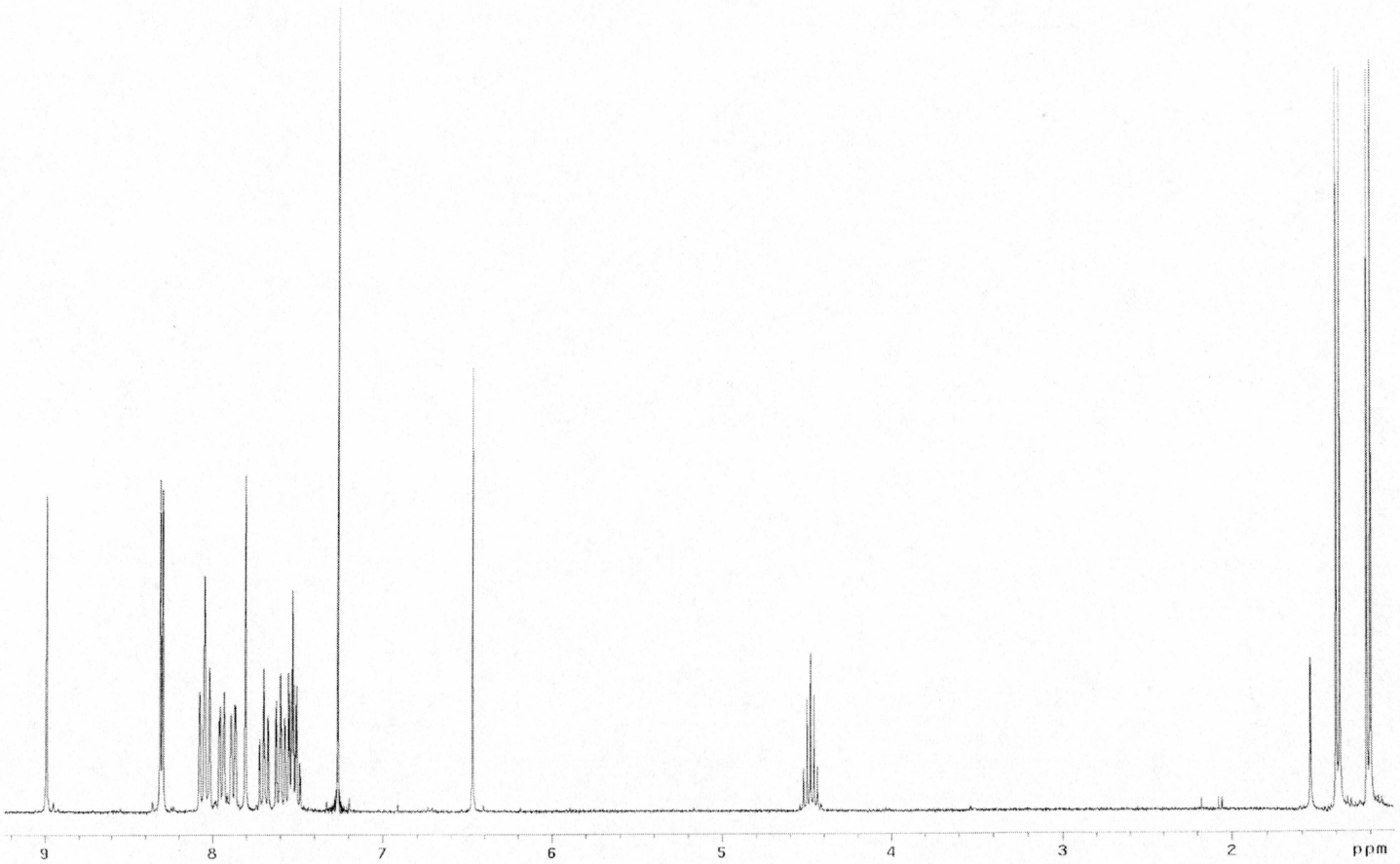

Figure C.3. ^{1}H NMR of the isopropyl ester derivative of **2** in $CDCl_3$

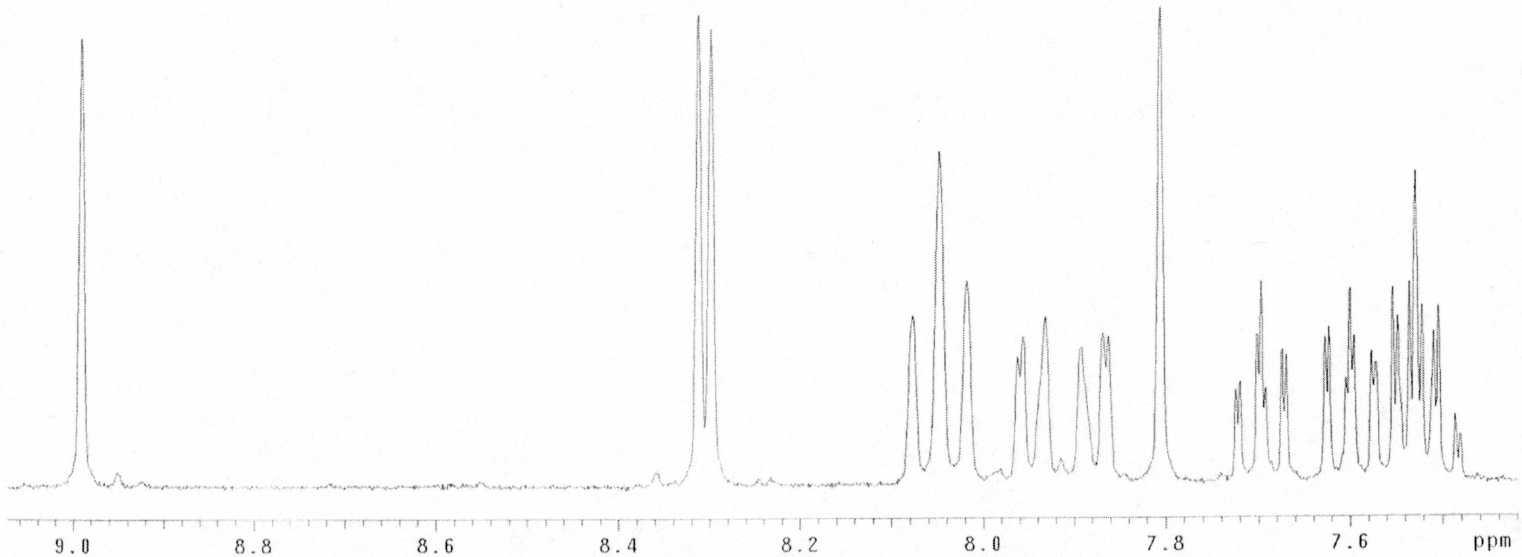

Figure C.4. Expanded ^{1}H NMR of the isopropyl ester derivative of **2** in $CDCl_3$, showing superior resolution in the couplings of the aromatic hydrogens

APPENDIX D

Supplementary Spectra for Product **4**

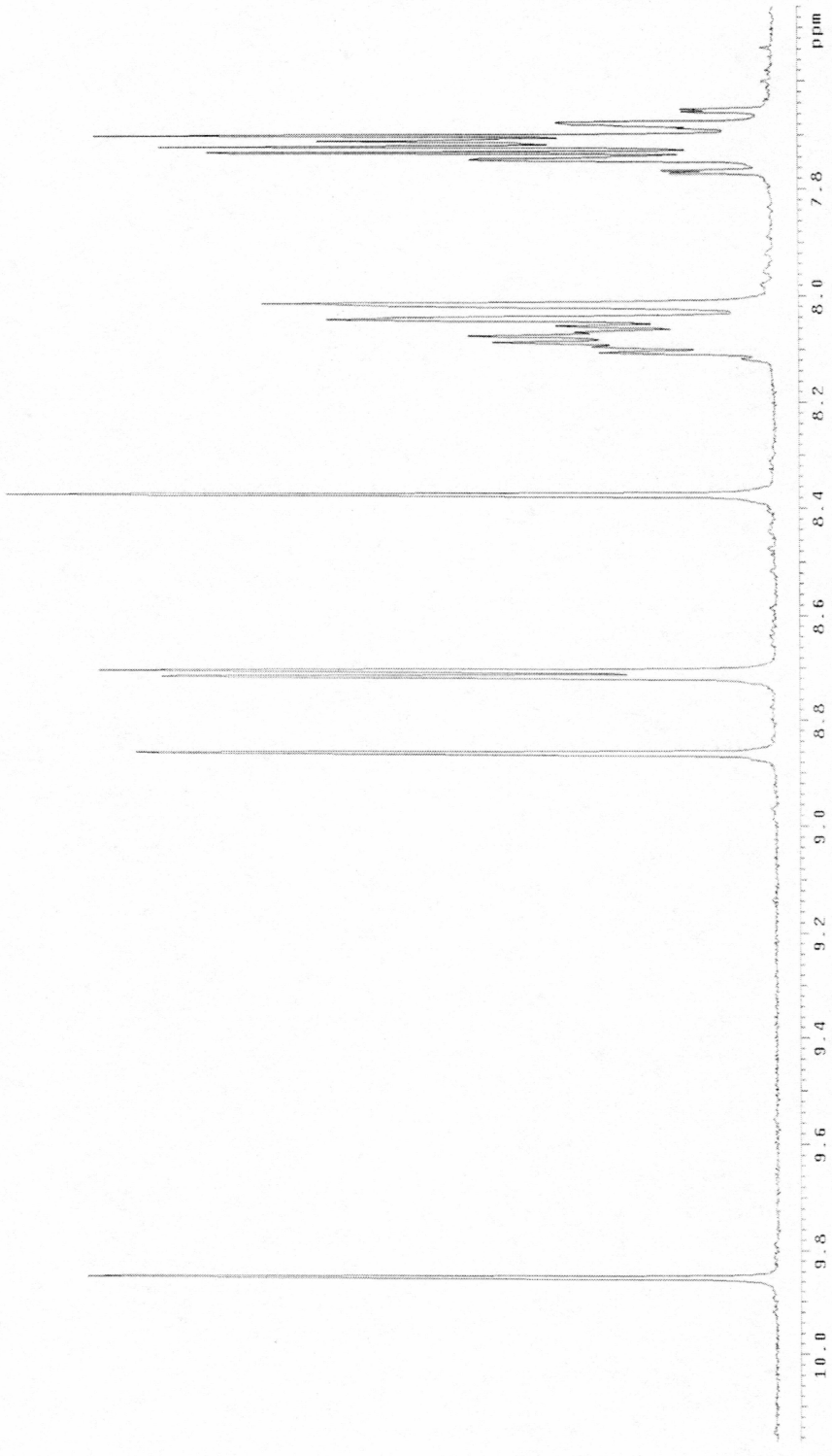

Figure D.1. ^{1}H NMR of Product **4** in $CDCl_3$

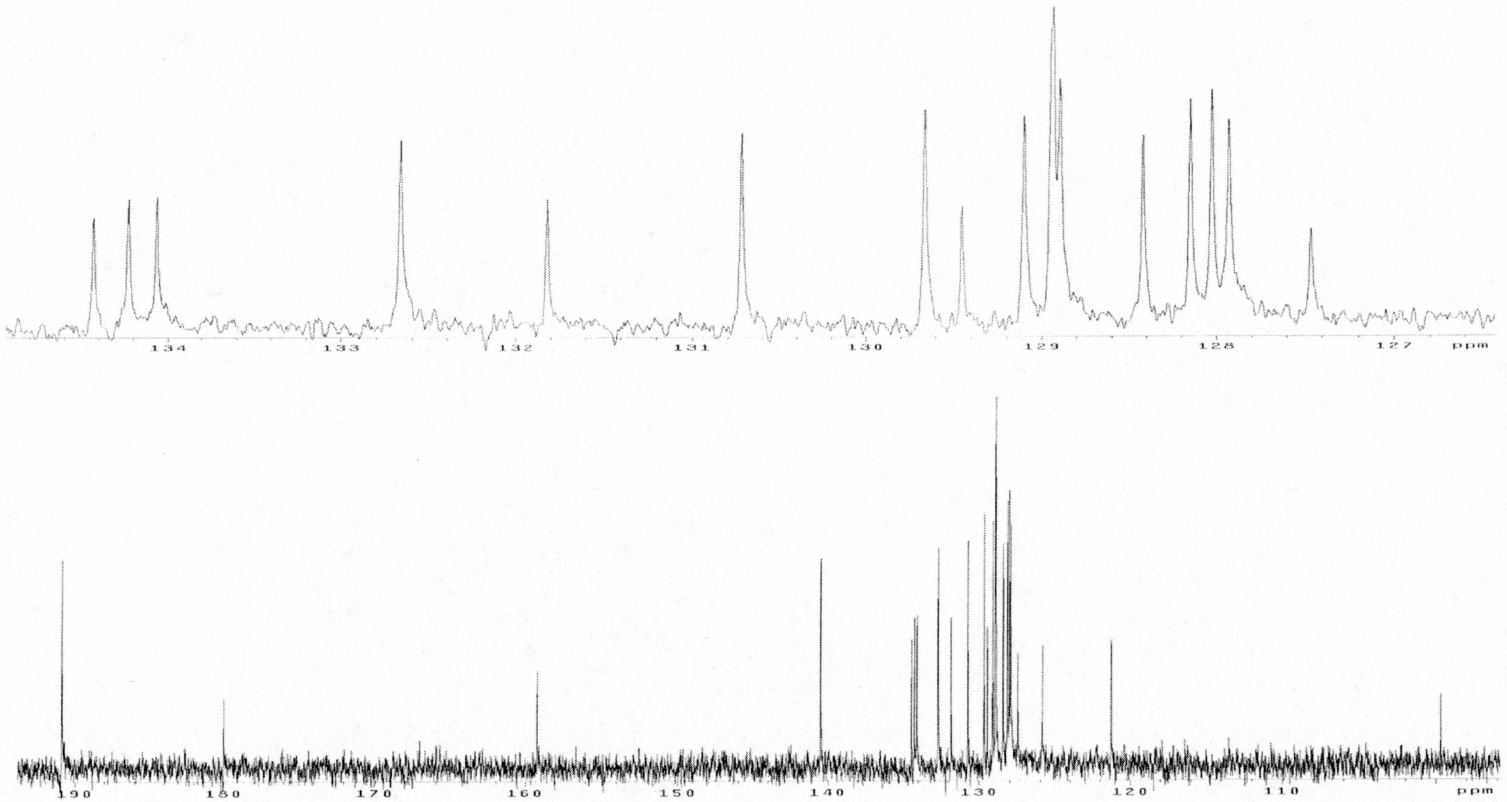

Figure D.2. ^{13}C NMR of Product **4** in $CDCl_3$

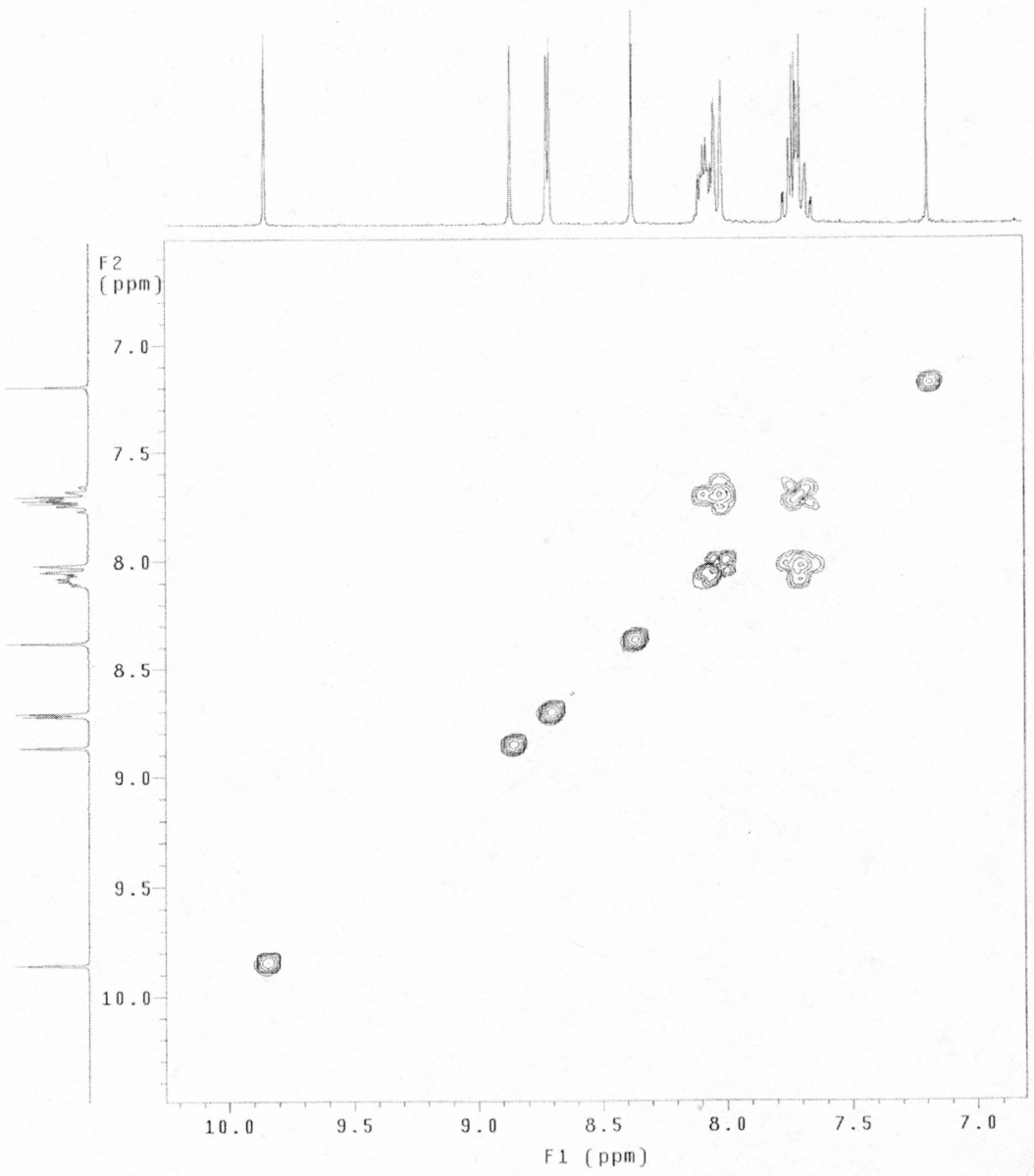

Figure D.3. gCOSY of Product **4** in $CDCl_3$

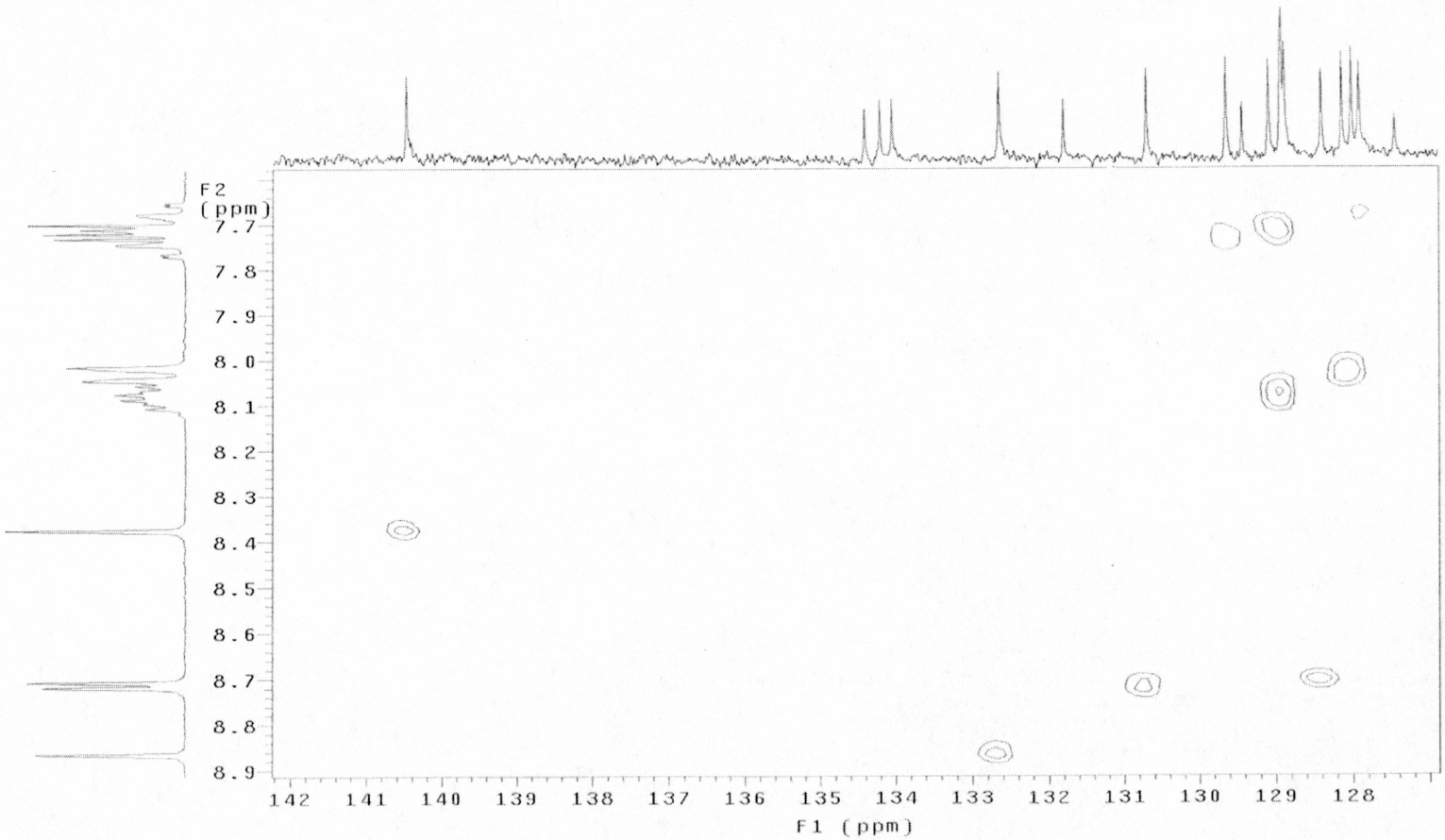

Figure D.4. Full gHSQC of Product **4** in $CDCl_3$

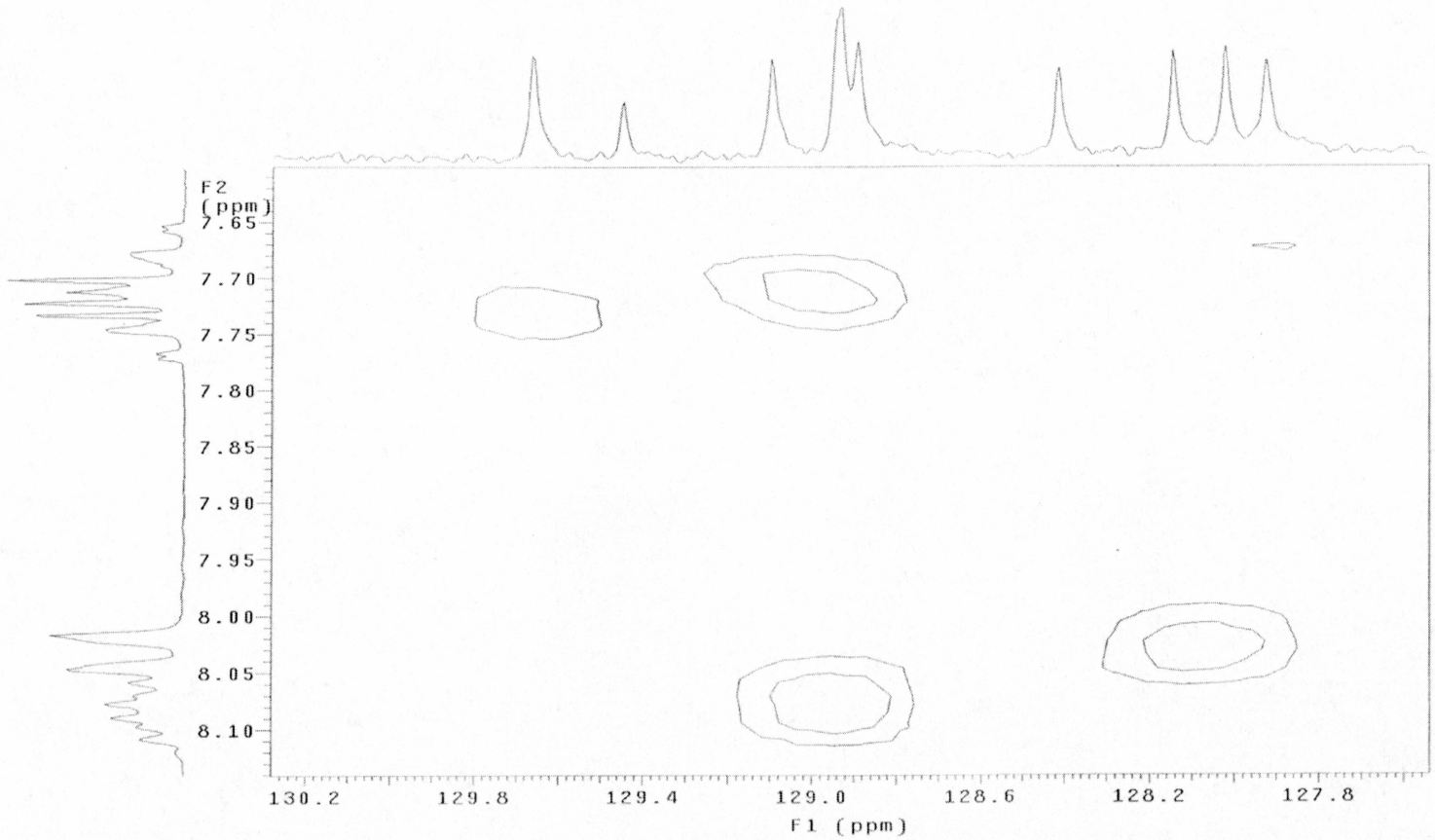

Figure D.5. Expanded gHSQC of **4** in $CDCl_3$. Note the overlapping resonances.

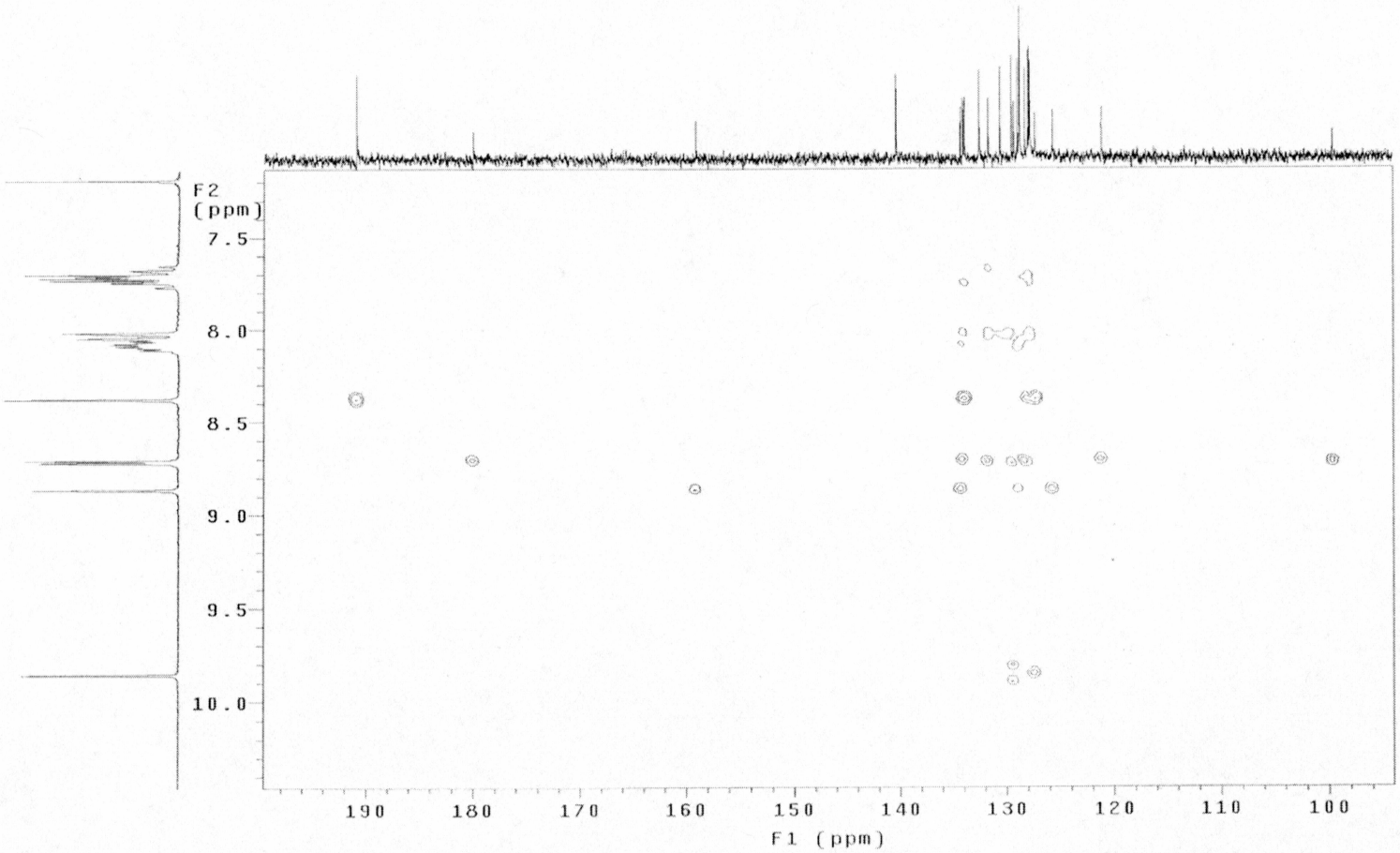

Figure D.6. Full gHMBC of Product **4** in $CDCl_3$

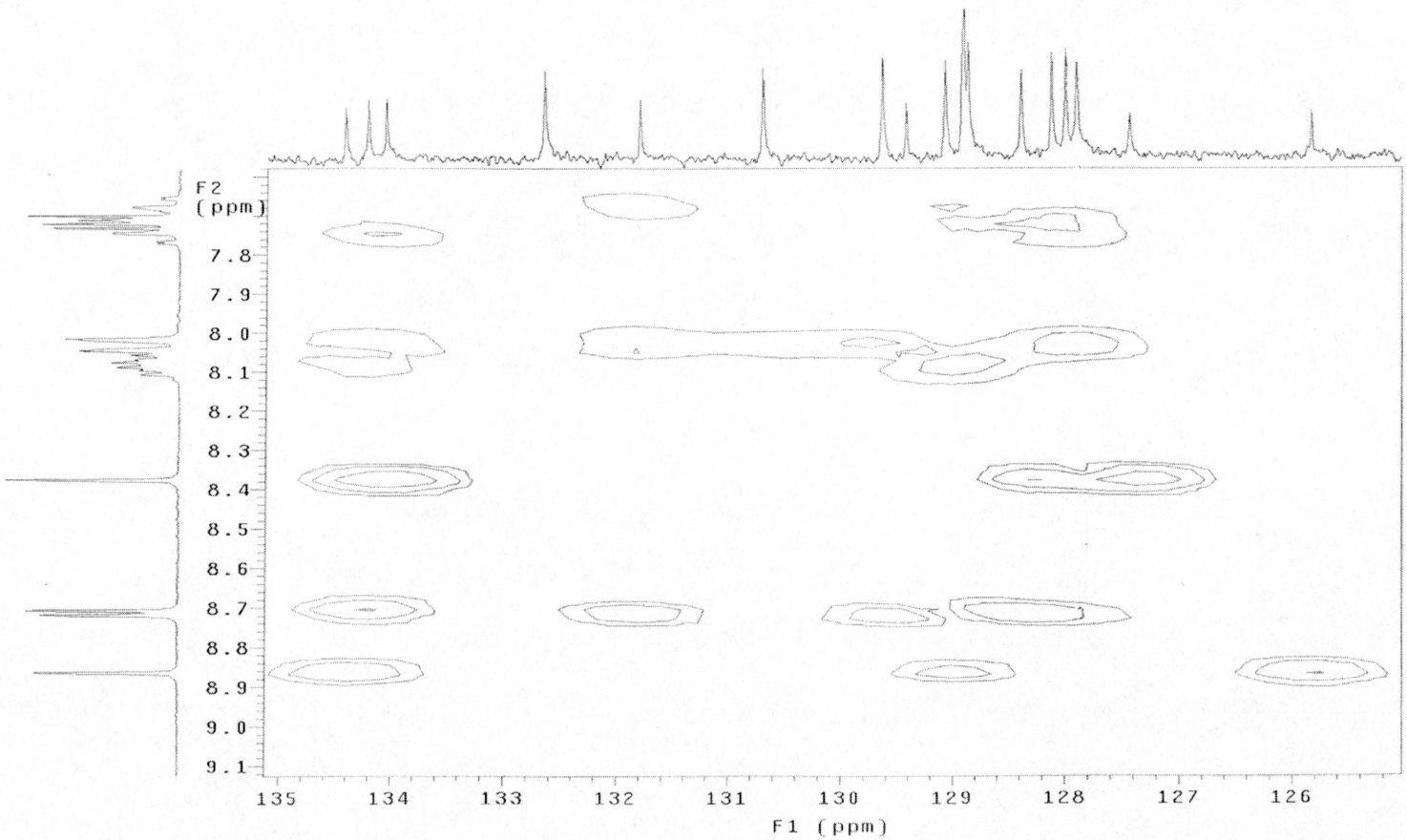

Figure D.7. Expanded gHMBC of **4** in $CDCl_3$

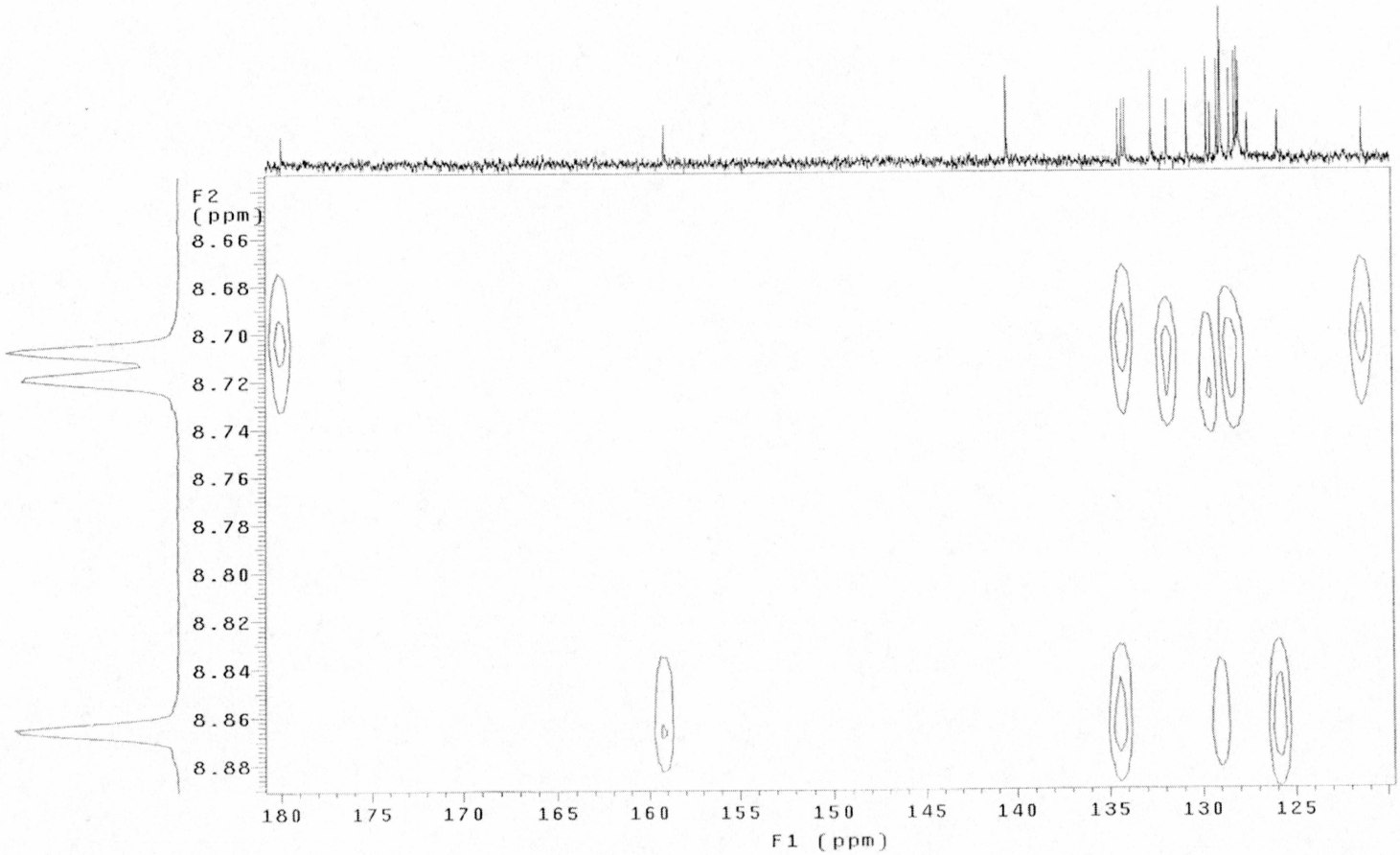

Figure D.8. Expanded gHMBC of **4** in $CDCl_3$, showing shift differences between H correlations

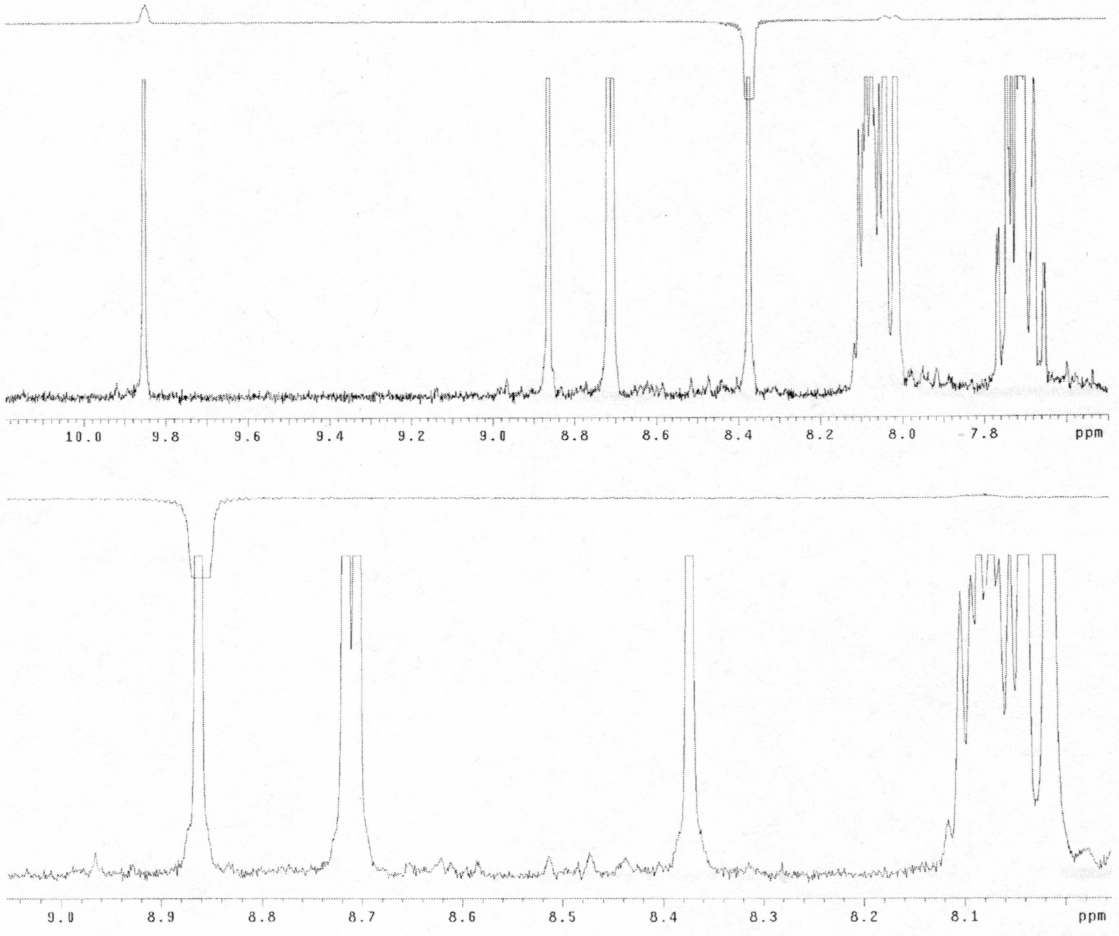

Figure D.9. NOESY 1D of **4** in $CDCl_3$ with irradiation at (from top to bottom) 8.36 and 8.86 ppm.

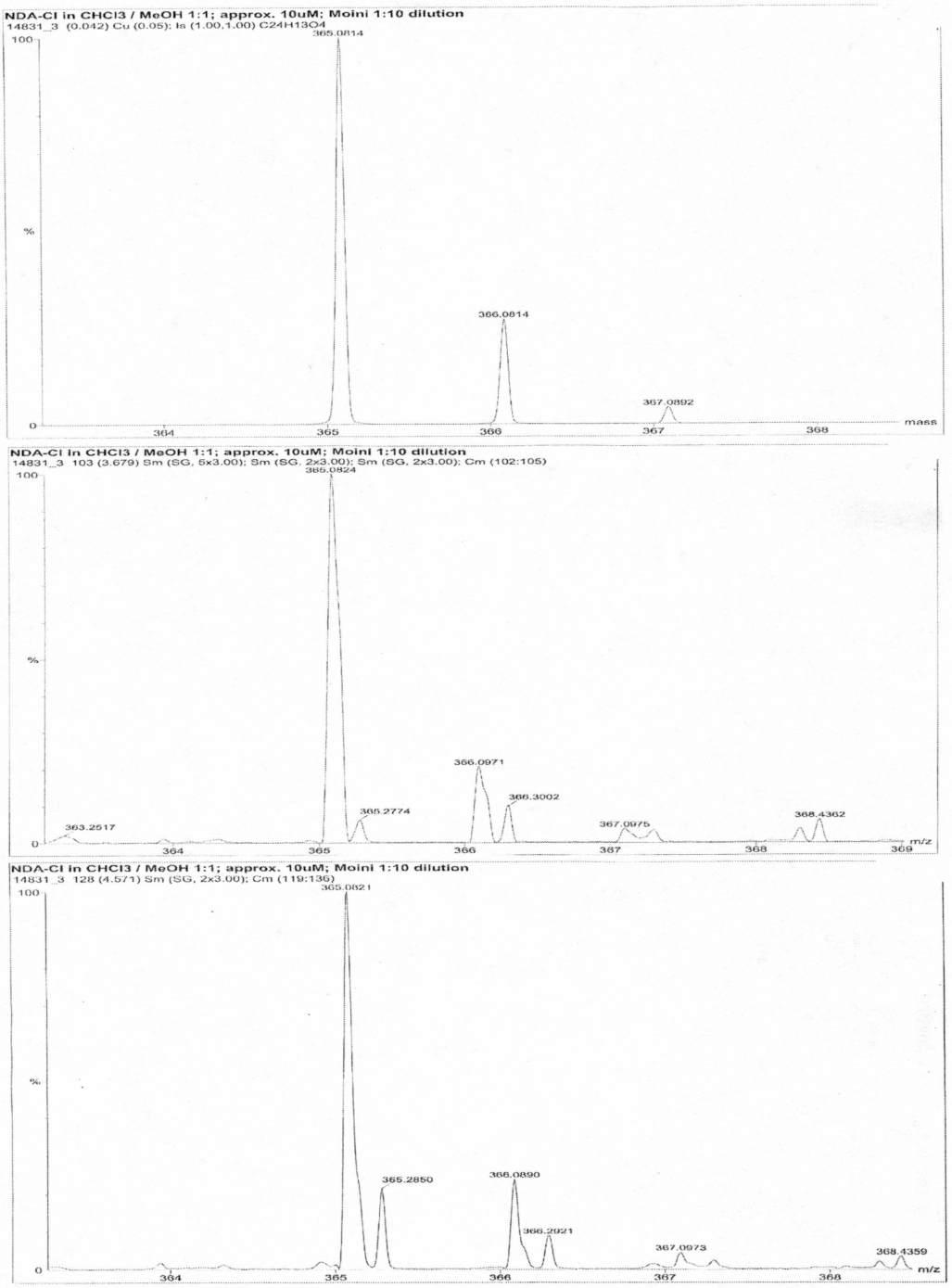

Figure D.10. ESI-MS of Product **4**

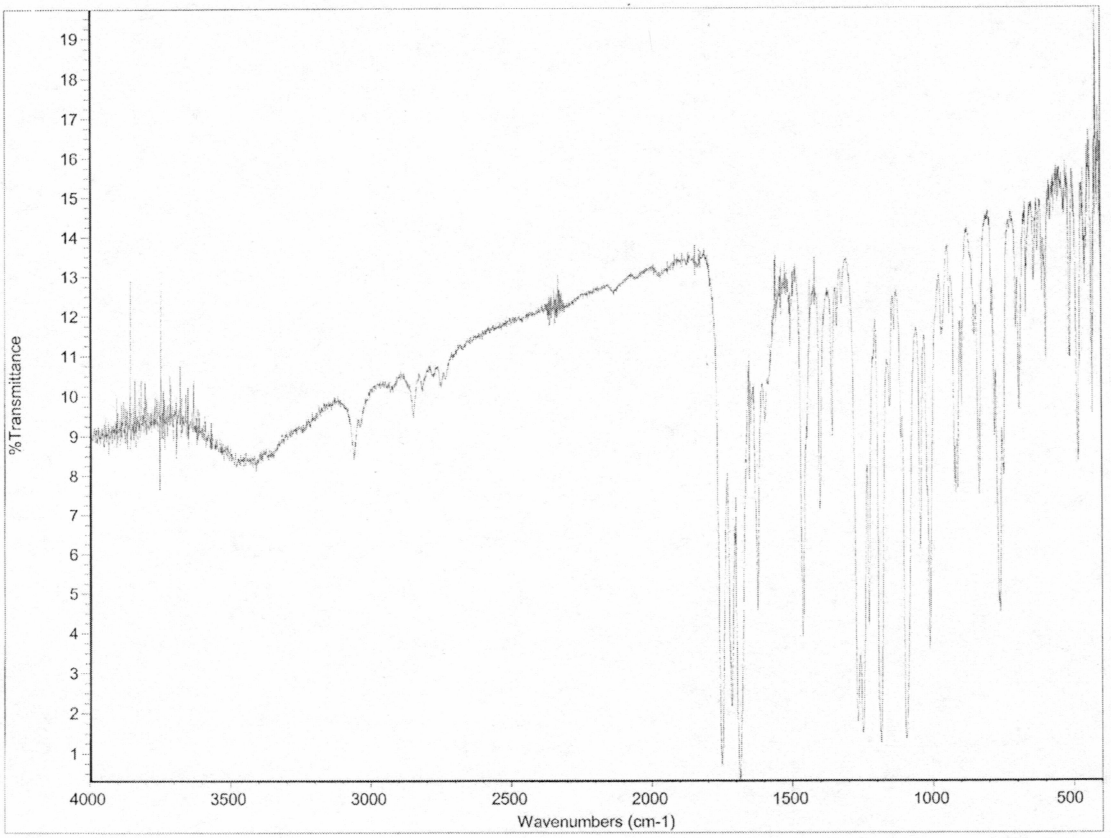

Figure D.11. IR (KBr) of Product **4**

APPENDIX E

Supplementary Spectra for Product **5**

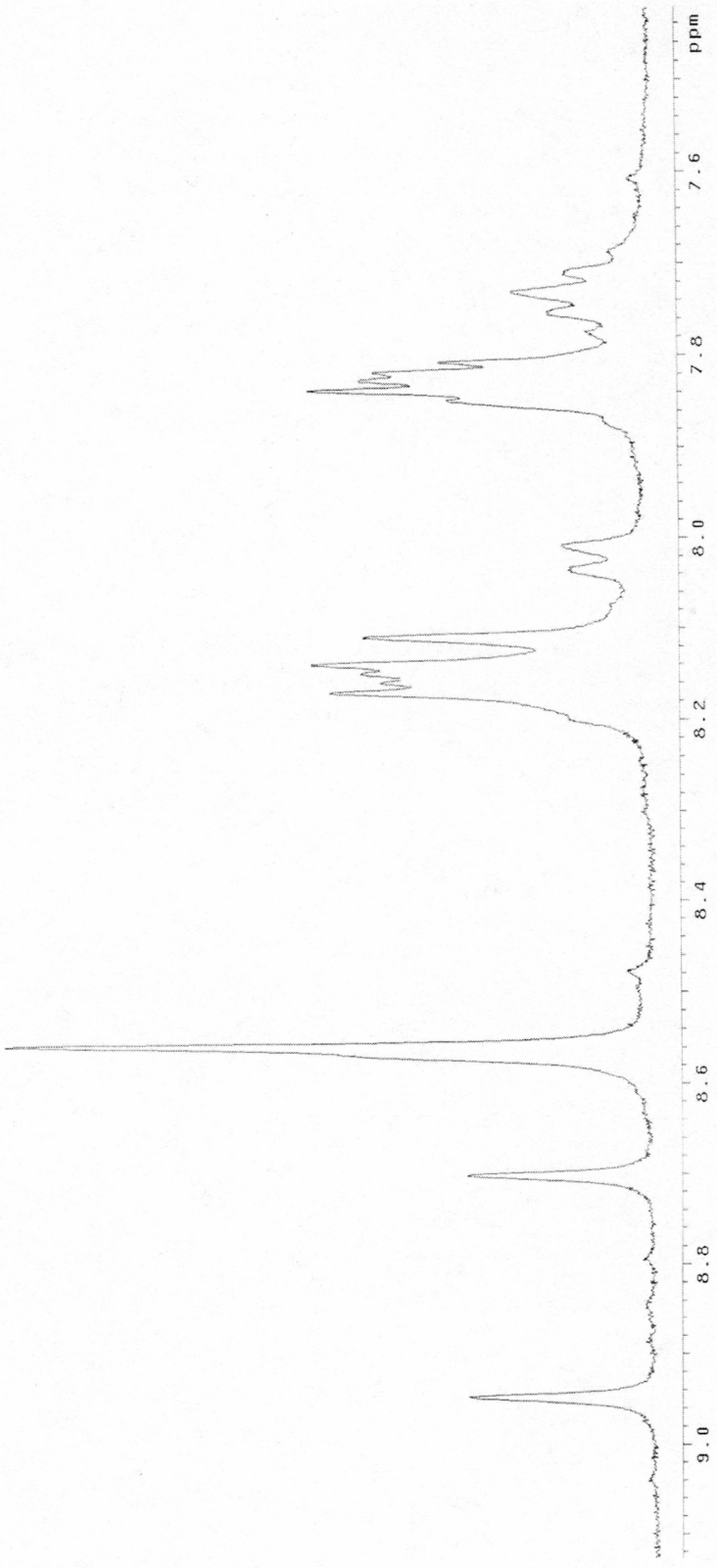

Figure E.1. ^{1}H NMR of unseparated product of PCC oxidation including starting material (**2**) and naphtho[2,3-c]furan-1,3-dione (**5**) in $CDCl_3$

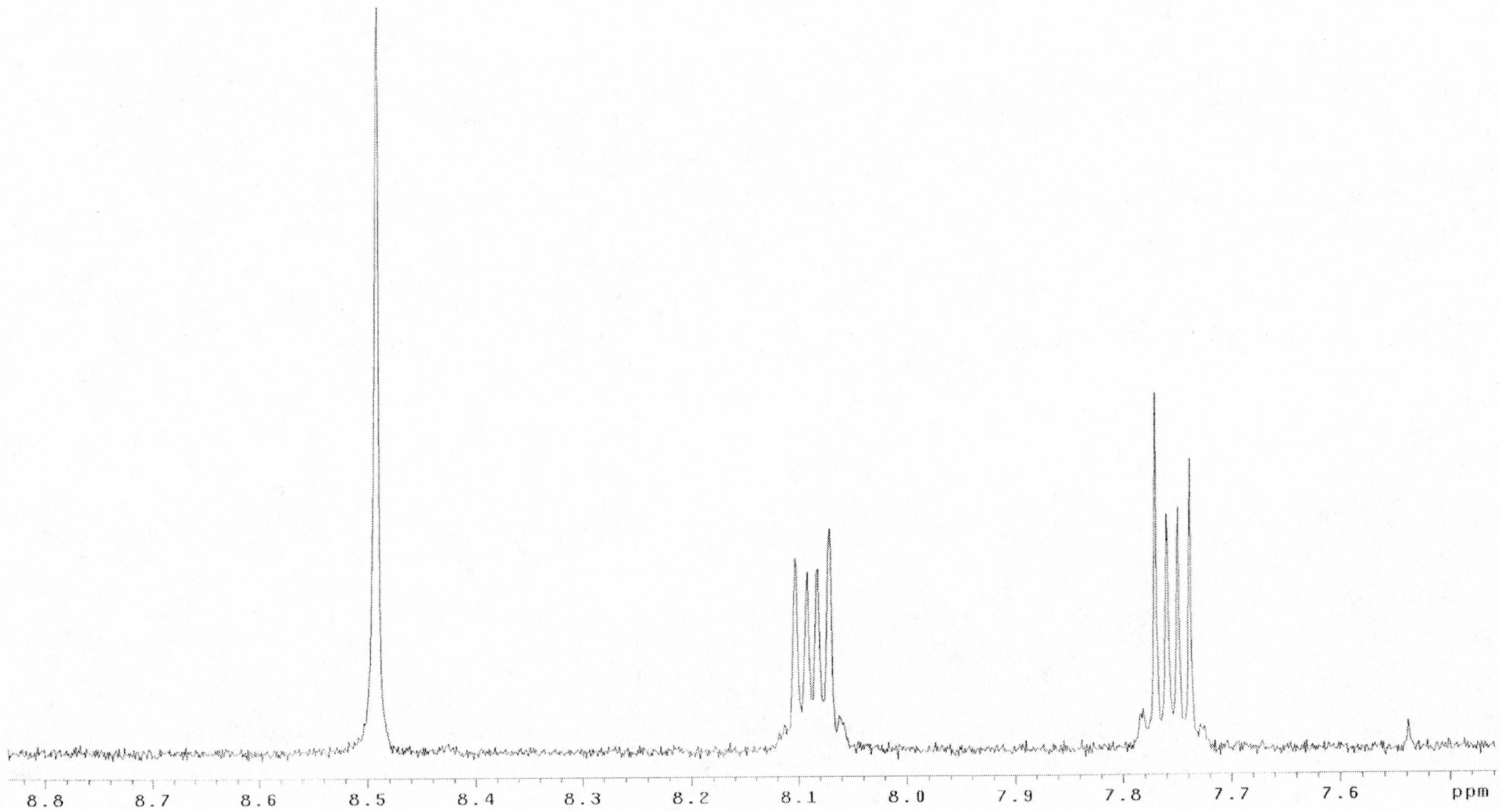

Figure E.2. ^{1}H NMR of naphtho[2,3-c]furan-1,3-dione (**5**) in $CDCl_3$

APPENDIX F

Supplementary Spectra for the Competitive Condensation

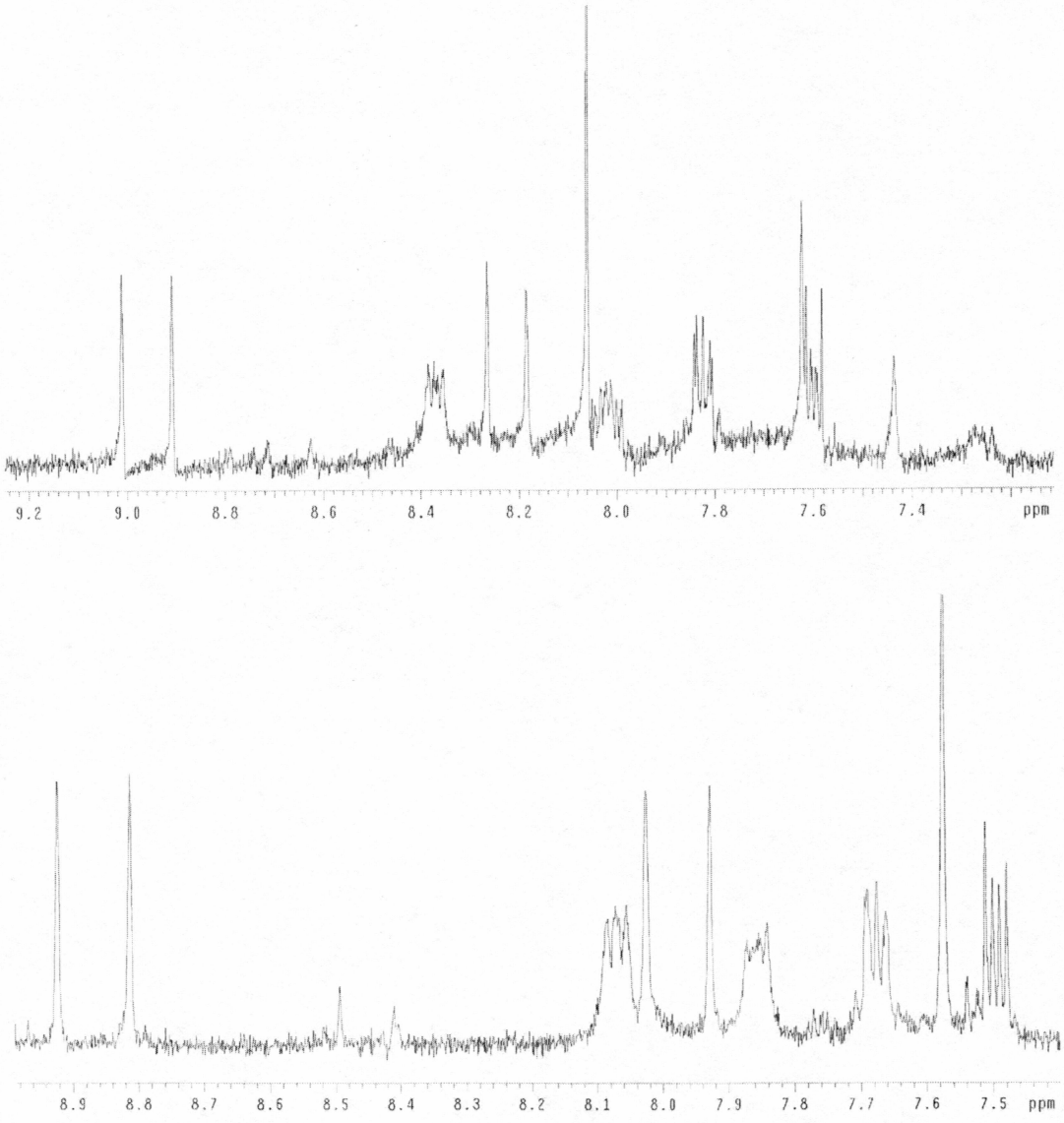

Figure F.1. ^{1}H NMR of the unidentified competetive condensation product isolated as a contaminant (top) and directly synthesized (bottom)